A SYSTEMS BIOLOGY APPROACH TO STUDY TYPE

III AND TYPE IV BACTERIAL EFFECTOR PROPERTIES

APPROVED BY SUPERVISORY COMMITTEE

Neal Alto, Ph.D.

Michael Shiloh, M.D., Ph.D.

Nan Yan, Ph.D.

Joel Goodman, Ph.D.

DEDICATION

Thinking of the numerous individuals whose support and guidance throughout my education gives me great joy, and I would initially like to thank Bert Chandler, the first professor to train me in laboratory work. Dr. Chandler dedicated hours of his time to teaching me how to design experiments and interpret data. I believe he is responsible for the development of my critical thinking skills that allowed me to easily transfer from the field of Chemistry to Microbiology. Next, I would like to thank my advisor Neal Alto. It was honestly a pleasure to work in his lab. He created an enthusiastic environment and motivated me through excitement. I overheard him once explain that he had chosen a faculty position at UT Southwestern because, even though the bar was set high, the university provided all of the necessary support to achieve those high aims. Neal has done the very same thing for all the members of his lab, including me. He expected the best, but did everything in his power to aid in that achievement. Additionally, the members of the Alto lab during my time here deserve a special thanks, especially Sarah Sutton, Robert Orchard, Andrey Selyunin, and Nikolay Burnaevskiy for their friendship and help through discussions and collaborations. I would also like to thank those on my thesis committee, Michael Shiloh, Joel Goodman, and Nan Yan for their helpful conversations and provision of essential reagents.

From a personal standpoint, I would like to thank my parents, Brad and Marianne Auten. I was raised to never doubt myself for a second, and that I could achieve anything I wanted. Thank you for always believing in me and for removing any barriers that might

come my way. I would also like to thank many of my friends for their camaraderie in Dallas and help watching Benjamin while I wrote my dissertation, especially Samantha Howard. Lastly, I would like to thank my husband, Adam, for sacrificing more than anyone else to help me get my Ph.D. It was a huge deal for you to leave your friends and family and come with me to Dallas. Thank you for all your support and love.

A SYSTEMS BIOLOGY APPROACH TO STUDY TYPE III AND TYPE IV BACTERIAL EFFECTOR PROPERTIES

by

BETHANY AUTEN WEIGELE

DISSERTATION

Presented to the Faculty of the Graduate School of Biomedical Sciences

The University of Texas Southwestern Medical Center at Dallas

In Partial Fulfillment of the Requirements

For the Degree of

DOCTOR OF PHILOSOPHY

The University of Texas Southwestern Medical Center at Dallas

Dallas, Texas

August, 2014

A SYSTEMS BIOLOGY APPROACH TO STUDY TYPE

III AND TYPE IV BACTERIAL EFFECTOR PROPERTIES

Publication No. _____

Bethany Auten Weigele, Ph.D.

The University of Texas Southwestern Medical Center at Dallas, 2014

Supervising Professor: Neal M. Alto, Ph.D.

The interaction between Type III and Type IV bacterial effector proteins and host signal transduction enzymes is a critical interface that, in many cases, determines the outcome of infectious disease. While many pathogenic strategies, such as evasion of phagolysosomal fusion, have been identified as necessary for microbial survival within the host, the effectors responsible are still largely unknown. Since most Gram-negative bacterial pathogens secrete between 5 to 300 effector proteins, a "systems biology" approach offers an enormous discovery potential. To approach the problem of effector protein biology from a global perspective, I first developed a comprehensive library of Type III and Type IV effector

proteins (from six diverse pathogens) and assayed this library of effectors for their ability to associate with eukaryotic membranes. Unexpectedly, 30% of the virulence factor repertoire exhibited transmembrane-spanning domains, fatty-acid acceptor sites, peripheral membrane-binding properties, and/or cryptic phospholipid-targeting motifs. From a global analysis of phospholipid-binding mechanisms and from specific studies on the *Shigella flexneri* invasion program, a membrane-dependent autocatalytic feedback loop that regulates bacterial effector protein functions in space and time was identified. Additionally, new tools to further understand the potential role(s) of bacteria effector molecules in usurping the tightly regulated endocytic trafficking pathway were developed. These tools were then used to identify and characterize the location at which three bacterial effectors EspG, VirA, and IpaJ disrupt the global secretory pathway. Lastly, the effector library was utilized in a bioinformatics approach to identify bacterial effectors from a newly sequenced pathogen found to encode a Type III secretion system. Exploiting previous knowledge of homologous characterized effectors within the library, the first bacterial effectors from the pathogen, *Providencia alcalifaciens* were identified. Taken together, these findings suggest that the evolution of bacterial membrane binding motifs promote higher-order signaling functions in host cells and provide a resource for further interrogation of these virulence properties across a broad range of bacterial pathogens.

TABLE OF CONTENTS

CHAPTER ONE 1

BACTERIAL SECRETED EFFECTORS HIJACK EUKARYOTIC MEMBRANES .. 1

TARGETING THE MASTER REGULATORS OF ENDOMEMBRANE TRAFFIC. 2

ALTERING FUSION MACHINERY COMPONENTS 4

LIPID PERTURBATIONS 6

ALTERNATIVE MECHANISMS TO EVADE PHAGOLYSOSOMAL DEGRADATION. 8

MECHANISMS OF EFFECTOR MEMBRANE LOCALIZATION 10

AIMS OF THIS STUDY 12

CHAPTER TWO 19

INTRODUCTION 19

RESULTS 21

SYSTEMATIC IDENTIFICATION OF BACTERIAL EFFECTOR/HOST MEMBRANE INTERATIONS 21

LOSS-OF-FUNCTION PI-KINASE SCREEN DEFINE MECHANISMS OF BACTERIAL PROTEIN LOCALIZATION 25

EXAMINATION OF A SPECIFIC CASE: IPGB1 LIPID BINDING MOTIF IS ESSENTIAL FOR SHIGELLA INFECTION 28

SHIGELLA ENGINEERS AN IPGB1-RAC1-PHOSPHOLIPID FEEDBACK CIRCUIT 29

GENERATING AN EXPERIMENTAL RESOURCE FOR FUNCTIONAL STUDIES IN MAMMALIAN CELLS 32
DISCUSSION 33
MATERIALS AND METHODS 59
MOLECULAR BIOLOGY 59
YEAST BASED ASSAYS 60
MAMMALIAN CELL STUDIES 62
RECOMBINANT PROTEIN 63
LIPID INTERACTIONS 63
SHIGELLA STRAINS AND INFECTIONS 64
CHAPTER THREE 67
INTRODUCTION 67
RESULTS 69
HUMAN GROWTH HORMONE SECRETION ASSAY 69
CONSTRUCTION OF CHEMICALLY REGULATED ENDOCYTIC TRAFFICKING ASSAY 70
TIME LAPSE STUDIES OF EFFECTOR TRAFFICKING USING THE CAD DOMAIN 73
DISCUSSION 74
MATERIALS AND METHODS 83
MOLECULAR BIOLOGY 83
HGH RELEASE ASSAY 83

BIOINFORMATICS 84
MAMMALAIN CELL STUDIES 84
CHAPTER FOUR 86
INTRODUCTION 86
RESULTS 87
BIOINFORMATIC INDENTIFICATION OF EFFECTOR HOMOLOGS 87
ACTIVATION OF THE T3SS 88
ANALYSIS OF PUTATIVE SSEJ HOMOLOG IN P. ALCALIFACIENS 90
ANALYSIS OF PUTATIVE STEC HOMOLOG IN P. ALCALIFACIENS..... 91
ANALYSIS OF PUTATIVE WXXXE HOMOLOG IN P. ALCALIFACIENS..... 92
DISCUSSION 93
MATERIALS AND METHODS 104
PLASMIDS 104
BIOINFORMATICS 104
INFECTION STUDIES..... 104
YEAST BASED ASSAYS 105
MAMMALIAN CELL STUDIES 105
RECOMBINANT PROTEIN 105
CHAPTER FIVE 107
ORIGINS OF NOVEL LIPID BINDING DOMAINS 107
MECHANISMS TO AMPLIFY EFFECTOR PROTEIN ACTIVITY IN SPACE AND TIME 108

NEW TOOLS TO STUDY BACTERIAL EFFECTORS 110
APPLYING OUR KNOWLEDGE 110
CONCLUSIONS 111
BIBLIOGRAPHY 119

PRIOR PUBLICATIONS

Andrey S. Selyunin, Lovett Evan Reddick, **Bethany A. Weigele**, Neal M. Alto. Selective Protection of an ARF1-GTP Signaling Axis by a Bacterial Scaffold Induces Bidirectional Trafficking Arrest. *Cell Reports*. 2014, 6: 1-14.

Burnaevskiy N, Fox TG, Plymire DA, Ertelt JM, **Weigele BA,** Selyunin AS, Way SS, Patrie SM, Alto NM. Proteolytic elimination of N-myristoyl modifications by the Shigella virulence factor IpaJ. *Nature*. 2013, 496(7443): 106-109.

Selyunin AS, Sutton SE, **Weigele BA**, Reddick LE, Orchard RC, Bresson SM, Tomchick DR, Alto NM. The assembly of a GTPase-kinase signaling complex by a bacterial catalytic scaffold. *Nature*. 2011, 469(7328): 107-111.

Weigele BA, Alto NM. Salmonella taking charge. Cell Host Microbe. 2010, 7(6): 421-422.

Auten, BJ.; Crump, CJ; Singh, AR; Chandler, BD; Dendrimer templates for Pt and Au catalysts. *Catalysis of Organic Reactions* Steve R. Schmidt, 2007, Ed. 1: 515-524.

Auten, B. Lang, H. and Chandler, B Dendrimer templates for heterogeneous catalysts: Bimetallic Pt-Au nanoparticles on oxide supports. *Applied Catalysis B: Environmental*. 2008, 81(3-4): 225-235.

Auten, B.; Hahn, B. Vijayaraghavan, G. Stevenson, K., Chandler, B D. Preparation and characterization of 3 nm magnetic NiAu nanoparticles. *J. Phys. Chem. C.* 2008, 112(14): 5365-5372.

Hoover, N**., Auten, B.,** Chandler, BD: Tuning supported catalyst reactivity with dendrimer-templated Pt-Cu nanoparticles, *J. Phys. Chem. B*. 2006, 110(17): 8606-8612.

LIST OF FIGURES

FIGURE 1. A BACTERIAL SECRETION SYSTEM..... 14

FIGURE 2. PHAGOLYSOSOMAL FUSION..... 15

FIGURE 3. MECHANISMS OF MEMBRANE INTERACTIONS..... 17

FIGURE 4. RAS-RESCUE SCREEN..... 37

FIGURE 5. CONFIRMATION OF THE RAS RESCUE SCREEN..... 38

FIGURE 6. PHENOTYPIC DIVERSITY AMONG SIMILAR EFFECTORS..... 40

FIGURE 7. MEMBRANE TARGETING OF THE 57 EFFECTORS IN YEAST STRAINS WITH ALTERED PHOSPHOINOSITIDE LEVELS..... 41

FIGURE 8. PI KINASE SCREEN..... 43

FIGURE 9. DIRECT PHOSPHOLIPID INTERACTIONS OF BACTERIAL EFFECTORS ……44

FIGURE 10. LIPID OVERLAY ASSAYS..... 45

FIGURE 11. THE IPGB1 MEMBRANE LOCALIZATION IS ESSENTIAL FOR SHIGELLA PATHOGENESIS..... 47

FIGURE 12. IPGB1 ASSEMBLES A GTPASE-PHOSPHOLIPID FEEDBACK LOOP.. 48

FIGURE 13. IPGB1 INDUCES A SHIGELLA SPECIFIC PHOSPHOLIPID RECRUITMENT PROFILE..... 50

FIGURE 14. IPGB1 SIGNALING CIRCUIT DURING INFECTION..... 52

FIGURE 15. BACTERIAL EFFECTOR LOCALIZATION AND FUNCTION..... 53

FIGURE 16. COLOCALIZATION STUDIES IN MAMMALIAN CELLS..... 54

FIGURE 17. DEVELOPMENT AND APPLICATION OF A GLOBAL SECRETORY PATHWAY ASSAY 76
FIGURE 18. VALIDATION OF ENDOMEMBRANE TRAFFICKING PROBES 77
FIGURE 19. ENDOMEMBRANE PROBES CAN BE USED TO IDENTIFY EFFECTORS POINT OF ATTACK 79
FIGURE 20. CAD TECHNOLOGY CAN BE USED TO STUDY BACTERIAL EFFECTOR TRAFFICKING 81
FIGURE 21. IDENTIFICATION OF *PROVIDENCIA ALCALIFACIENS* HOMOLOGS TO KNOWN TYPE III AND TYPE IV EFFECTORS 96
FIGURE 22. T3SS ACTIVATION STUDIES WITH *P. ALCALIFACIENS* 97
FIGURE 23. CHARACTERIZATION OF THE SSEJ HOMOLOG IN *PROVIDENCIA ALCALIFACIENS* 99
FIGURE 24. CHARACTERIZATION OF THE STEC HOMOLOG IN *PROVIDENCIA ALCALIFACIENS* 100
FIGURE 25. CHARACTERIZATION OF THE WXXXE HOMOLOG IN *PROVIDENCIA ALCALIFACIENS.* 102

LIST OF TABLES

TABLE ONE 18

TABLE TWO 56

LIST OF APPENDICES

APPENDIX A 113

LIST OF DEFINITIONS

AMP – ampicillin

ATPase – adenosine triphosphatase

Bh – *Bartonella henselae*

ca – constitutively active

CAD – conditional aggregation domain

CAM – chloramphenicol

cfu – colony forming units

DMEM – Dulbecco's modified Eagle media

Dox – doxycycline

Ec – enterohemorrhagic *Escherichia coli* O157:H7

EDTA – ethylenediaminetetraacetic acid

EHEC – Enterohemorrhagic *Escherichia coli*

ELISA – enzyme-linked immunosorbent assay

ER – endoplasmic reticulum

ERGIC – Endoplasmic Reticulum Golgi Intermediate Compartment (ERGIC

F-actin – filamentous actin

faf – fatty acid free

FBS – fetal bovine serum

Gal – galactose

GAP – GTPase activating protein

GEF – guanine nucleotide exchange factor

GFP – green fluorescent protein

GGTase – geranylgeranyltransferase

Glu – glucose

GSP – global secretory pathway

GTPase – guanosine triphosphatase

hGH – human growth hormone

HRP – horse radish peroxidase

HOPS complex – homotypic fusion and vacuole protein sorting complex

INV – invertase

KAN – kanamycin

LCV – *Legionella* containing vacuole

LiAc – lithium acetate

Lp – Legionella pneumophila

M6PR – mannose-six phosphate receptor

MEM – minimal essential media

MOI – multiplicity of infection

NBD-PC – 1-palmitoyl-2-6-[(7-nitro-2-1,3-benzoxadiazol-4-yl)amino]hexanoyl-*sn*-glycero-3-phosphocholine

PA – phosphatidic acid

PBS – phosphate buffered saline

PC – phosphatidylcholine

PEG – polyethylene glycol

Pel – Prenylated effectors of *Legionella* (Pel)

PH – pleckstrin homology

PI – phosphatidylinositol

PIP – phosphatidylinositol phosphate

PM – plasma membrane

PS – phosphatidylserine

Ps – *Pseudomonas syringae*

SCV – *Salmonella* containing vacuole

Sf – *Shigella flexneri*

St – Salmonella typhimurium

TBS – Tris buffered saline

TBST – Tris buffered saline plus tween

Tet-off – tetracycline off

TM – transmembrane

TMPred – transmembrane prediction

TNT – *in vitro* transcription and translation

T3SS – type III secretion system

T4SS – type IV secretion system

Vp – Vibrio parahaemolyticus

Wt – wild type

Ye – Yersinia enterocolitica

YopH – *Yersinia* outer protein H

Yp – Yersinia pestis

YPAD – yeast extract - peptone - dextrose plus adenine

CHAPTER ONE
Literature Review and Introduction

Bacterial secreted effectors hijack eukaryotic membranes

Microbial infectious diseases pose a challenge to human health and a large economical burden worldwide. Many of the most deadly Gram-negative bacterial pathogens use conserved protein translocation machines (e.g. Type III and Type IV) to deliver anywhere from 5 to 300 "effector" proteins directly into host cells (Figure 1) (Cascales & Christie, 2003; Dean, 2011). These effectors mimic or copy eukaryotic enzymatic function, hijack important host signaling pathways, and are required for the pathogen to successfully cause disease. Now, after 20 years of research, common themes in effector functions and targets are becoming apparent and can be used as a directive for further discovery. For example, many pathogens rewire the host endomembrane system through a variety of effector-mediated biochemical mechanisms. Discussed in this review are the currently known bacterial effector proteins that usurp the organellar architecture of the host in order to provide a pathogenic advantage.

Targeting the Master Regulators of Endomembrane Traffic

Perhaps the most ubiquitous targets of bacterial effectors are small GTPases. These signaling proteins cycle between an active (GTP bound) and inactive (GDP bound) state.

Regulating this process are two groups of proteins. The Guanine nucleotide Exchange Factors (GEFs) that facilitate the release of GDP and subsequent GTP reloading, which turns the GTPases on, and the Guanine Activating Proteins (GAPs) that facilitate the hydrolysis of GTP, which consequently turns the GTPases off. GTPases serve as master regulators of the cell and are critical for many basal cellular functions (Hall, 1998; Nobes & Hall, 1995). In particular, small GTPases from the Arf and Rab families are responsible for controlled fusion events throughout the endomembrane pathway (D'Souza-Schorey & Chavrier, 2006; Mizuno-Yamasaki, Rivera-Molina, & Novick, 2012). Several effectors have been shown to activate or deactivate these small GTPases, thereby directing traffic through either inhibiting deleterious fusion events or overstimulating beneficial ones.

Several examples of effectors that target small GTPase proteins are encoded in *Legionella pneumophila*, the causative agent of a severe pneumonia called *Legionnaires'* disease that is transmitted via aerosolized water droplets (Heidtman, Chen, Moy, & Isberg, 2009). During infection, this bacterium invades host cells and replicates in its own *Legionella*-containing vacuole (LCV). The first *Legionella* effector protein characterized, RalF is a GEF specific for Arf1 – one of the GTPases that regulates traffic from the endoplasmic reticulum (ER) to the Golgi apparatus (D'Souza-Schorey & Chavrier, 2006). Over-activation of Arf1 during *Legionella* infection allows for the redirection of ER vesicles to the LCV (Allombert, Fuche, Michard, & Doublet, 2013). Additionally, six secreted effectors from *Legionella* target Rab1 (another important regulator of ER to Golgi traffic) (Mizuno-Yamasaki et al., 2012). First, the *Legionella* effector LidA binds to Rab1 in the GTP bound active state in the low picomolar range and protects it from turnover by host

GAPs (Neunuebel, Mohammadi, Jarnik, & Machner, 2012; Schoebel, Cichy, Goody, & Itzen, 2011). Another *Legionella* effector, SidM, is a multidomain protein that not only covalently links an adenosine monophosphate (AMP) moiety to Rab1, but also serves as a GEF for Rab1 (Brombacher et al., 2009; Muller et al., 2012). Both these functions overstimulate Rab1 activity, further enhancing ER fusion to the LCV (Allombert et al., 2013). Interestingly, *Legionella* also encodes effectors to turn off both of these functions – SidD deAMPylates Rab1 and LepB is a GAP for Rab1 (Tan & Luo, 2011; Q. Yu et al., 2013). Lastly, *Legionella* performs another level of regulation on Rab1 through its effectors AnkX and Lem3, a phosphocholinase and dephosphocholinase, respectively (Mukherjee et al., 2011; Tan, Arnold, & Luo, 2011). The concerted effect is a highly re-regulated Rab1 by the pathogen *Legionella pneumophila*.

While pathogens encode effectors that facilitate beneficial Arf- and Rab-mediated fusion events, they also need to deactivate Arf and Rab GTPases on compartments they wish to evade. One particular arm of the endomembrane system commonly blocked by microbes is the lysosomal degradation pathway. Lysosomes are essential for the catabolism of macromolecules and clearance of invasive microbes. Cargo within any vesicle that fuses to the lysosome is destroyed by the acid hydrolases present in the lumen of this organelle (Figure 2A) (Saftig & Klumperman, 2009). The autophagy system aids in the removal and recycling of unwanted material in the cytosol (Figure 2A). Double membrane organelles (autophagosomes) engulf old organelles, aggregated proteins, and pathogens and specifically target them to the lysosome for degradation (Figure 2A) (Tanida, 2011). It is therefore critical for microbes to develop methods to evade exposure to this degradative pathway. One

effector that confers evasion of phagolysosomal fusion is VipD, a Type IV *Legionella* secreted protein that binds Rab5 and Rab22 at nanomolar range and blocks recruitment and interaction with their downstream targets, such as rabosyn and Eea1, respectively (Figure 2B) (Ku et al., 2012; Shohdy, Efe, Emr, & Shuman, 2005). The result of inhibiting Rab signaling is nonfunctional lysosomes, as DQ-red BSA is not degraded in cells expressing VipD. This indicates that VipD potentially plays a role in preventing bacterial lysosomal degradation (Ku et al., 2012).

The manipulation of Arf and Rab host proteins is not restricted to *Legionella* as it is also observed during *Salmonella* infection. *Salmonella* is a Gram-negative facultative intracellular pathogen that causes illnesses such as typhoid fever and severe gastroenteritis (Steele-Mortimer, 2008). Through the efforts of the Type III effector SifA, the *Salmonella* containing vacuole (SCV) matures by acquiring first early and then late endosomal markers. This process is essential for recruitment of the Lysosomal Associated Membrane Protein (LAMP1), the persistence of *Salmonella* within its vacuole, and, ultimately, disease as shown in mouse models (Browne, Hasegawa, Okamoto, Fierer, & Guiney, 2008; Brumell, Goosney, & Finlay, 2002). SifA binds the host protein SKIP and competitively prevents SKIP binding to the small GTPase Rab9 (Jackson, Nawabi, Hentea, Roark, & Haldar, 2008). More mechanistic characterization will be necessary to fully understand how SifA can alter LAMP1 localization.

Altering fusion machinery components

Another mechanism for evasion of phagolysosomal fusion is through the inhibition of other components necessary for host fusion machinery. In addition to small GTPases, fusion events in all eukaryotes require functional SNARE pairing of the vesicle (v-) and target (t-) SNARES and proper membrane phospholipid composition (Wickner, 2010). A few effectors have been found to target SNARE pairing as a method to block phagolysosomal fusion. For example, IncA, a secreted effector from *Chlamydia trachomatis*, the bacteria that causes the most prevalent sexually transmitted disease in the United States, is able to block endocytic membrane fusion (Figure 2B) (Subtil, Parsot, & Dautry-Varsat, 2001). Secondary structure analysis of IncA displayed several coiled-coils similar to the ones found in host SNARE proteins. Interestingly, the effector could be incorporated on either the v- or t-SNARE-containing membrane producing a general block in SNARE pairing (Scidmore, Fischer, & Hackstadt, 2003). While IncA is non-specific for the v- or t- membrane, it is specific for inhibiting endocytic machinery as no defect in exocytic fusion was observed (Figure 2B) (Scidmore et al., 2003). This finding is consistent with the *Chlamydia* lifecycle that requires fusion events with exocytic vesicles for delivery of nutrients to the pathogenic vacuole (Scidmore et al., 2003). Similarly, several *Legionella* effectors encode coiled-coil motifs. Indeed, one such effector, LegC3, blocks homotypic fusion *in vitro* in a dose-dependent manner. Though the particular host substrate and mechanism are still unknown, LegC3 *in vivo* fragments yeast vacuoles – an organelle similar to mammalian lysosomes (de Felipe et al., 2008). While more biochemical studies are necessary, these findings indicate effector-regulated inhibition of the fusion machinery, likely through SNARE pairing, as a possible method for persistence by avoiding exposure to the toxic lysosome (Bennett et al., 2013).

Lipid perturbation

Perturbation of phospholipid composition inhibits phagolysosomal fusion. For example, *Salmonella* is internalized into non-phagocytic epithelial cells through the alteration of the eukaryotic plasma membrane phosphoinositide (PI) composition. This manipulation is done by the phosphatidylinositol phosphatase, SopB, which dephosphorylates PI(4,5)P_2 to produce PI5P, causing bacterial internalization in an actin-dependent manner (Zhou, Chen, Hernandez, Shears, & Galan, 2001). Once *Salmonella* is inside the cell, SopB dissociates from the plasma membrane through a polymonoubiquitinated signal and is retargeted to the *Salmonella* containing vacuole (Marcus, Knodler, & Finlay, 2002; Patel, Hueffer, Lam, & Galan, 2009). At this second site of localization, SopB creates an overall neutral charge on the SCV by lowering the levels of both PI(4,5)P_2 and phosphatidylserine (PS) (Figure 2B) (Bakowski et al., 2010). The consequence of a loss of negative charge on the membrane was shown when a series of small GTPases that share a polycationic-prenyl plasma membrane targeting domain were absent on the SCV membrane of wild type but localized to the SCV membrane of the Δ*sopB* strain (Bakowski et al., 2010). Importantly, the GTPases excluded from the SCV belong to the Rab subclass of membrane traffic control molecules such as Rab8, Rab13, Rab23 and Rab35 (Smith et al., 2007). It appears that the absence of negative charge on the SCV plays a fundamental role for marking this intracellular compartment as "self" and selectively inhibiting lysosomal fusion events by restricting the accumulation of Rab GTPases at electrically neutral sites.

Legionella pneumophila employs several tactics to alter membrane identity through phosphatidylinositol modifications. For example, SidF a newly characterized PI phosphatase localizes to the *Legionella* containing vacuole and metabolizes $PI(3,4,5)P_3$ and $PI(4,5)P_2$ to the phosphoinositide found primarily on the Golgi – PI4P (Hsu et al., 2012). Another *Legionella* effector, LpnE, directly recruits the host PI phosphatase, OCLR1 to the LCV membrane further biasing the lipid population to PI4P (Newton et al., 2007). Marking the LCV with this lipid serves two purposes. First, it directs fusion of ER vesicles to the LCV, providing *Legionella* with nutrients. Second, it labels the LCV as the Golgi – an organelle that does not fuse with the lysosome in uninfected cells (Allombert et al., 2013).

Other bacteria also encode PI phosphatases that have been demonstrated to play different roles in pathogenesis. For example, the Type III effector Vpa0450 from *Vibrio parahaemolyticus (Vp),* the most common cause of food-borne illness from eating shellfish, is a homolog to the mammalian PI phosphatase Synaptojanin and targets $PI(4,5)P_2$ (Broberg, Zhang, Gonzalez, Laskowski-Arce, & Orth, 2010). $PI(4,5)P_2$ serves not only as an anchor for cytoskeletal proteins, directly tethering the plasma membrane to actin, but also as a regulator of actin polymerization through N-WASP activation (H. Miki, Miura, & Takenawa, 1996; Raucher et al., 2000). Reduction in $PI(4,5)P_2$ by this bacterial effector protein causes membrane blebbing and, ultimately, cell lysis (Broberg et al., 2010). Similarly, IpgD from *Shigella flexneri,* a pathogen that causes bloody diarrhea and severe abdominal cramping, also uncouples the plasma membrane from the actin cytoskeleton through its dephosphorylation of $PI(4,5)P_2$. Its function, however, is to reduce the tethering force during the *Shigella* invasion process, causing a larger phagocytic cup directly underneath the

bacteria (Niebuhr et al., 2002). Changes in the local concentration of $PI(4,5P)_2$ play a critical role in host cell membrane identity and integrity and are a common point of manipulation by diverse pathogens.

Alternative mechanisms to evade phagolysosomal degradation

An entirely different way to avoid the toxic contents of the lysosome is to inhibit bacterial phagocytosis. *Yersinia pestis (Yp),* the microbe responsible for the bubonic plague, encodes a tyrosine phosphatase YopH that disrupts Fcγ receptor- and ß1 integrin-mediated internalization, allowing the bacteria to persist attached to the exterior of the host cell (Fallman et al., 1995). Since tyrosine phosphorylation regulates a plethora of signaling cascades, it is likely that YopH inhibits the phosphorylation of a protein in the phagocytosis signaling pathway, although the specific host substrate has not been identified. Consistent with this hypothesis, *Yersinia*-encoding phosphatase-dead YopH mutants are readily engulfed by professional phagocytes and ultimately degraded via phagolysosomal fusion (Fallman et al., 1995). Another method applied by pathogens to inhibit phagocytosis is the targeting of Rho family small GTPases – the master regulators of the actin cytoskeleton. For example, enteropathogenic *E. coli* (EPEC) inhibits its internalization with the *E. coli* secreted protein H (EspH). EspH binds directly to the DH-PH domain of RhoGEF, blocking its ability to activate the small GTPase, RhoA. This block in activation of RhoA inhibits actin polymerization – a necessary step in the engulfment of extracellular bacteria (Dong, Liu, & Shao, 2010).

While bacterial persistence outside host cells allows for the evasion of phagolysosomal degradation through mechanisms described above, it does not confer avoidance of immune detection. As discussed earlier, common tactics for intracellular pathogens involve the targeting of fusion machinery, but alternative mechanisms have also been observed. For example, *Vibrio parahaemolyticus* was recently observed to induce its own internalization through VopC deamidation of another Rho family small GTPase, Cdc42 that also regulates actin polymerization (Okada et al., 2013). The observation of intracellular *V. parahaemolyticus,* a once thought to be a solely extracellular pathogen, now explains why this pathogen encodes an effector that prevents lysosomal degradation. VopQ recognizes the vATPase on lysosomal membranes and forms pores that are 18 Å in diameter. These pores cause the rapid neutralization of the lysosomal luminal pH (Figure 2B) (Sreelatha et al., 2013). Importantly, the potential for lysosomes to clear pathogens requires functional acid hydrolases, which are much less active at a pH above five (Saftig & Klumperman, 2009). With a neutralized lysosome, the destructive hydrolases are no longer functional, resulting in the pathogenic colonization of the host.

Some pathogens target the autophagy pathway to avoid clearance and persist within host cells. Normal activation of autophagy requires the conjugation of phosphoethanolamine (PE) to the host protein LC3 on its C-terminal glycine residue and the subsequent localization of LC3 to autophagosomal membranes (Tanida, 2011). Interestingly, *Legionella pneumophila* encodes a cysteine protease, RavZ, which cleaves the C-terminal glycine of LC3. This modification irreversibly blocks LC3 lipidation and, thus, activation of autophagy (Figure 2B) (Choy et al., 2012). RavZ deletion mutants, however, grow to equal levels as

wild type *Legionella* even though LC3 is successfully recruited to the autophagic membrane. This suggests additional effectors in *Legionella* are also targeting this pathway, although they have not yet been identified. Alternatively, autophagy may not be vital to control *Legionella*. Further studies will be needed to determine the interplay between the host autophagy system and *Legionella*. Other pathogens, like *Shigella flexneri,* avoid detection by the autophagy machinery through targeting essential autophagy proteins. For example, IcsB targets the autophagy protein Atg5 and prevents recognition of *Shigella* by autophagosomes, allowing for bacterial cytoplasmic persistence (Ogawa et al., 2005). Avoidance of autophagy is so critical that pathogens of various lifestyles often apply robust strategies to shut down the pathway to guarantee their survival.

Mechanisms of effector membrane localization

Although the mechanisms by which many bacterial effectors rewire the endomembrane system are characterized, there are still many trafficking phenotypes observed during infection in which the bacterial effectors responsible are still unknown. Bacterial effector proteins that localize to host cellular membranes are likely candidates for these observed trafficking phenotypes. Three main methods for membrane interaction have been observed: phospholipid interactions, transmembrane insertion, and protein lipidation (Figure 3).

Phosphatidylinositol phosphates (PIPs) are an evolutionarily conserved class of anionic phospholipids that act as site-specific signals on membranes and recruit and/or activate proteins for the assembly of spatially localized functional complexes. While some

effectors have been shown to dephosphorylate PIPs to alter membrane dynamics, as discussed previously, other effectors have been shown to require PIPs for proper localization within the endomembrane system. For example, the *Legionella* effectors LpnE, LidA, SidC, and SidM have been shown to bind to PI3P or PI4P (Haneburger & Hilbi, 2013). Additionally, a handful of Type III effectors (VopR^{Vp} from *V. parahaemolyticus*, YpkA^{Ye} from *Y. entercolitica*, and HopA1^{Ps} from *P. syringae*) were discovered to all contain a conserved membrane-binding motif that recognized various phosphoinositides (Salomon et al., 2013). The functional consequence of this motif, however, remains to be discovered.

Several effectors encode transmembrane domains. The best characterized is the translocated intimin receptor (TIR) encoded in pathogenic *E. coli* strains. This effector has two transmembrane domains that integrate into the plasma membrane. From that site, TIR facilitates both bacterial attachment through its extracellular domain and actin pedestal formation through its cytosolic tails (Luo et al., 2000; Weiss et al., 2009). Transmembrane-prediction software and truncation studies have also suggested that other bacterial effectors such as SseFSt, SseGSt, YlfA^{Lp}, YlfB^{Lp}, LegC3^{Lp}, and SidF^{Lp} encode transmembrane domains (Abrahams, Muller, & Hensel, 2006; Hsu et al., 2012). How these effectors integrate their transmembrane domains into eukaryotic membranes remains unknown.

Lipid modification allows for the spatial regulation of many important signaling proteins. Several types of lipidation have been observed on bacterial effectors. For example, N-terminal myristoylation has been shown in the *Pseudomonas syringae* effectors AvrPto1 and HopF2 (Robert-Seilaniantz, Shan, Zhou, & Tang, 2006). C-terminal prenylation of the *Salmonella* effector SifA as well as the Prenylated Effectors of *Legionella* (Pel) occurs on the

cysteine of a CaaX box motif and is necessary for membrane localization (Boucrot, Beuzon, Holden, Gorvel, & Meresse, 2003; de Vries, Andriotis, Wu, & Rathjen, 2006; Price, Jones, Amundson, & Kwaik, 2010; Reinicke et al., 2005). Additionally, the Hang group recently screened and identified effectors that are lipidated at more cryptic sites by host machinery (Ivanov, Charron, Hang, & Roy, 2010). While a handful of effectors have been shown to localize to membranes through a variety of mechanisms, a "systems biology" approach to exhaustively identify the effectors that target and/or disrupt the endomembrane system of host cells has enormous discovery potential.

Aims of this study

To approach the problem of effector protein biology from a global perspective, a plasmid-based library of Type III and Type IV effector proteins that can be exploited for large scale screening approaches will be developed. These genes will provide the templates necessary to assay cellular functions that are commonly subverted by multiple bacterial pathogens (i.e. membrane trafficking). Importantly, this library will be constructed with the TOPO Gateway system. This system does not require the use of PCR and restriction enzymes to shuttle genes between various expression plasmid, but rather uses site-specific recombination to accurately transfer genes from a parent vector (pENTR) to the destination vector of choice (i.e. yeast, bacteria, or mammalian expression). This system reduces the time and effort in cloning, allowing for efficient screening of multiple effector proteins using several systems. The library will be comprised of confirmed translocated effectors from six

different pathogens: *Salmonella enterica* serovar *typhimurium, Shigella flexneri, EHEC H7:O157, Legionella pneumophila,* as well as the plant pathogen *Pseudomonas syringae*, and the pathogen responsible for Cat Scratch disease *Bartonella henselae* (Table 1). Importantly, this large repertoire of effector proteins will allow for the assessment of the global conservation and functional contributions of effector/endomembrane interactions over a wide-range of bacterial species with distinct tropisms (plant and animal), tissue specificities (respiratory, blood, gut), cellular lifecycles (extracellular, cytoplasmic, vacuole), and disease outcomes (dysentery, pneumonia, fever).

Large-scale screening efforts will then be performed with the library. First, effector proteins that localize to host membranes will be identified through the use of yeast genetics. Once candidates are discovered, biochemistry, fluorescence imaging, and bacterial infection tools can be used to determine the mechanisms of interaction and their functional purpose. The development of this library will also be used to screen effectors for phenotypes already observed to occur during infection. As mentioned previously, the rewiring of endomembrane trafficking is known to occur during infection of many pathogens and is dependent on functional secretion systems. To this end, screens to identify the effectors that regulate host trafficking systems will be designed. Lastly, these findings can be applied to more quickly characterize pathogens recently sequenced and found to encode secretion systems by finding similarities between their putative effectors and those that are already well characterized by other studies.

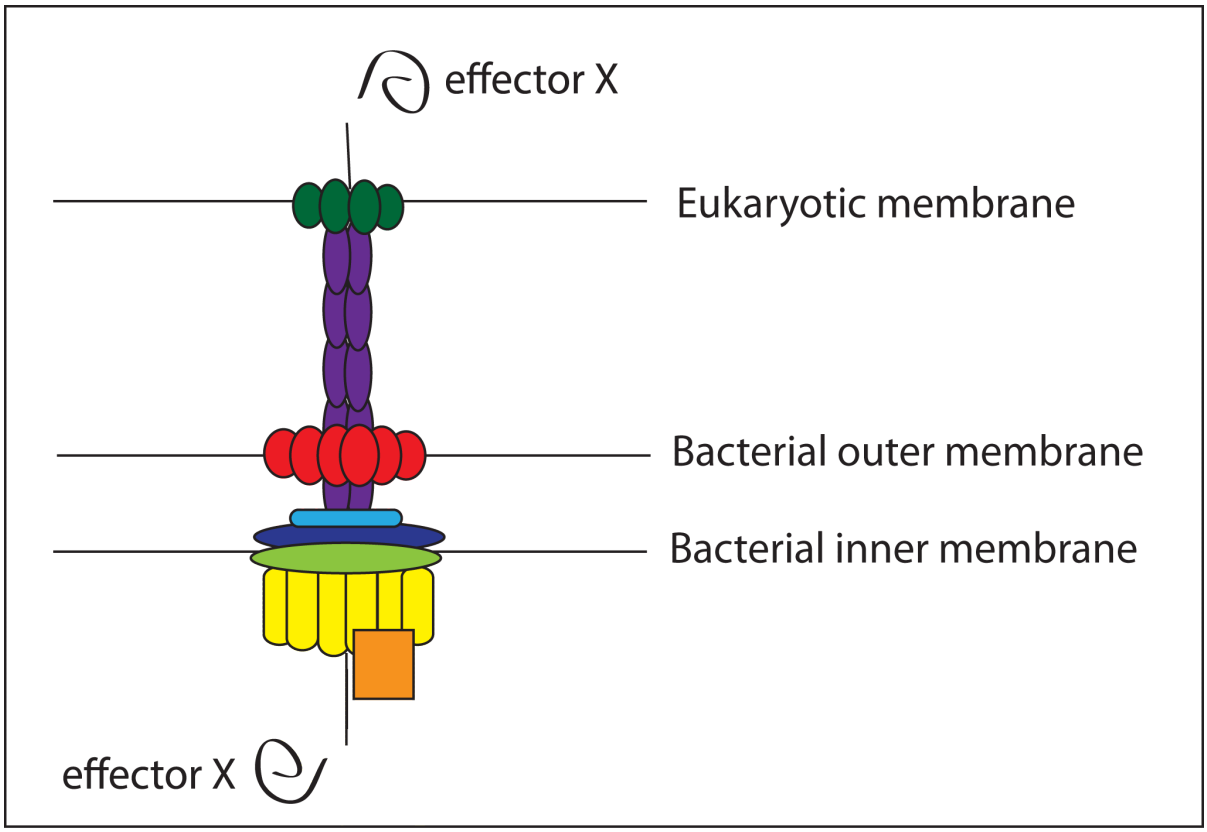

Figure 1: A **Bacterial secretion system**
Pictorial representation of the multiprotein Type III secretion system that facilitates the translocation of bacterial "effector" proteins directly into the host cell. Each unique protein is a different color.

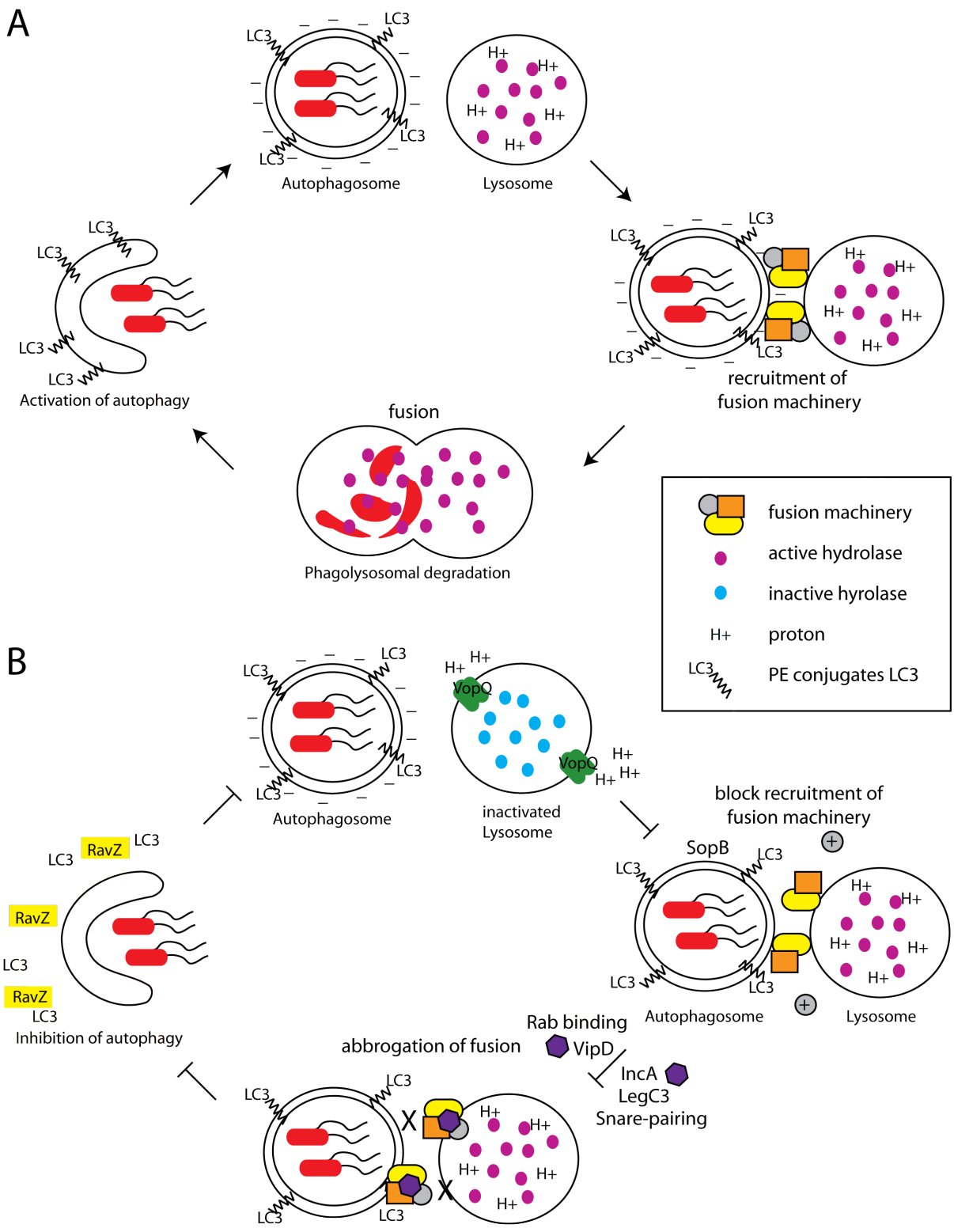
A
LC3
Autophagosome
H+
Lysosome
recruitment of
fusion machinery
fusion
Phagolysosomal degradation
Activation of autophagy
fusion machinery
active hydrolase
inactive hyrolase
proton
PE conjugates LC3
B
VopQ
inactivated
Lysosome
block recruitment of
fusion machinery
SopB
RavZ
Inhibition of autophagy
Rab binding
VipD
abbrogation of fusion
IncA
LegC3
Snare-pairing

Figure 2: Phagolysosomal fusion

(A) In healthy cells, the autophagy system is activated during modes of starvation or microbial invasion to engulf cargo and deliver it to the lysosome for degradation. LC3 is recruited to the membrane of the autophagosome, fusion machinery is then recruited to the lysosome and autophagosome, and contents are degraded by the harsh acidic environment and acid hydrolases.

(B) Several bacterial secreted effectors target this pathway and arrest phagolysosomal fusion through a variety of mechanisms, which allow for pathogenic persistence. RavZ cleaves LC3 and prevents its association to the autophagosome; VopQ forms pores in the lysosome and neutralizes the acidic pH. SopB reduces the negative charge on the autophagosome, blocking the recruitment of fusion machinery. LegC3 and IncA interact with the fusion machinery and prevent fusion events. Lastly, VipD binds Rab GTPases to prevent adaptor protein recruitment necessary for fusion.

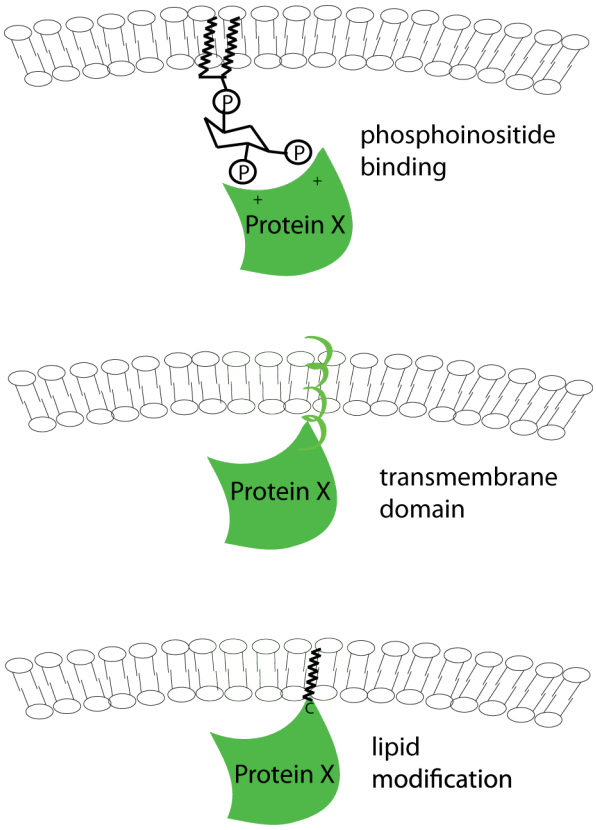

Figure 3: Mechanisms of Membrane Interaction
Proteins that interact with eukaryotic membranes do so by phospholipid interactions, transmembrane insertion, or fatty acid modification as shown above.

Table 1: Pathogens discussed in this review

Pathogen	Secretion system	Lifestyle	Used in these studies
Salmonella typhimurium	Type III	vacuolar	x
Shigella flexneri	Type III	intracellular	x
EHEC H7:O157	Type III	extracellular	x
Pseudomonas syringae	Type III	extracellular	x
Vibrio parahaemolyticus	Type III	extracellular/intracellular	
Chlamydia trachomatis	Type III	vacuolar	
Legionella pneumphila	Type IV	vacuolar	x
Bartonella henselae	Type IV	vacuolar	x

CHAPTER TWO
A Systematic Exploration of Host-Membrane Interactions that Shape Bacterial Virulence Factor Functions

Introduction

The protein secretory systems (SS) of Gram-negative bacterial pathogens are among the most thoroughly studied microbial virulence determinants. Many of these systems are evolutionarily related to ancient molecular machines, including flagellum (e.g. T3SS), the conjugation pili (T4SS), and phage tail spike apparatus (e.g. T6SS), and all function to deliver "effector" proteins from the bacterial cytoplasm directly into host cells. Once inside the host, these virulence factors reprogram host cellular behaviors to promote bacterial replication, colonization, and inhibition of the host immune system. Due to the importance of this pathogenic strategy across numerous bacterial species, research in this field has largely been focused on determining how effector molecules modify host substrates at the biochemical and structural level. Interestingly, however, recent studies suggest that effector proteins can induce more complex host signaling behaviors including autocatalytic feedback reactions, non-linear signaling dynamics, and network crosstalk (Dong et al., 2012; Ohlson et al., 2008; Orchard et al., 2012; Selyunin et al., 2011). However, the global conservation of this pathogenic strategy – and particularly the molecular mechanisms driving "higher order" bacterial effector protein functions – is poorly understood.

Here, I sought to identify conserved features of host cells that may regulate bacterial effector protein functions in space and time. It is well known that targeting proteins to the

plasma membrane and membrane-bound organelles is an essential feature of dynamic interaction networks that exhibit precise signaling fidelity and efficacy (Grecco, Schmick, & Bastiaens, 2011; Scott & Pawson, 2009). In fact, several aspects of host membrane architecture make it a critical site for enzyme-substrate organization and signal amplification. First, the ability of lipids to recruit cytosolic proteins onto a two dimensional membrane surface has a powerful concentration effect within the cell, which promotes signal organization. Second, protein movement within membranes is much slower than in the cytoplasm, providing a physical barrier to protein diffusion, which limits non-specific interactions. Third, certain lipid-types can be geographically restricted within the cell, building spatially defined membrane microdomains that generate selectivity in many signal transduction systems. Finally, membrane surfaces are often used as physical scaffolds for the assembly of multi-protein complexes that display robust detection, amplification, and decoding of input signals. In these contexts, I predicted that bacterial effector protein acquisition of lipid binding domains would offer a simple, yet flexible, strategy for bacterial pathogens to "rewire" host signaling systems in both space and time.

To systematically identify bacterial virulence factors that alter host lipid dynamics, a library of Type III and Type IV secreted bacterial effector genes, (encoded by six distinct bacterial species: *Salmonella typhimurium* [*St*], *Shigella flexneri* [*Sf*], Enterohemorrhagic *Escherichia coli* O157:H7 [*Ec*], *Legionella pneumophila* [*Lp*], *Bartonella henselae* [*Bh*], and *Pseudomonas syringae* [*Ps*]) were screened for interaction with yeast cellular membranes. This broad-based approach allowed for the examination of the convergence of effector protein functions across pathogens with vastly different host tropisms, tissue specificities,

cellular life cycles, and infectious disease outcomes. By integrating an unbiased genetic approach with high-content fluorescence microscopy, I identified 57 bacterial effector proteins that interacted with host cellular membranes, 80% of which were previously uncharacterized. A secondary screen of over 342 genetic perturbations uncovered sixteen bacterial effector proteins that directly interacted with host acidic phospholipids, significantly extending the repertoire of bacterial lipid binding proteins. Importantly, this experimental design provided a framework for the identification of molecular events that orchestrate complex host-pathogen interactions. Indeed, an in-depth analysis of the *Shigella flexneri* invasion program suggested a phospholipid-assisted autocatalytic sensor that regulates the dynamics of the Type III secreted IpgB1. When taken together, these findings greatly expand the field's understanding of bacterial effector protein dynamics across multiple pathogens, further demonstrates the utility of functional genomic screens to interrogate virulence factor complexity in model organisms, and provides a powerful resource for defining higher order signaling dynamics during bacterial infection. These results are discussed in light of the current understanding of spatiotemporal regulation of host-pathogen interactions, leading to the proposal that host-assisted autocatalytic feedback reactions are a common protein design principle.

Results

Systematic identification of bacterial effector/host membrane interactions

To develop a library of virulence factors for functional comparison, I curated the literature for confirmed Type III secreted effectors encoded in the SPI-I and SPI-2 genetic

loci of *Salmonella typhimurium,* the Hrp pathogenicity island of *Pseudomonas syringae,* the pWR100 virulence plasmid of *Shigella flexneri,* and the locus of enterocyte effacement (LEE) as well as the nine other effector loci (non-LEE) of *EHEC H7:O157* (see Appendix A for references). Additionally, the library was expanded to include the Type IV secreted effectors from the Icm/Dot and VirB/D4 systems from *Legionella pneumophila* and *Bartonella henselae*, respectively (Appendix A). In total, 208 bacterial effector genes were cloned and sequence confirmed (Appendix A).

Next, an unambiguous (life or death) genetic screen in yeast to identify bacterial effector proteins that interact with intracellular membranes of a model eukaryotic organism was adapted (Figure 4A) (Isakoff et al., 1998). Each bacterial effector gene was fused in-frame to the C-terminus of constitutively active (Q61L), non-farnesylated (ΔCaaX) Ras mutant (herein referred to as Ras*) and then transformed into a cdc25 temperature sensitive mutant strain (cdc25t/s) of yeast. If the bacterial effector protein of interest drives Ras* to a cellular membrane, it will promote yeast replication at the non-permissible temperature (37°C) by complementing the growth defects in the cdc25t/s mutant background (Figure 4A). This screen is much more reliable than GFP subcellular determination, which can give false positives from protein aggregates or luminal trafficking proteins as well as false negatives from seemingly disperse proteins that have transient or cyclical membrane localization. Furthermore, the robust sensitivity of the Ras system can easily overcome artifacts caused by overexpression, as demonstrated with a fusion of a cytosolic truncation of dynamin, which resulted in no yeast growth (Figure 4C). In contrast to this negative control, PLC, a PI(4,5)P_2 binding protein, grew rapidly at 37°C and served as a positive control (Figure 4C).

Before conducting the screen, growth-inhibition assays revealed that 13 effector proteins from the library caused growth arrest at the permissible temperature (25°C; data not shown). However, inactivating point mutations of eight of these effectors (whose catalytic activity is known) abrogated the yeast growth arrest phenotype, allowing these effectors to be included in the Ras rescue screen (Figure 4B). Subsequent expression profiling revealed that 190 of the 203 effector genes that did not cause yeast growth arrest produced full-length proteins in yeast. It is important to note that the choice of yeast as a model organism relies on the conservation of the effector substrates being studied (i.e. membranes) between yeast and mammalian cells. The evolution of membrane bound organelles was the key defining event that distinguished eukaryotes from the prokaryote and archea domains of life. Because these organelles and their interconnected membrane trafficking systems play an essential role for compartmentalizing enzymes with their chemical reactants, they are highly conserved across eukaryotic taxa, permitting this study to be performed in yeast.

From a total of 190 bacterial effector-Ras* fusion proteins validated, 60 promoted yeast growth at the non-permissible temperature of 37°C (Figure 4C). This value was unexpectedly high, indicating that ~30% of the bacterial effector protein repertoire tested associated with yeast cellular membranes (Figure 4D). To confirm these results, all 60 bacterial effector proteins were fused to Green Fluorescent Protein (GFP) and the subcellular distributions were recorded by confocal microscopy (Figure 5A). Twelve effector proteins associated with the plasma membrane (PM), the primary site of Ras signal transduction, while 45 bacterial effector proteins bound to internal sites. These findings are consistent with previous reports showing that Ras* fusion proteins may signal from various subcellular

organelles (J. W. Yu et al., 2004). In total, 57 effector proteins accumulated at a discrete location in yeast, whereas only three were soluble (CegC4, LegL1, and LegLC8) and deemed false-positives (however, it cannot be ruled out that membrane binding of these effector proteins is transient or that their sites of interaction are readily saturated).

Of the 57 bacterial effector proteins identified that accumulated at particulate locations or at the plasma membrane, 17 had been previously shown to localize to a host membrane compartment (Table 2). Importantly, well-known mechanisms of protein and lipid-bilayer interactions could be reconstituted in yeast. These included effectors with transmembrane spanning domains (e.g. Tir^{Ec}, SidF^{Lp}, YlfA^{Lp}, YlfB^{Lp}, and SseGSt), post-translational fatty acid modifications (e.g. SifASt), and peripheral membrane protein interactions (e.g. SseJSt) (Figure 5B-E). In confirmation of these specific mechanisms, point mutations in SifASt that abolished its site of fatty acylation (Boucrot et al., 2003) or in SseJSt that inhibits its known interaction with membrane-bound RhoA GTPase (LaRock, Brzovic, Levin, Blanc, & Miller, 2012) failed to rescue yeast growth in the Ras screen (Figure 5D and 5E). It is also notable that only a small percentage of transformants in the screen were false-negatives. For example, the *Pseudomonas syringae* effectors HopF2 and AvrPto1 are targeted to membranes via N-terminal myristoylation (de Vries et al., 2006; Robert-Seilaniantz et al., 2006). However, the N-terminal Ras* fusion protein likely masked the myristoylation machinery from acylating the bacterial effector protein and, thus, prevented rescue in this assay. Additionally, SseI and SspH2 were previously reported to be palmitoylated within their N-terminus (Hicks, Charron, Hang, & Galan, 2011). Since yeast

encode only two palmitoyltransferases, compared to 23 in humans, I hypothesize that these effector proteins were unmodified in yeast.

Literature inquiries suggested host membrane association can evoke multiple mechanisms of virulence as bacterial effector proteins identified in the Ras-rescue screen displayed a wide variety of enzymatic activities; the positive hits included three lipid phosphatases (SopBSt, IpgD^{Sf}, SidF^{Lp}), three Rho-family GEFs (SopE2St, SifASt, and IpgB1^{Sf}), three actin nucleation factors (VipA^{Lp}, EspF^{Ec}, and EspFu^{Ec}), an E3 ubiquitin ligase (SopASt), a cholesterol esterase (SseJSt), a protein kinase (NleH^{Ec}), a phospholipase (CegC1^{Lp}), and a sphingosine-1 phosphate lyase (LegS2^{Lp}). Besides revealing potentially new modes of enzyme regulation, these data suggest that the evolution of membrane-targeting motifs may drive phenotypic diversity among closely related pathogens. For example, several members of the SopE/WxxxE family of bacterial GEFs interacted with eukaryotic membranes through distinct molecular mechanisms (SopE2St, SifASt, and IpgB1^{Sf}), while other family members did not bind membranes at all, despite sharing a common catalytic core (Figure 6A and 6B). Because these GEFs regulate host GTPases in a variety of cellular contexts (e.g. *E. coli, Salmonella, Shigella* infection), differential membrane binding patterns might contribute significantly to substrate selectivity and the functional discrepancies among these pathogens. However, this hypothesis requires further investigation.

Loss-of-function PI-kinase Screen Identifies Novel Lipid Binding Domains:

Since the molecular mechanisms of bacterial effector protein localization remain to be determined, genetic tractability of yeast was further leveraged to identify specific genes

that are required for host membrane targeting. To this end, I focused on the phosphatidylinositol kinases. These evolutionarily conserved kinases phosphorylate the 3', 4' or 5' positions of phosphatidylinositol, generating a class of negatively charged inositol-containing phospholipids (known as PIPs). Furthermore, PIPs act as site-specific signals on membranes and recruit proteins for the assembly of spatially localized functional complexes (Figure 7A) (Di Paolo & De Camilli, 2006; Strahl & Thorner, 2007). Inactivation of PI-kinase gene expression would, in theory, cause mislocalization of EGFP-tagged bacterial effector proteins that require phospholipid interactions for membrane targeting, providing a visual readout to identify new modes of membrane association (Figure 7B).

The expression of PI-kinase genes was inhibited by either isogenic knockout of the non-essential PI-kinase genes (VPS34, FAB1, LSB6) (Baudin, Ozier-Kalogeropoulos, Denouel, Lacroute, & Cullin, 1993) or by doxycycline-mediated (Dox) repression of $TetO_7$-promoter alleles of essential PI-kinase genes (PIK1, STT4, MSS4) (Mnaimneh et al., 2004). Next, the 57 GFP-tagged bacterial effector genes were transformed into the PI-kinase mutant strains in a one-to-one format, generating a mini-array of 342 potential host-pathogen interactions (Figure 7C). In comparison to the subcellular localization in wild type yeast, 26 bacterial effector proteins were differentially localized when expressed in one or more of the PI-kinase mutant strains. (Figure 7C and 8). In most cases, the bacterial effector proteins did not lose membrane localization per se but redistributed to a new membrane site. For example, *Shigella* IpgB1 relocated from the plasma membrane to internal membrane sites via loss of PIK1, STT4, MSS4, and VPS34, but not LSB6 or FAB1 (Figure 7D). Similar protein redistribution in response to PI-kinase depletion has been observed previously for

endogenous PIP binding proteins, including Osh2, which shuttles between the plasma membrane and Golgi apparatus upon depletion of the PI4-kinases PIK1 and STT4, respectively (Figure 7D) (Roy & Levine, 2004). Similar to the Osh2 control, the changes in subcellular localization of bacterial effector proteins often correlated with the primary site of a PI-kinase function. For example, SopASt and HopS1^{Ps} were redirected from the PM to internal membrane sites by deletion of Mss4, a PI-5 kinase that generates the major PM phospholipid – PI(4,5)P_2 (Figure 7E). Depletion of PI(4,5)P_2 did not simply disrupt membrane integrity, however, since the peripheral localization of several bacterial proteins was unaltered under these conditions (Figure 7E).

To validate the genetic analysis, the 26 full-length Strep-tagged bacterial effector proteins that changed localization in the PI kinase screen were purified from HEK293T cell lysates (via Strep-Tactin affinity chromatography) and overlaid onto nitrocellulose membranes spotted with a variety lipid species. Six of the bacterial effectors bound non-specifically to nitrocellulose. Subsequent transmembrane prediction programs predicted at least one transmembrane spanning domain in each of these proteins, potentially explaining the insolubility of these six proteins. Four other effectors tested showed no interaction with any lipid tested. This observation may indicate that these four proteins interact with host proteins that have direct phospholipid interactions. The remaining sixteen bacterial effector proteins were identified to have direct affinity for anionic phospholipids. (Figure 7C, 9A, and 10A). Interestingly, 12 of the 16 proteins recognized several lipid types, consistent with their sensitivity to loss of multiple PI-kinase genes in yeast. In contrast, four bacterial effector proteins (HopO1-2^{Ps}, SseJSt, SteASt, and PipB2St) exhibited lipid isoform selectivity under

these experimental conditions (Figure 9A and 10A). These findings significantly expand the repertoire of bacterial effector proteins with affinity for host acidic phospholipids (Brombacher et al., 2009; Haneburger & Hilbi, 2013; Salomon et al., 2013).

Neither sequence- nor structural-based bioinformatics revealed canonical lipid-binding domains in the 16 bacterial effectors analyzed (e.g. PH, PHOX, FYVE etc.). However, several possessed non-catalytic domains at the N-terminus enriched in basic and aromatic residues and exhibited isoelectric points greater than 8.5, indicating that they are positively charged at physiological pH (Figure 9B). These properties are often found in domains that bind phospholipids (McLauphlin et al. 2002). Indeed, the N-terminus of 3 candidate effector proteins, IpgB1^{Sf}, SteASt, and SopASt, was sufficient for membrane localization in yeast and mammalian cells (Figure 9C, 10B, and 10C). Closer examination of *Shigella* IpgB1 revealed a cluster of positively charged residues (R25, K27, K30, K31, R41) that when mutated to alanine (A) (herein referred to as IpgB1^{5XA}) attenuated its ability to complement Ras* in cdc25t/s yeast, to localize to the plasma membrane, and to interact with phospholipids arrayed on a solid-phase support (Figure 9C and 9D). These findings are consistent with the necessary region identified for IpgB1 localization through an unknown mechanism (Costa & Lesser, 2014). To then determine if these residues facilitate membrane bilayer interactions, velocity sedimentation assays were performed with liposomes of known phospholipid composition. Only background levels of IpgB1 sediment with vesicles composed of 100% phosphatidyl choline (PC). In contrast, vesicles containing 20% phosphatidic acid (PA) sediment the majority of IpgB1 protein but failed to interact with IpgB1^{5xA} mutant protein (Figure 9E). Although these data suggest that IpgB1 has some

selectivity toward PA *in vitro*, they may more globally indicate that charge-mediated lipid binding interactions direct IpgB1 and potentially other bacterial effectors localization in eukaryotic cells.

Examination of a Specific Case: IpgB1 Lipid Binding Motif is Essential for Shigella Infection.

While having identified a significant number of bacterial effectors that recognize eukaryotic membranes, the overarching goal of this study was to determine how bacterial effector proteins regulate host cellular systems at both spatial and temporal resolution during infection. Unfortunately, the biological functions of a large majority of bacterial effector proteins characterized here have not yet been determined. However, previous studies have shown that IpgB1 induces actin-rich membrane protrusions by catalyzing guanine-nucleotide exchange on Rac1 GTPase (Alto et al., 2006; Z. Huang et al., 2009). This signaling cascade is essential for *Shigella* invasion of non-phagocytic cells (Ohya, Handa, Ogawa, Suzuki, & Sasakawa, 2005a). Thus, a series of bacterial genetic studies were used to determine if the membrane targeting of IpgB1 is necessary for *Shigella* infection. Consistent with previous reports, *Shigella* induced phagocytic cup biogenesis and invaded HeLa cells in an IpgB1-dependent manner (Figure 11A and 11B) (Ohya, Handa, Ogawa, Suzuki, & Sasakawa, 2005b). The phagocytic cup and invasion defects of the parental *ShigellaΔipgB1*strain could be complemented to comparable levels with both plasmid-based IpgB1 and IpgB1^{5xA} but not the catalytically dead IpgB1^{E80A} (Figure 11A and 11B). These findings confirm that the IpgB1^{5xA} mutant is successfully translocated in spite of mutations near the recently identified

chaperone binding domain (Costa & Lesser, 2014). Importantly, the requirement for membrane recruitment of IpgB1 was readily apparent after 5.5 hours of infection. Bacterial loads of *ShigellaΔipgB1*-pIpgB1^{5xA} was decreased by over three orders of magnitude in population studies (Figure 11C), and replicating bacteria were nearly undetectable at the single cell level (Figure 11D). While it is clear that the basic motif in IpgB1 is essential for *Shigella* survival within eukaryotic cells, further determination of the mechanisms deployed is necessary. One possibility is that the IpgB1 basic motif redirects IpgB1 to the pathogenic vacuole, resulting in lipid and protein composition alteration that is conducive for *Shigella* escape. Under this idea, the IpgB1^{5xA} mutant would result in *Shigella* trapped in its vacuole and, as a consequence, destroyed by phagolysosomal fusion. Alternatively, the observation of a decreased bacterial load 5.5 hours after invasion may be due to gentamycin that is internalized during *Shigella* invasion, killing only pathogens retained within a vacuole. New approaches to study these mechanisms must first be developed before these possibilities can be differentiated.

Shigella Engineers an IpgB1-Rac1-Phospholipid Feedback Circuit

Because phospholipids play a critical role in amplifying signal transduction by spatially recruiting multi-protein complexes (Balla, 2005), it was attractive to think that the newly defined phospholipid binding domain of IpgB1 amplifies Rac1 activation at the sites of *Shigella* invasion (Z. Huang et al., 2009; Ohya et al., 2005b). On the basis of previously published studies and from work performed here, a four-step reaction scheme of IpgB1 function is proposed: (1) Entry into cells upon Type III secretion of IpgB1 triggers Rac1

signal transduction (IpgB1→Rac1) (Z. Huang et al., 2009; Ohya et al., 2005b). (2) Rac1 signal transduction induces the accumulation of anionic phospholipids at the plasma membrane (Rac1→phospholipid) (Weernink et al., 2004; Weiner et al., 2002). (3) Additional IpgB1 molecules are recruited to the plasma membrane through acidic phospholipid interactions as found in this study (phospholipid → IpgB1) (Figure 9). (4) Finally, IpgB1 plasma membrane localization is promoted by Rac1-dependent phospholipid accumulation in a positive feedback loop (IpgB1→Rac1→phospholipid→IpgB1) (Figure 12A).

Each step in the reaction scheme was examined using an *in vitro* cell system that reconstituted IpgB1 function. Ectopic expression of EGFP-tagged IpgB1 induced robust Rac1 activation as monitored by the generation of actin-rich membrane ruffles as outlined by the first step in the reaction scheme (IpgB1 → Rac1) (Figure 12B) (Alto et al., 2006). Assays were then conducted to test if IpgB1-mediated activation of Rac1 alters the distribution of phospholipids as proposed in reaction step two (Rac1 → phospholipid). Indeed, ectopic expression of IpgB1 induced the redistribution of binding probes to PA, phosphatidylserine (PS), PI(4)P, and PI(4,5)P_2, to cell surface membrane ruffles (Figure 13A). Next, the question of whether IpgB1 localization is controlled by phospholipids as predicted in step three was tested (phospholipid→IpgB1). Wild-type EGFP-tagged IpgB1 localized within membrane ruffles as well as endocytic vesicles (Figure 12B). This localization pattern was dependent on phospholipid interactions, as the phospholipid-binding mutant, IpgB1^{5xA}, was cytosolic (Figure 12C). Finally, the ability of IpgB1 induced phospholipid accumulation to generate a membrane-assisted autocatalytic feedback loop was examined as proposed in step

4 (IpgB1→Rac1→phospholipid→IpgB1). In contrast to wild-type IpgB1, the catalytically dead IpgB1^{E80A} localized exclusively to trafficking vesicles, allowing this mutant to be used as a reporter of Rac1 activation and subsequent phospholipid accumulation. Indeed, ectopic activation of Rac1 by FLAG-tagged wild-type IpgB1 caused a redistribution of EGFP-IpgB1^{E80A} from intracellular vesicles to actin-rich membrane ruffles at the plasma membrane (compare Figure 12D to 12E). These patterns of localization all suggest that IpgB1 utilizes its GEF activity to drive the accumulation of phospholipids necessary for its membrane localization in a feed-forward mechanism (Figure 12A).

To begin to validate the IpgB1 signaling circuit in context of *Shigella* infection, analogous experiments as those described above were performed, except that delivery of IpgB1 was achieved through *Shigella's* Type III secretion system (Figure 14A). IpgB1 activation of Rac1 was necessary for *Shigella* phagocytic cup formation (Figure 14B and 14D) (Ohya et al., 2005a). Similar to the transfection studies, increased levels of phospholipids (PA, PS, and PI(3,4,5)P_3) were recruited to the site of *Shigella* invasion (Figure 13B). Importantly, this pattern of phospholipid accumulation was unique to *Shigella* infection as compared to other enteric pathogens (Figure 13C). Next, EGFP-tagged IpgB1^{E80A} was used as a biosensor to track endogenously secreted IpgB1 location of activity during *Shigella* infection. As shown in Figure 14B and 14E, EGFP-IpgB1^{E80A} was recruited to the site of *Shigella* invasion. Time-lapse imaging revealed that the biosensor rapidly accumulated in the phagocytic cup and was released from the plasma membrane shortly after bacterial internalization (Figure 14C, arrows). In contrast, *Shigella*Δ*ipgB1* strain failed to recruit EGFP-IpgB1^{E80A} to sites of bacterial attachment, indicating that Rac1 activation is

necessary for biosensor recruitment (Figure 14D). Finally, the phospholipid-binding mutant of the biosensor (GFP-IpgB1$^{E80A\text{-}5xA}$) failed to concentrate in the *Shigella* phagocytic cup (Figure 14E). Taken together, these data support the existence of a phospholipid positive feedback loop that amplifies IpgB1 activation of Rac1 at the sites of *Shigella* invasion (Figure 14F). While additional studies will be needed to further confirm this circuit architecture, the low levels of IpgB1 expressed and secreted by *Shigella* have posed significant technical challenges.

Generating an Experimental Resource for Functional Studies in Mammalian Cells.

Determining if membrane-binding motifs in other bacterial effectors function as higher order regulatory mechanisms similar to IpgB1 is an exciting avenue of research. However, studying the subcellular localization during infection is experimentally challenging due to visual limitations caused by the extremely low levels of each secreted effector molecule. Interestingly, the findings on IpgB1 reported here suggest that ectopic expression can reveal physiological relevant sites of action. Thus, I determined the subcellular localization of the bacterial effectors identified in the Ras-rescue screen in mammalian cells to create an informational platform for future studies. Microscopic analysis of 54 EGFP-tagged bacterial effector proteins (the plant pathogen effectors were omitted from this study) expressed in HeLa cells revealed greater than 85% of bacterial effector proteins associated with membrane compartments (Figure 15). Further co-localization studies revealed binding interactions with the ER, Golgi, endosomes, lysosomes, mitochondria, and plasma membrane (Figure 16A). Additional studies with constitutively active Rab5 (ca-Rab5) allowed for the

identification of bacterial effector proteins that associate with the endocytic trafficking system that were not easily defined by a panel of subcellular markers in HeLa cells (Figure 16B). In many instances, the localization patterns matched previous reports (e.g. LegS2^{Lp} on mitochondria (Degtyar, Zusman, Ehrlich, & Segal, 2009) and SopBSt (Dukes et al., 2006) on the early endosomes). Additional sites of localization for previously characterized bacterial effector proteins were also identified (Figure 16A). However, the localization described here of the majority of bacterial effector proteins has not yet been reported. Notably, these studies provide an experimental resource that can be used to expand the field's understanding of the complex mechanisms by which bacterial effector proteins hijack host cellular signaling networks.

Discussion

Here, I present a systematic analysis of nearly 200 bacterial Type III and Type IV secreted effector protein localization across six pathogens in two model organisms and a general methodology for studying the functional consequence of membrane targeting. By focusing on these host-pathogen interactions, I have identified 60 bacterial effector proteins that target RAS-fusion proteins to yeast cellular membranes, of which 57 can be visualized at subcellular organelles in yeast, 26 are mislocalized by loss of one or more PI-kinase genes, and 16 exhibit affinity for immobilized anionic phospholipids. These findings combined with the evidence suggesting a membrane-assisted autocatalytic feedback system, significantly extend the field's understanding of bacterial secreted effector protein design. That is, I

predict that many bacterial pathogens have integrated three features into bacterial effector protein design. First, these proteins encode a core enzyme domain that inhibits or activates host cellular substrates. Second, they encode secondary interaction motifs that dictate their subcellular location and site of function. Third, they operationally couple these two physical elements (subcellular targeting and enzyme activity) through host reaction products that generate feedback circuits as mechanisms of bacterial signaling specificity and signal amplification in the host cell.

Several lines of evidence presented here support the fundamental nature of these virulence factor design principles. First, nearly 30% of the bacterial effector protein repertoire was found to encode mechanisms of membrane localization (Figure 4). Importantly, this data complement and extend studies on *Pseudomonas syringae*, *Salmonella,* and *Legionella* that focused primarily on post-translational fatty acid modifications (Hicks et al., 2011; Ivanov et al., 2010; Nimchuk et al., 2000), as well as anionic phospholipids (Brombacher et al., 2009; Salomon et al., 2013) as mechanisms of membrane targeting. Thus, the cross-species analysis presented here greatly expands the number of known functional membrane interactions that occur during infection. Additionally, the fact that these mechanisms are physically separate from the core catalytic activity strongly indicates a co-evolutionary process by which effector localization motifs and enzymatic domains are coupled through the natural selection of more robust signaling capabilities. Indeed, by focusing on IpgB1, a series of self-perpetuating molecular events that play a critical role in promoting *Shigella* persistence with host cells have been proposed (Figure 14F). This work found that the membrane binding motif and the GEF domain of IpgB1 coordinate the

activities of the membrane-bound signaling molecule Rac1 GTPase and the negatively charged phospholipids to promote *Shigella* invasion, to amplify virulence factor activity, and to make these events auto-regulated over time (Figure 14F). Taken together, these findings potentially broaden the utilization of autocatalytic feedback mechanisms for amplifying the activities of low abundant virulence proteins.

It is clear, however from this integrated study of protein-lipid interactions that a membrane-centric model can only partially explain the spatiotemporal regulation of virulence factor function, as many bacterial effector proteins do not contain membrane-binding motifs (only 60 out of the 190 effector proteins from the library). However, the in depth study on *Shigella* invasion lends credence to the hypothesis advanced by Orchard et al. (2012) that bacterial effector proteins can engineer positive feedback circuits from multiple host cellular components (Orchard et al., 2012). A theoretical analysis of the Enteropathogenic *E. coli* signaling-network revealed how the Type III effector protein Map (a structural homolog of *Shigella* IpgB1) directly connects Cdc42 GTPase activation to the polymerization of the actin cytoskeleton to amplify signals within spatially defined regions of the host cell. The architectural uniformity of these two higher-order virulence systems (Map and IpgB1) indicates that host-assisted feedback reactions are a generalizable mechanism for microbial signal amplification. As additional information on bacterial enzyme mechanisms become available (less than 15% of the bacterial effector library used in this screen harbor characterized catalytic activities), it will be possible to define the functions and necessity of the plethora of effector-membrane interactions reported here.

Of equal importance, this study also conveys the power of yeast genetics to define novel mechanisms of virulence factor localization in eukaryotic cells. Indeed, this interrogation revealed 16 bacterial effectors from a diverse set of animal and plant pathogens with either stereoselective or charge-mediated recognition of host phospholipids. While this analysis of these membrane-binding domains, so far, indicates that they have no structural or sequence similarity to canonical eukaryotic membrane binding domains, it is intriguing to speculate that these bacterial lipid-binding modules are structural mimics of currently unidentified membrane interacting domains within eukaryotic proteins. These hypotheses are supported by the fact that the presently characterized eukaryotic phospholipid binding domains (e.g. PH, PX, ANTH ENTH) cannot account for all the proteins that require these lipids for localization. Further sequence and fold analysis of these motifs will need to be performed to identify conserved mechanisms among the subset that can then be used to probed eukaryotic genomes for similar motifs. Likewise, the autocatalytic regulatory mechanisms found in this study may also be utilized for eukaryotic protein regulation as well. Future studies on eukaryotic proteins must be performed to know if this is a common method to regulate signaling networks.

In total, these findings provide significant new insights into bacterial effector protein design. The sophisticated mechanisms dynamically linking prokaryotic proteins with eukaryotic membranes also emphasize the intimate evolutionary relationship between host and pathogen. Furthermore, a powerful genetic and biochemical approach to reveal conserved virulence factor features has been developed, which will allow for rapid advances in the field. Lastly, the studies on IpgB1 highlights the physiological importance of these

membrane binding modules, as it was essential for *Shigella* persistence, and, conceivably, offer many new targets for therapeutic intervention against a wide range of microbial infectious diseases.

Figure 1

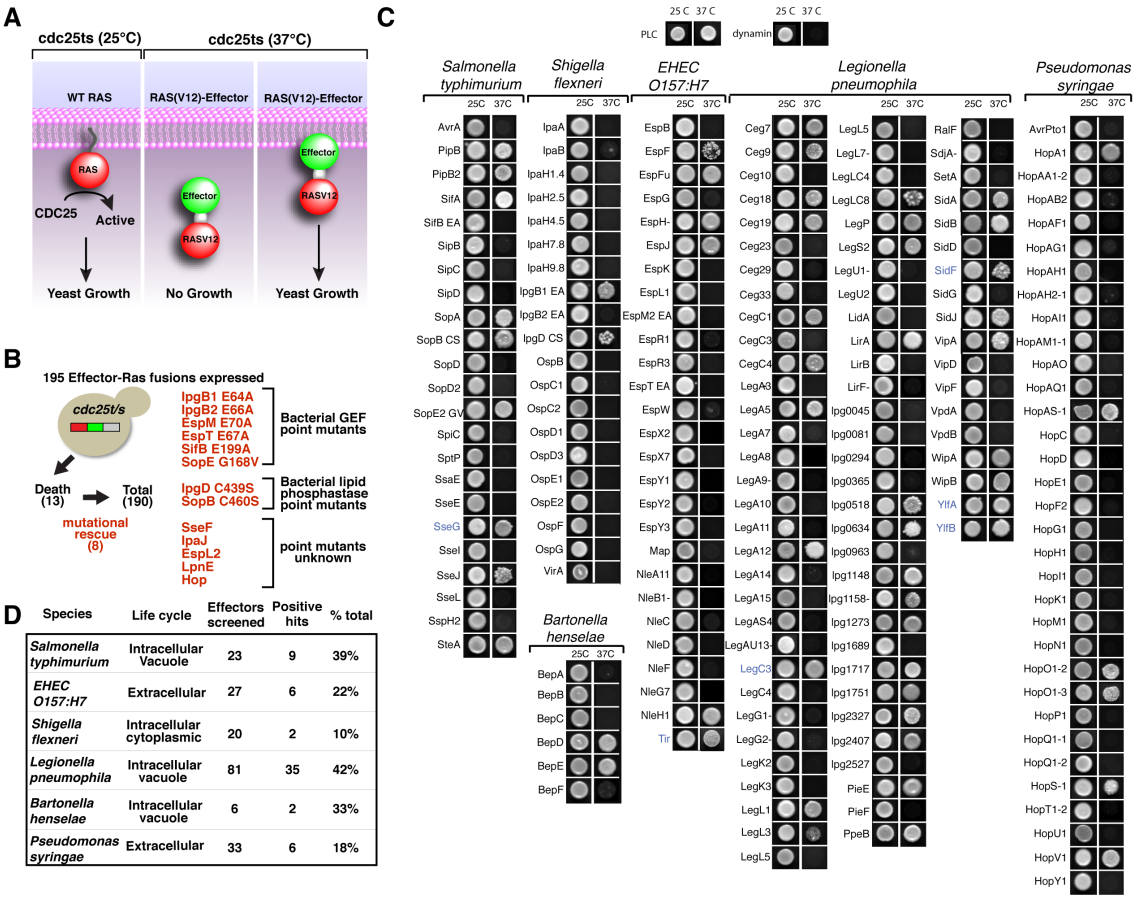

Species	Life cycle	Effectors screened	Positive hits	% total
Salmonella typhimurium	Intracellular Vacuole	23	9	39%
EHEC O157:H7	Extracellular	27	6	22%
Shigella flexneri	Intracellular cytoplasmic	20	2	10%
Legionella pneumophila	Intracellular vacuole	81	35	42%
Bartonella henselae	Intracellular vacuole	6	2	33%
Pseudomonas syringae	Extracellular	33	6	18%

Figure 4: Ras-rescue screen

(A) Schematic diagram of the temperature sensitive Ras-rescue system used to identify membrane-associated effectors in yeast.

(B) Experimental setup for construction of the Ras-effector fusion library and mutants that alleviated yeast growth inhibition. Ras-effector-HA fusion proteins (labeled red-green-grey) were expressed in cdc25t/s and assayed for growth inhibition. Catalytically dead mutations (if known) were made in each effector that caused yeast growth defects, allowing for those effectors to be included in the screen.

(C) Growth assay for the cdc25t/s yeast strain harboring the indicated effector genes grown at the non-restrictive temperature (25° C) or the restrictive temperature (37° C). The yeast proteins PLC (known to bind $PI(4,5)P_2$) and dynamin (known to not localize to yeast membranes) were used as positive and negative controls, respectively. Effectors that allow for yeast growth at the restrictive temperature reconstituted Ras* localization to the membrane.

(D) Table of results summarizing the pathogens studied, number of effectors screened, and percentage of effector repertoire from each pathogen that localized to eukaryotic membranes.

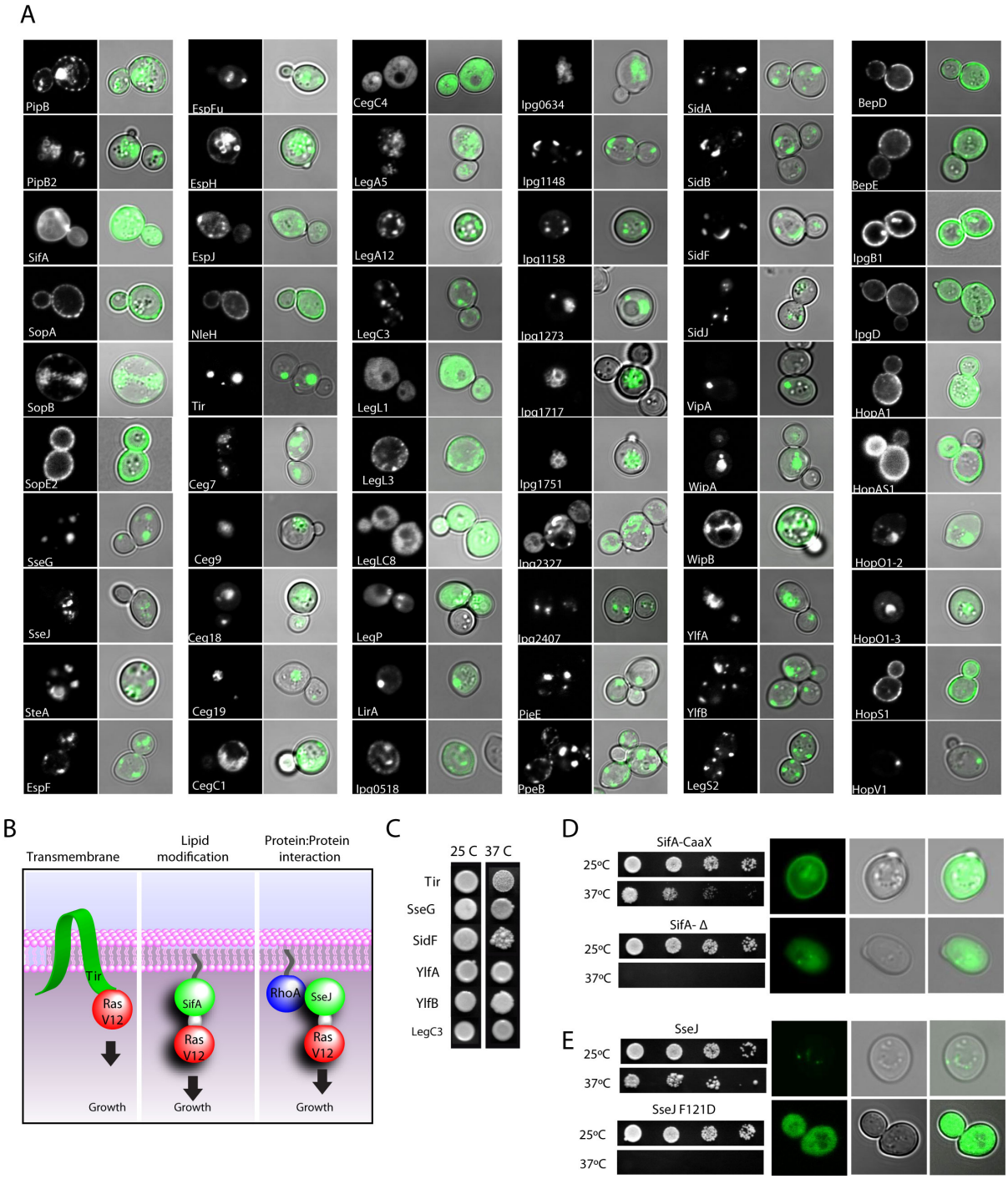
A
PipB
PipB2
SifA
SopA
SopB
SopE2
SseG
SseJ
SteA
EspF
EspFu
EspH
EspJ
NleH
Tir
Ceg7
Ceg9
Ceg18
Ceg19
CegC1
CegC4
LegA5
LegA12
LegC3
LegL1
LegL3
LegLC8
LegP
LirA
Ipg0518
Ipg0634
Ipg1148
Ipg1158
Ipg1273
Ipg1717
Ipg1751
Ipg2327
Ipg2407
PieE
PpeB
SidA
SidB
SidF
SidJ
VipA
WipA
WipB
YlfA
YlfB
LegS2
BepD
BepE
IpgB1
IpgD
HopA1
HopAS1
HopO1-2
HopO1-3
HopS1
HopV1
B
Transmembrane
Lipid modification
Protein:Protein interaction
Tir
Ras V12
Growth
SifA
Ras V12
Growth
RhoA
SseJ
Ras V12
Growth
C
25 C
37 C
Tir
SseG
SidF
YlfA
YlfB
LegC3
D
SifA-CaaX
25°C
37°C
SifA- Δ
25°C
37°C
E
SseJ
25°C
37°C
SseJ F121D
25°C
37°C

Figure 5: Confirmation of the Ras-rescue screen

(A) Fluorescent images of the 60 effectors that rescued in the Ras screen fused to EGFP and transformed into *S. cerevisiae*. For each effector, the GFP channel is shown in white (left) and pseudocolored green (right) overlaid with the brightfield channel.

(B) Cartoon representation of well-characterized effectors with different mechanisms of membrane association, TIR^{Ec} (transmembrane), $SifA^{St}$ (prenylation), and $SseJ^{St}$ (protein:protein) that were capable of growing at the restrictive temperature (37 °C) in the RAS-rescue screen.

(C) Ras-rescue screen results of other effectors known to have transmembrane domains $SseG^{St}$, $SidF^{Lp}$, $YlfA^{Lp}$, $YlfB^{Lp}$, $LegC3^{Lp}$ that were capable of Ras* recruitment to the membrane as shown by growth at the restrictive temperature (37 °C).

(D) Serial dilutions of cdc25t/s yeast expressing Ras fused to wild type SifA (SifA-CaaX) or mutant SifA that is no longer prenylated (SifA-Δ). Fluorescent images of GFP fusions of wild type SifA and GFP-SifA-Δ. Representative images show GFP channel (left), brightfield (middle), and merged image (right) of GFP (pseudocolored green) and brightfield.

(E) Serial dilutions of cdc25t/s yeast expressing Ras-SseJ and Ras-$SseJ^{F121D}$ mutant that cannot interact with membrane localized RhoA and fluorescent images of GFP-fused and GFP-$SseJ^{F121D}$ mutant in *S. cerevisiae* cells. Representative images organized similarly as in panel D.

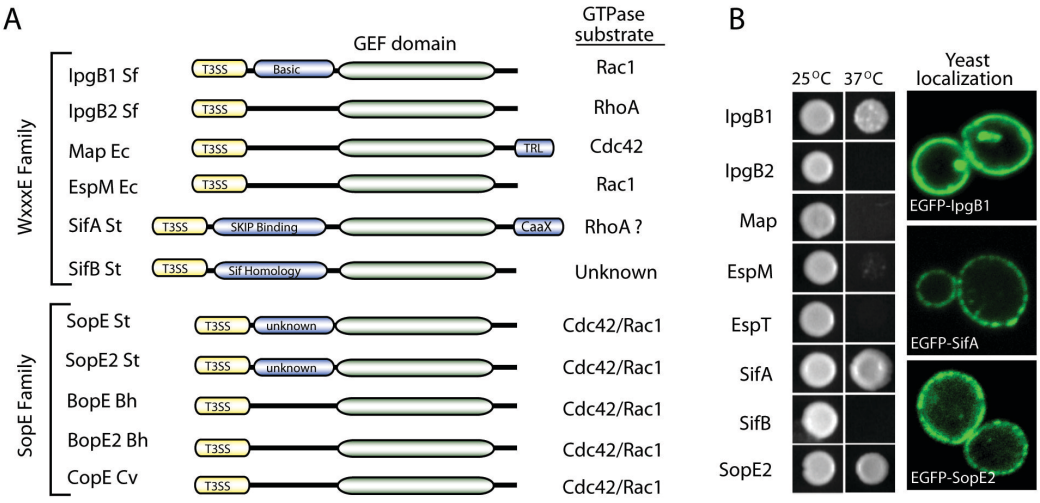

Figure 6: Phenotypic diversity among similar effectors

(A) Domain organization and substrate selection of bacterial GEFs of the WxxxE and SopE family. T3SS: Type III Secretion Signal; TRL: Threonine-Arginine-Leucine PDZ-Ligand; CAAX: lipidation signal.

(B) Ras-rescue screen of bacterial GEFs and fluorescent micrographs of yeast expressing EGFP-tagged IpgB1, SifA, and SopE2 are shown to the right.

Figure 2

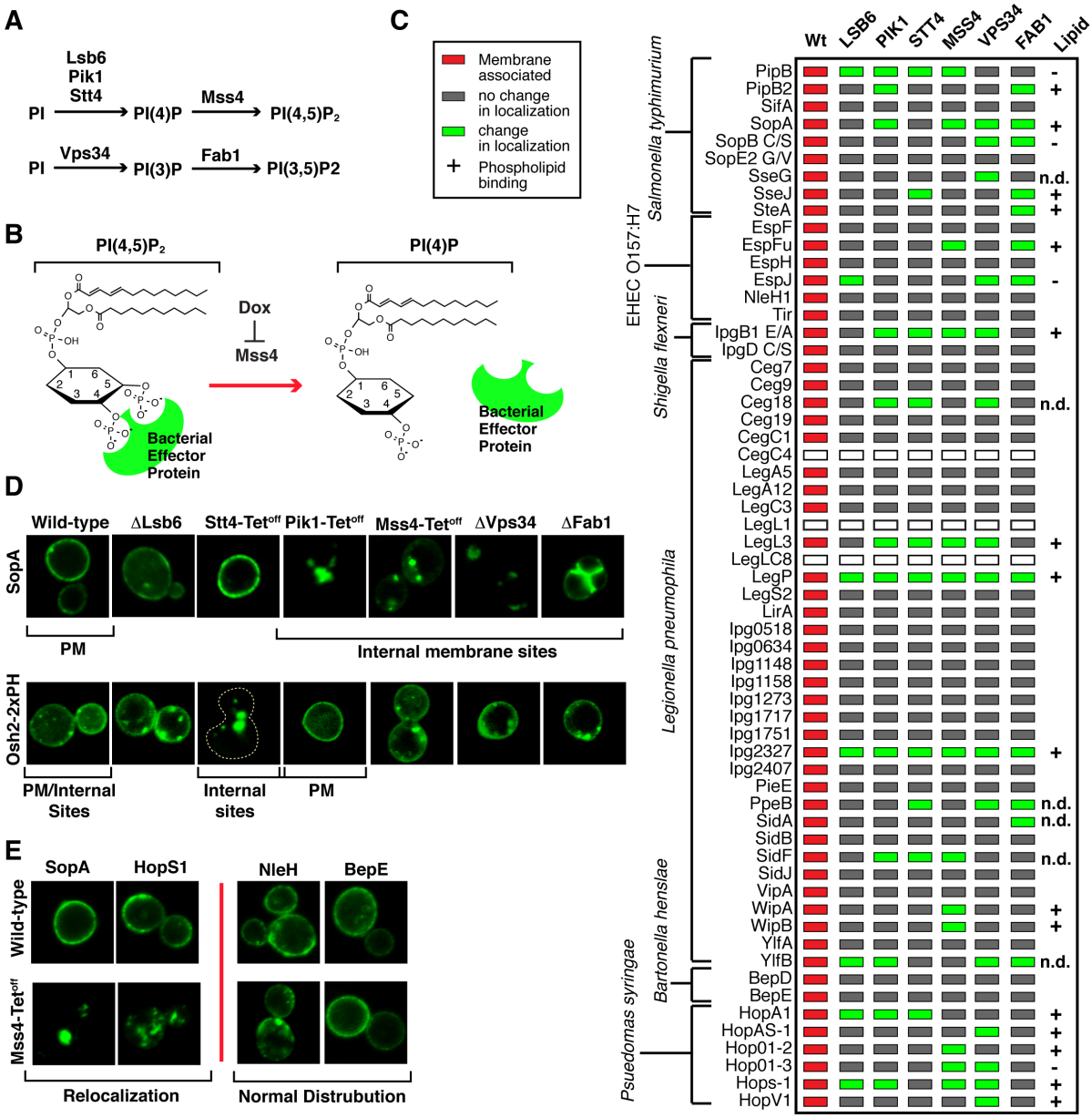

Figure 7: Membrane targeting of the 57 effectors in Yeast Strains with Altered Phosphoinositide levels.

(A) PIP synthesis is regulated by 6 PI kinases in yeast as indicated by the pathways below.

(B) Design of the PI kinase screen as demonstrated with Mss4. Doxycycline repression of Mss4 depletes PI(4,5)P_2, causing loss of localization of effectors that have a membrane localization governed by PI(4,5)P_2.

(C) Graphical representation of all the membrane associated effectors localization upon depletion of each of the six PI kinases compared to localization in wild type yeast.

(D) Fluorescent images of GFP-fused IpgB1^{Sf} in wild type *S. cerevisiae* cells and the six PI kinase yeast strains, as well as fluorescent images of GFP-Osh2 (a known PI4P binding protein) in *S. cerevisiae* (wild type) and the six PI kinase strains.

(E) Representative images of plasma membrane-localized effectors that were redistributed when MSS4 was repressed by the presence of doxycycline (example: SopA and HopAS1) and those that did not redistribute with MSS4 repression (example: NleH and BepE).

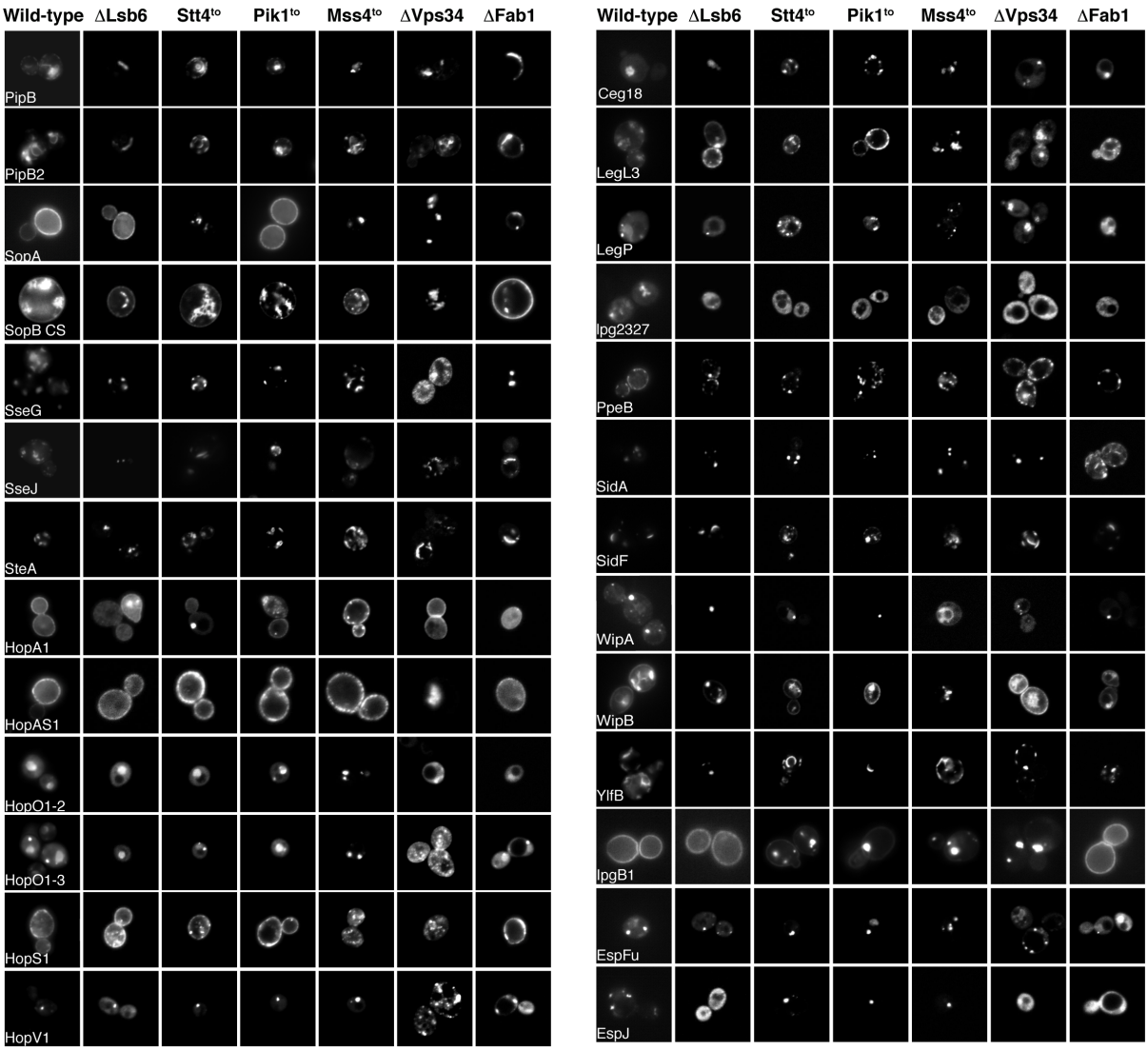

Figure 8: PI kinase screen

Localization of GFP fused effector proteins were examined in the six PI kinase deletion or tet-off (to) strains. All images are representative of at least 75% of expressing cells for each of the 26 effectors that changed localization in one or more PI kinase strains.

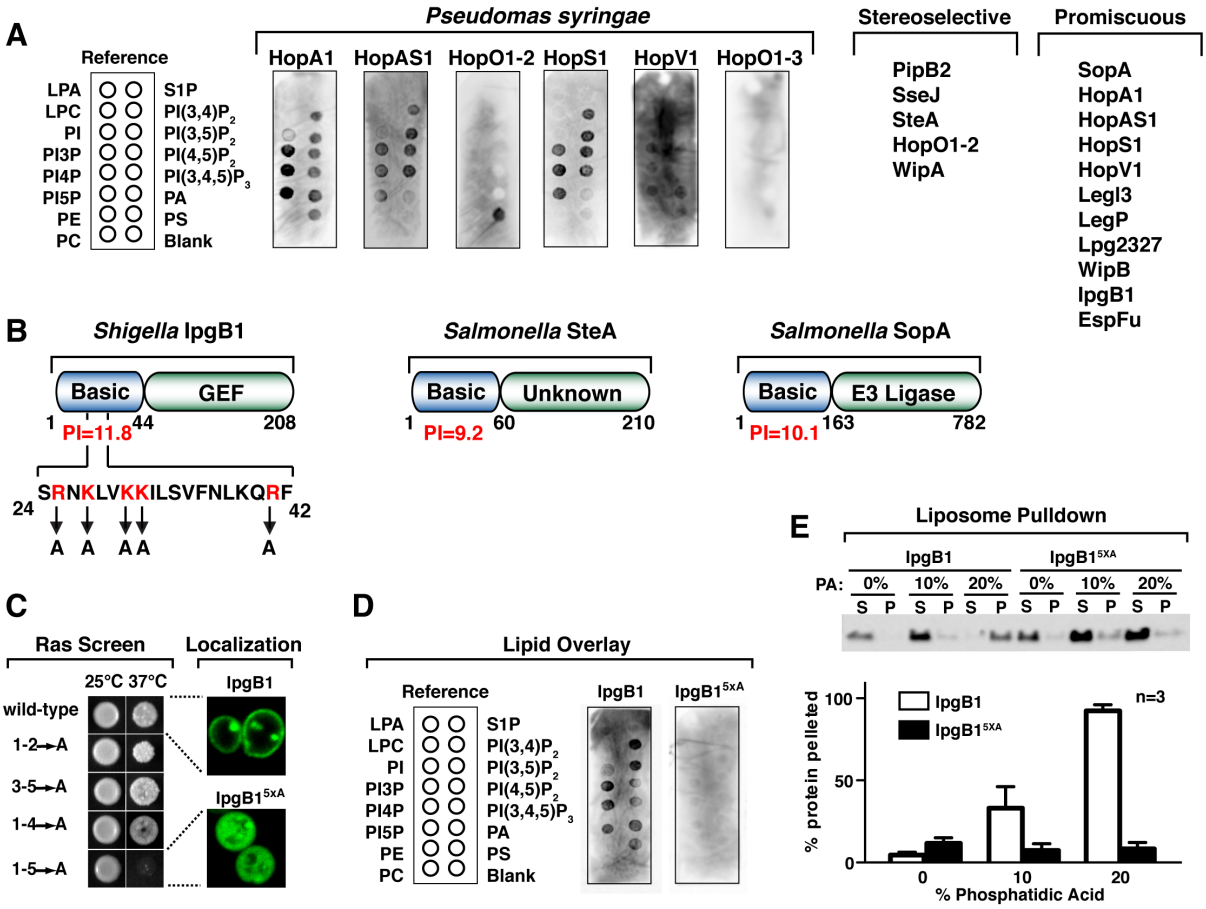

Figure 9: Direct phospholipid interactions of bacterial effectors.
(A) Representative protein-lipid overlay assay of *Pseudomonas syringae* effector proteins.
(B) Domain architecture and pI of the N-terminus of three candidate proteins that changed localization in the PIK screen.
(C) Ras rescue screen results on combinatorial mutations of the five basic residues in the N-terminus (marked in red in panel B) mutated to alanine in IpgB1 (left). Fluorescent images showing the localization of GFP-IpgB1 and GFP-IpgB1^{5xA} (right).
(D) Lipid overlay of wild type IpgB1 and mutant IpgB1^{5xA}.
(E) Vesicle sedimentation studies on IpgB1 and the IpgB1^{5xA} mutant using vesicles that contain 0-20% (mole/mole) phosphatidic acid. Mean ± standard deviation is plotted for three independent experiments.

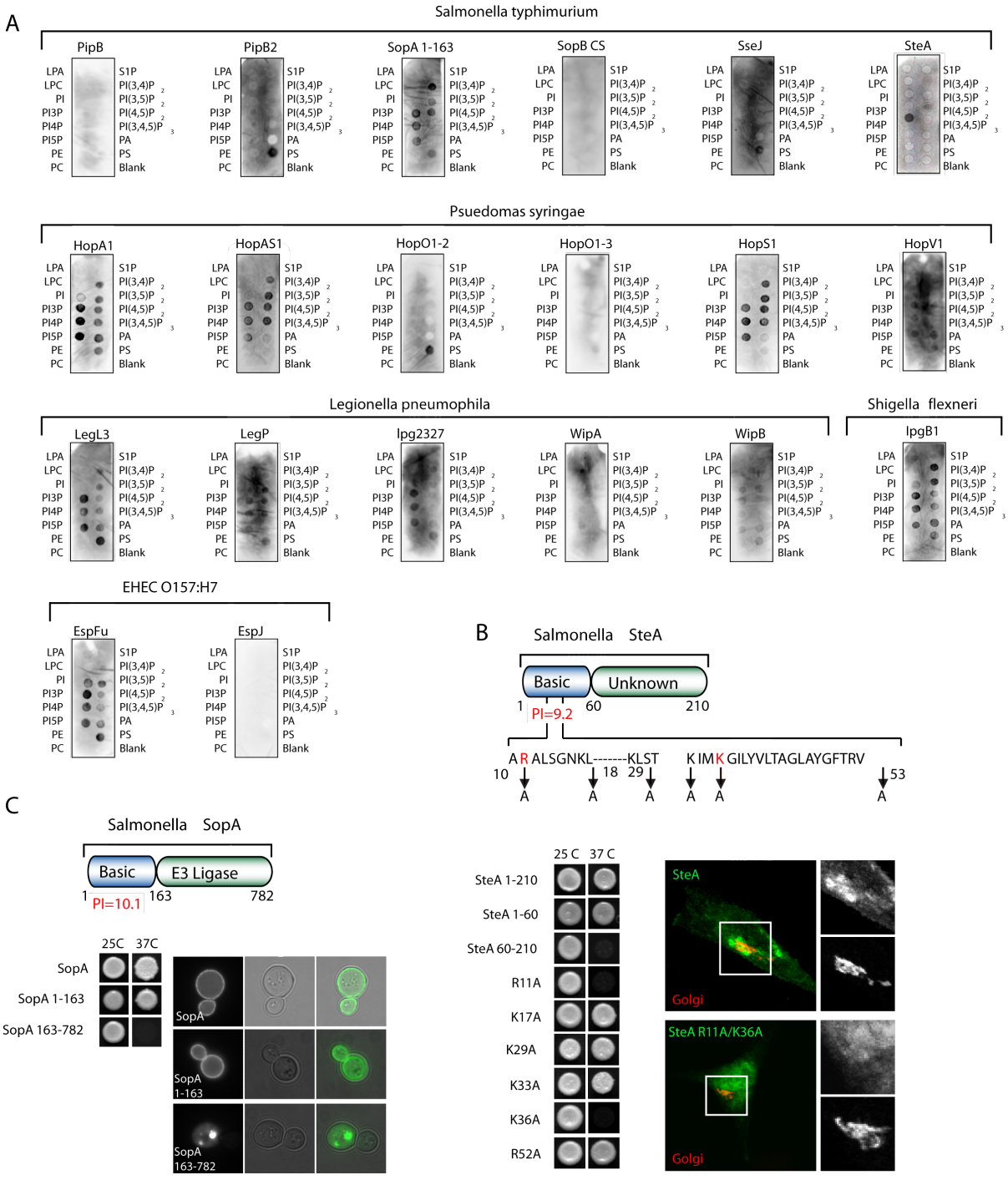

Figure 10: Lipid overlay assays

(A) PIP strips of the twenty effectors that changed localization in the PI kinase screen but were not predicted to have TM domains.

(B) SteA truncations and mutants as listed were fused to the C-terminus of Ras* and assayed for growth at the non-permissible temperature. Fluorescent microscopy of wild type SteA or $SteA^{R11AK36A}$ co-expressed with Golgi apparatus marker in HeLa cells (SteA:green, GM130:red).

(C) Ras-rescue screen using the full-length, N-terminus (1-163), and C-terminus (163-end) of SopA. Fluorescent micrographs of GFP fusions with full-length, N-terminus, and C-terminus of SopA.

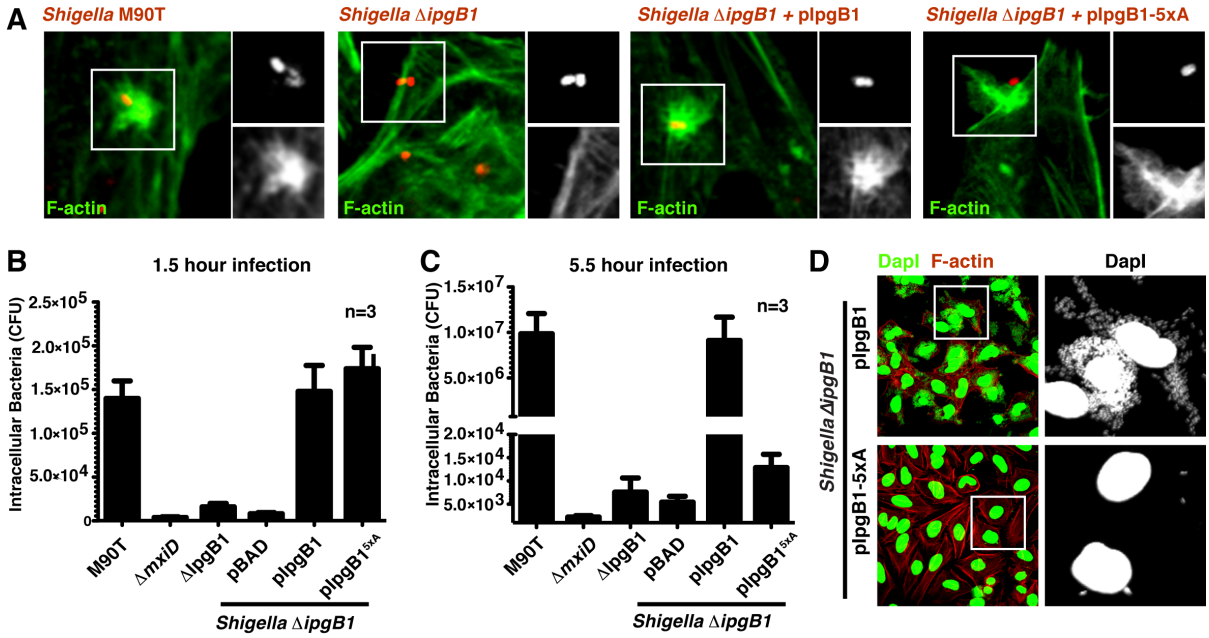

Figure 11: The IpgB1 membrane localization is essential for Shigella pathogenesis
(A) Representative fluorescent micrographs of indicated *Shigella* strains (red) inducing F-actin rearrangements (FITC-phalloidin; green). The boxed region is enlarged 2x and the fluorescence signal from the bacteria (top) and F-actin (bottom) are displayed.
(B-C) Gentamicin protection assay of HeLa cells infected for 1.5 hours (B) or 5.5 hours (C) with the indicated strains (M90T – wild type *Shigella*, mxiD – T3SS deficient, pBAD – empty vector). Intracellular bacteria were enumerated through quantifying the total colony forming units (cfu).
(D) Representative fluorescent micrographs of HeLa cells infected with for 5.5 hours with either S*higella* Δ*ipgB1* complemented with wild-type IpgB1 (top), or IpgB1^{5xA} (bottom). 594-phalloidin was used to label the actin cytoskeleton (red) and DNA was labeled with DAPI (green). The DAPI signal in the boxed region is magnified 4x.

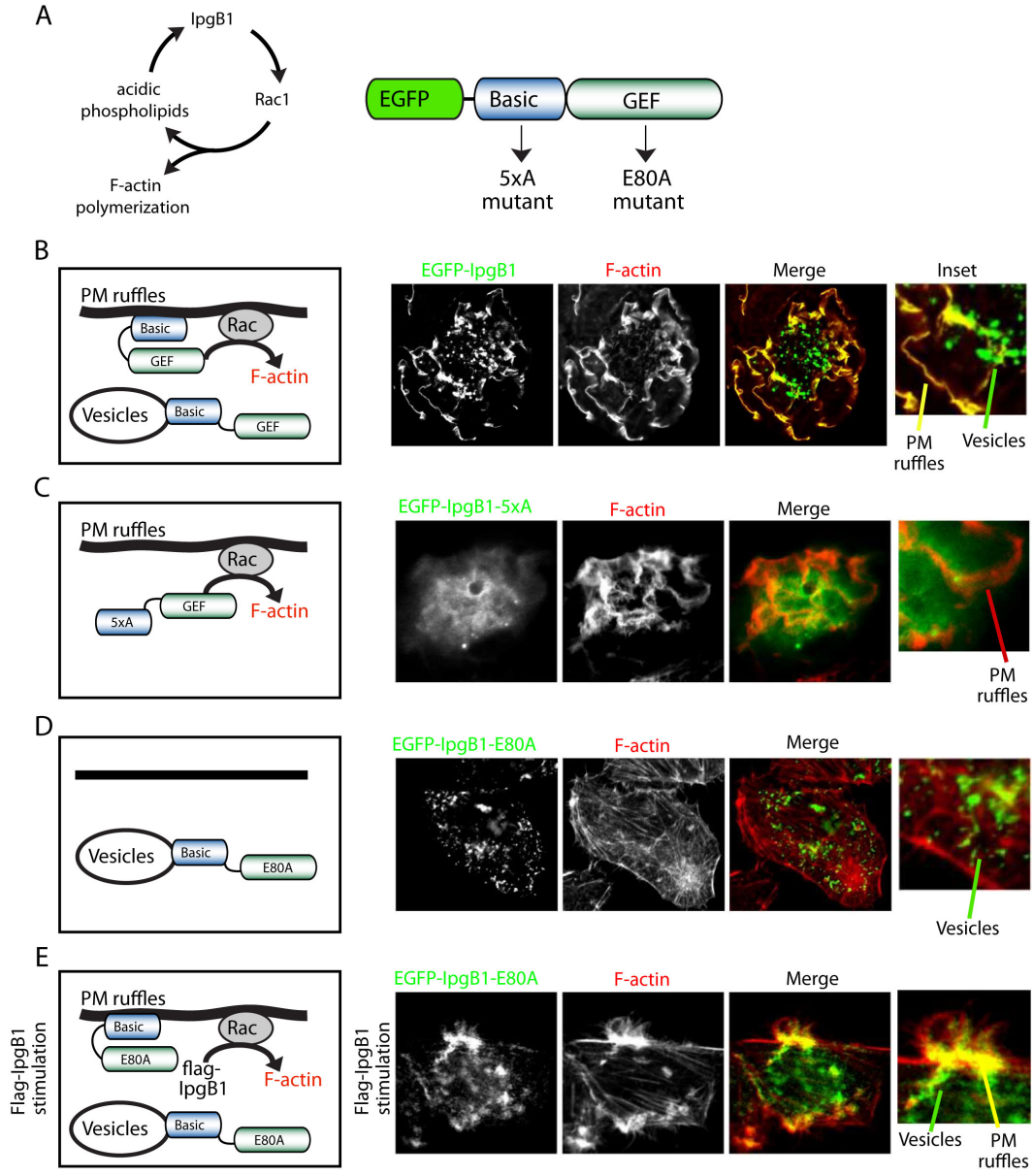

Figure 12: IpgB1 assembles a GTPase-Phospholipid feedback loop
(A) Diagram of the proposed IpgB1 induced GTPase-phospholipid feedback loop.
(B) (Left) Cartoon diagram of the localization of wild-type EGFP- IpgB1transiently transfected in HeLa cells. (Right) Representative fluorescent micrographs of HeLa cells expressing EGFP-IpgB1. The localization of EGFP-IpgB1 (green) the architecture of the actin cytoskeleton (594-Phalloidin, Red) is displayed. The inset is a 2x magnification of the boxed region. IpgB1 localization on the plasma membrane ruffles and on endocytic vesicles are marked.

(C-D) (Left) Cartoon diagram of the localization of EGFP- IpgB1^{5xA} **(C)** and EGFP-IpgB1^{E80A} **(D)**. (Right) Representative fluorescent micrographs of HeLa cells expressing indicated IpgB1 mutants. Data is presented similarly to panel B.

(E) (Left) Cartoon diagram of the localization of EGFP-IpgB1^{E80A} in a Flag-IpgB1 stimulated cell. (Right) Representative fluorescent micrographs of a HeLa cell expressing both Flag-IpgB1 and EGFP-IpgB1^{E80A}. Data is presented similarly to panel B.

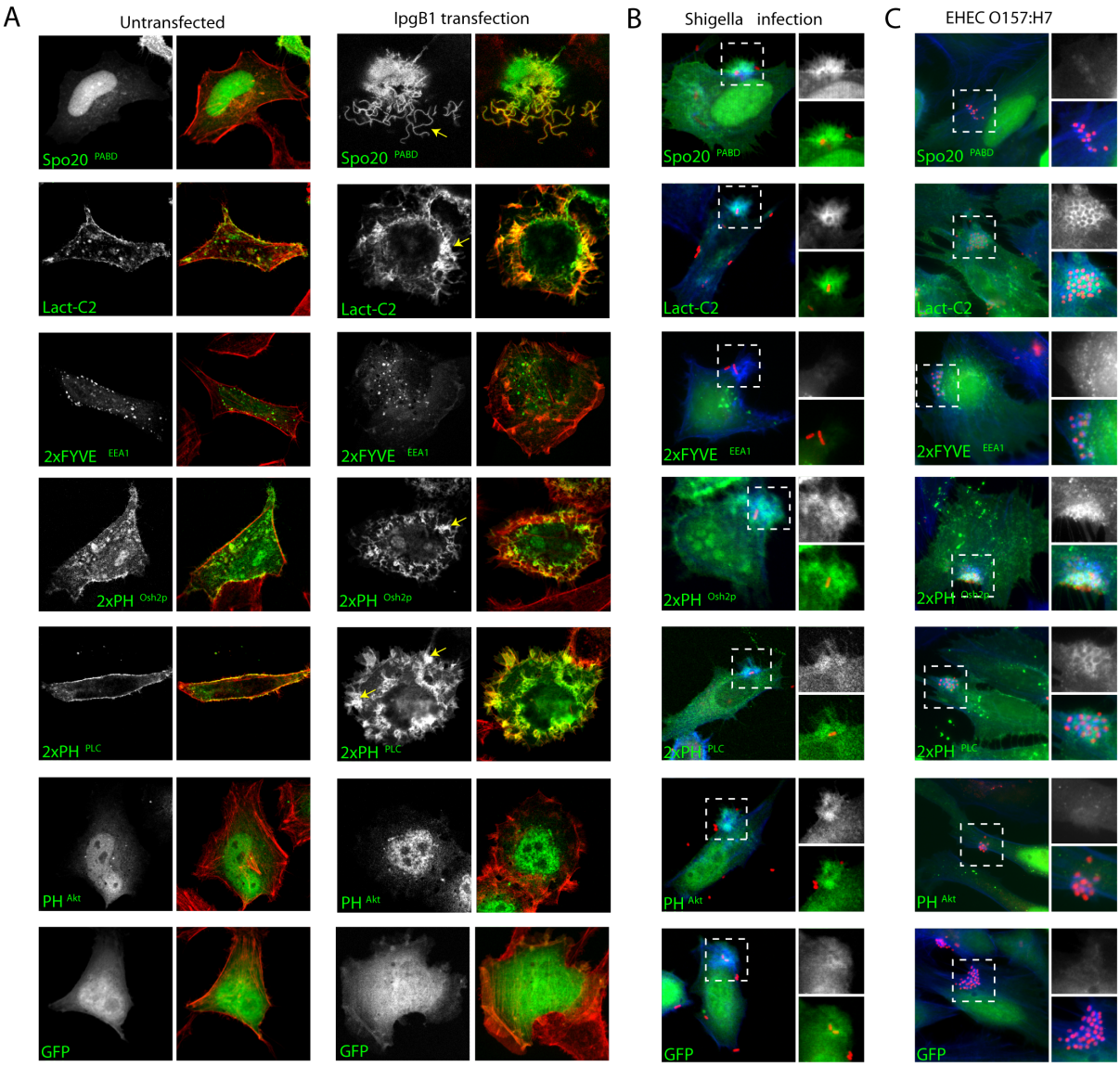

Figure 13: IpgB1 induces a *Shigella* specific phospholipid recruitment profile.
(A) HeLa cells were either transiently transfected with EGFP-tagged lipid binding probes (green) alone (left) or cotransfected with FLAG-IpgB1 (right). The actin cytoskeleton was labeled with 594-phalloidin (red) to depict Rac1-induced F-actin rearrangements. Soluble

GFP was used as a control to determine nonspecific elevation in fluorescence due to an increase in cytosolic volume within the membrane ruffle.
(B) Wild type mCherry-expressing Shigella M90T (red) infecting HeLa cells transiently transfected with indicated EGFP-tagged lipid binding probes (green) or GFP alone as a control. Phagocytic cup formation (F-actin in blue) was monitored similar to Figure 13A. The box region is enlarged 2x showing the EGFP-tagged lipid probe (top) and the bacteria (red) and lipid probe (green) together (bottom).
(C) HeLa cells transiently transfected with the indicated lipid binding probes (green) were infected for 4 hours with mCherry expressing EHEC 0157:H7. F-actin (blue) pedestals were used to identify infected cells. The box region is enlarged 2x showing the EGFP-tagged lipid probe (top) and the full merge are shown as well (bottom).

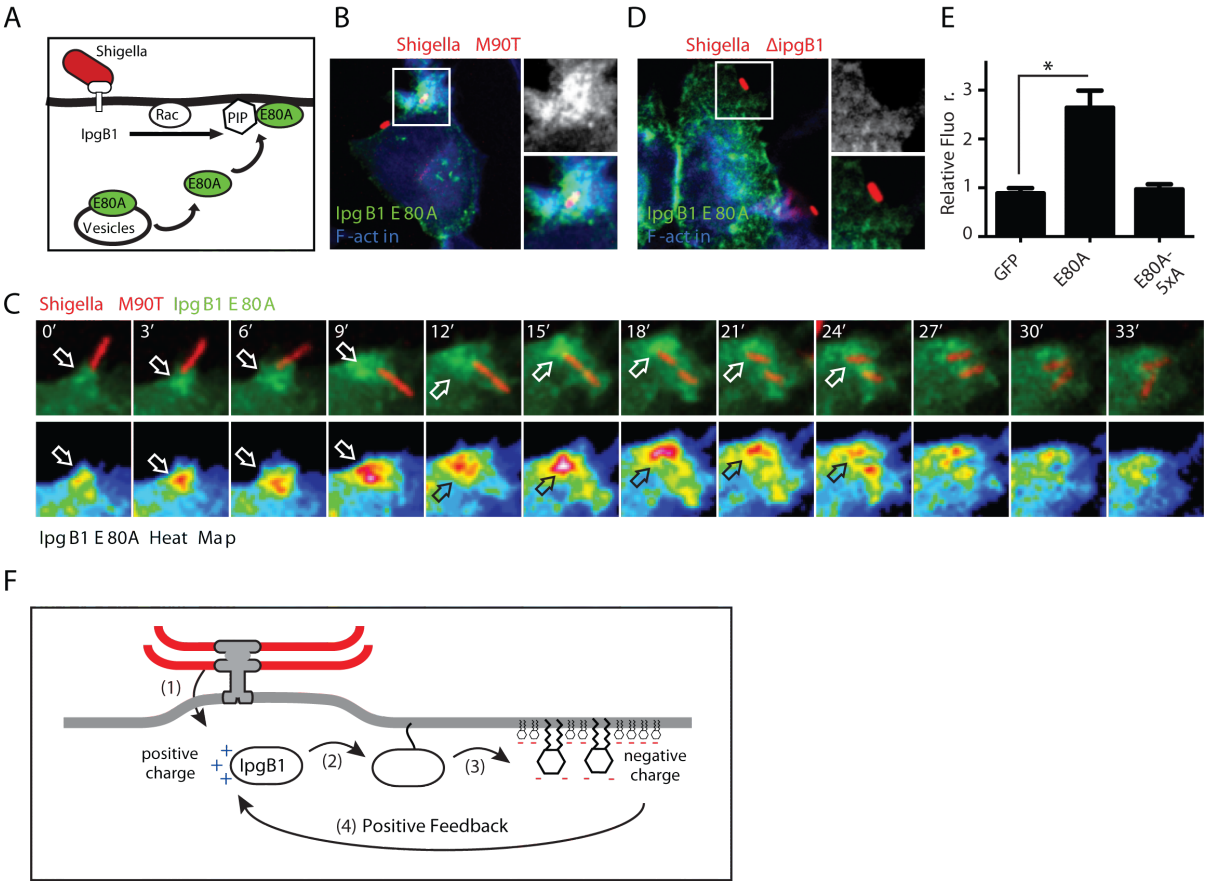

Figure 14: The IpgB1 Signaling Circuit During Infection

(A) Diagram of the strategy to monitor the GTPase-phospholipid feedback loop during *Shigella* infection. mCherry expressing *Shigella* inject IpgB1 into host cells expressing the activity probe EGFP-IpgB1^{E80A}.

(B) Fluorescent micrographs of cells expressing EGFP-IpgB1^{E80A} (green) and infected *Shigella* (red). The actin cytoskeleton (Alexa Fluor 350-Phalloidin; blue) illustrates phagocytic cup formation. The boxed region is magnified two times depicting the EGFP-IpgB1E80A signal (top) and the merged image (bottom).

(C) (Top) Time-lapse fluorescent microscopy of Shigella-mCherry (Red) infecting an EGFP-IpgB1^{E80A} (Green) expressing HeLa cell. (Bottom) Heat map of the pixel intensity of EGFP-IpgB1E80A at the indicated time points.

(D) Fluorescent micrographs of cells infected with *Shigella*Δ IpgB1 mutant strain and labeled as in (B).

(E) Quantification of recruitment of IpgB1 mutants or GFP into the phagocytic cup during *Shigella* infection. Values reported as a fold increase of fluorescent signal in the phagocytic cup over the cytosol. Significance determined by ANOVA.

(F) Diagram of the IpgB1 autocatalytic circuit.

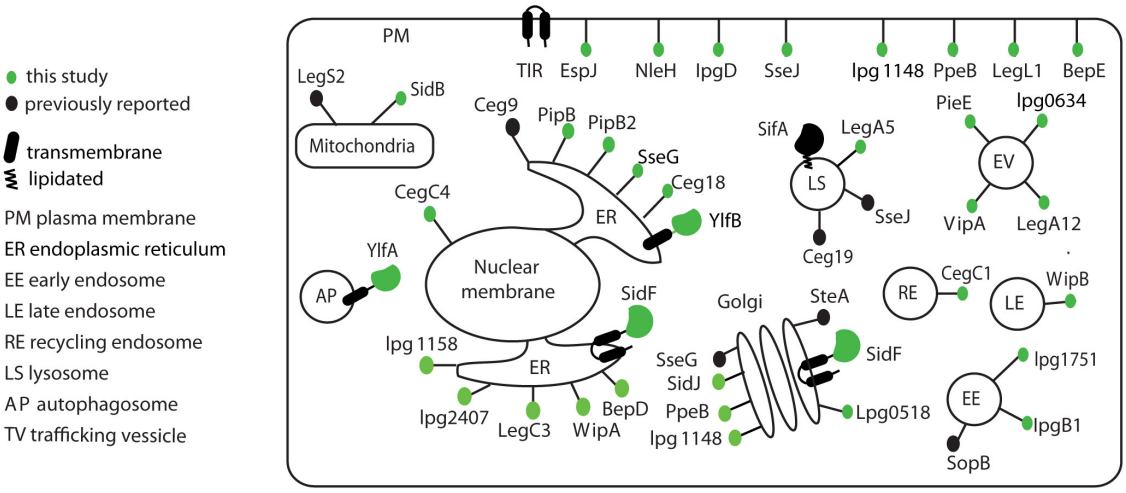

Figure 15: Bacterial effector protein localization and function.
Summary of colocalization studies using EGFP membrane effectors and a series of mCherry fused eukaryotic markers in HeLa cells. See also Figure 16.

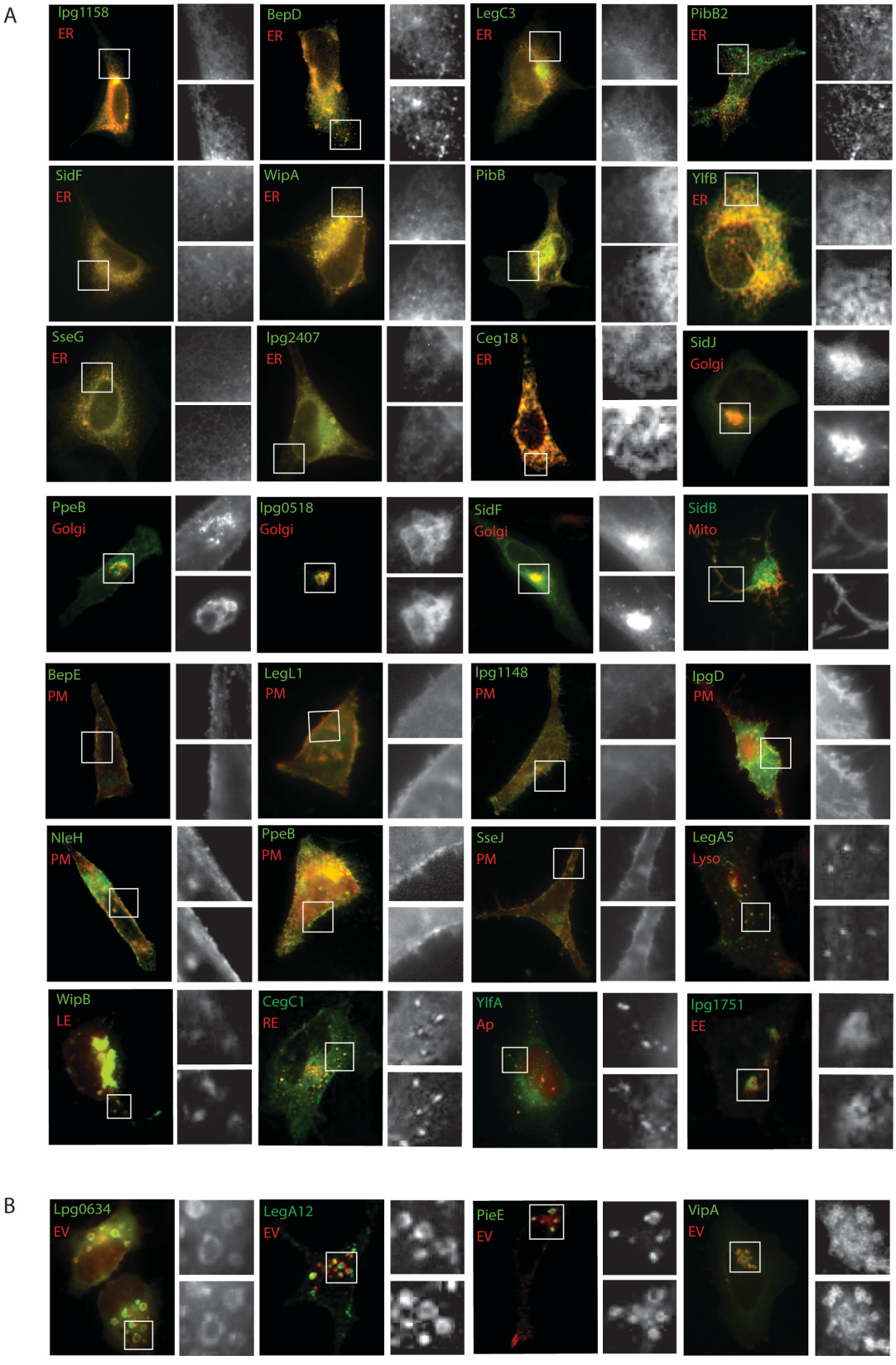
A
Ipg1158
ER
BepD
ER
LegC3
ER
PibB2
ER
SidF
ER
WipA
ER
PibB
YlfB
ER
SseG
ER
Ipg2407
ER
Ceg18
ER
SidJ
Golgi
PpeB
Golgi
Ipg0518
Golgi
SidF
Golgi
SidB
Mito
BepE
PM
LegL1
PM
Ipg1148
PM
IpgD
PM
NleH
PM
PpeB
PM
SseJ
PM
LegA5
Lyso
WipB
LE
CegC1
RE
YlfA
Ap
Ipg1751
EE
B
Lpg0634
EV
LegA12
EV
PieE
EV
VipA
EV

Figure 16: Colocalization studies in mammalian cells

(A) Fluorescent images of colocalization studies with EGFP-effector fusions coexpressed with a panel of mCherry subcellular markers in HeLa cells. Merged images are displayed. The white box indicates the enlarged images with the effector (green) on top and the marker (red) on bottom.

(B) Effectors that did not colocalize with anything in the panel of subcellular markers used were cotransfected with ca-Rab5 that causes the fusion of the endosomal system allowing for potential classification of effector localization to some type of trafficking vesicles (green:effector of interest, red:ca-Rab5).

Effector	Reported membrane localization	Reported mechanism of membrane interaction	Reported function
HopA1		this study	Bhattacharjee et al., 2011
HopAS1		this study	
HopO1-2		this study	
HopO1-3			
HopS1		this study	
HopV1		this study	
PipB	Knodler et al., 2003		
PipB2	Knodler et al., 2003	this study	
SifA	Stein et al., 1996	Boucrot et al., 2003; Reinicke et al., 2005	Ohlson et al., 2008
SopA	Layton et al., 2005	this study	Zhang et al., 2006; Lin et al., 2012
SopB	Dukes et al., 2006		Marcus et al., 2002; Cain et al., 2004
SseG	Salcedo and Holden, 2003	Abrahams et al., 2006	
SseJ	Freeman et al., 2003	this study	Lossi et al., 2008; Christen et al., 2009
SteA	van Engelenburg and Pamer, 2010	this study	
EspF	Marches et al., 2006		Weflen et al., 2010; Alto et al., 2007
EspFu		this study	Campellone et al., 2008
EspH	Tu et al., 2003		Dong et al., 2010; Wong et al., 2012
EspJ	Kurushima et al., 2010		
NleH	Hemrajani et al., 2010		Gao et al., 2009
Tir	Kenny and Finlay, 1997	Luo et al., 2000	Weiss et al., 2009
Ceg7			
Ceg9	Heidtman et al., 2009		
Ceg18	this study	this study	
Ceg19	Heidtman et al., 2009		
CegC1	this study		Aurass et al., 2013
CegC4	this study		
LegA5	this study		
LegA12	this study		

Effector	Reported membrane localization	Reported mechanism of membrane interaction	Reported function
LegC3	de Filipe et al., 2008	de Filipe et al., 2008	Bennett et al., 2013
LegLC8	this study		
LegL1	this study		
LegL3	this study	this study	
LegP		this study	
LegS2	Degtyar et al., 2009		Degtyar et al., 2009
LirA	this study		
lpg0518	this study	this study	
lpg0634	this study		
lpg1148	this study		
lpg1158	this study		
lpg1273	this study		
lpg1717	this study		
lpg1751	this study		
lpg2327	this study	this study	
lpg2407	this study		
PieE	this study		
PpeB	this study	this study	
SidA		this study	
SidB	this study		
SidF	Banga et al., 2007	Hsu et al., 2012	Hsu et al., 2012; Banga et al., 2007
SidJ	this study		Liu and Luo, 2007
VipA	Shohdy et al., 2005		Franco et al., 2012
WipA	this study	this study	
WipB	this study	this study	
YlfA/LegC2	de Filipe et al., 2008	de Filipe et al., 2008	
YlfB/LegC7	de Filipe et al., 2008	de Filipe et al., 2008	
BepD	this study		
BepE	this study		
IpgB1	Ohya et al., 2005	this study	
IpgD	Niebuhr et al., 2002		Niebuhr et al., 2002

Table 2: Membrane localization, enzymatic activity, host substrates of the 60 membrane localized effectors.

Table References:

(Abrahams et al., 2006; Alto et al., 2007; Aurass et al., 2013; Banga et al., 2007; Bennett et al., 2013; Bhattacharjee, Halane, Kim, & Gassmann, 2011; Boucrot et al., 2003; Cain, Hayward, & Koronakis, 2004; Campellone et al., 2008; Christen et al., 2009; de Felipe et al., 2008; Degtyar et al., 2009; Dong et al., 2010; Dukes et al., 2006; Franco, Shohdy, & Shuman, 2012; Freeman, Ohl, & Miller, 2003; Gao et al., 2009; Heidtman et al., 2009; Hemrajani et al., 2010; Hsu et al., 2012; Kenny & Finlay, 1997; Knodler et al., 2003; Kurushima, Nagai, Nagamatsu, & Abe, 2010; Layton, Brown, & Galyov, 2005; Lin, Diao, & Chen, 2012; Liu & Luo, 2007; Lossi, Rolhion, Magee, Boyle, & Holden, 2008; Luo et al., 2000; Marches et al., 2006; Marcus et al., 2002; Niebuhr et al., 2002; Ohlson et al., 2008; Ohya et al., 2005b; Reinicke et al., 2005; Salcedo & Holden, 2003; Shohdy et al., 2005; Stein, Leung, Zwick, Garcia-del Portillo, & Finlay, 1996; Tu, Nisan, Yona, Hanski, & Rosenshine, 2003; Van Engelenburg & Palmer, 2010; Weflen, Alto, Viswanathan, & Hecht, 2010; Weiss et al., 2009; Wong, Raymond, Collins, Crepin, & Frankel, 2012; Zhang, Higashide, McCormick, Chen, & Zhou, 2006)

Materials and Methods

Molecular Biology

Full-length effectors were PCR amplified from genomic DNA from *Pseudomonas syringae pathovar tomato* and *Legionella pneumophila Philadelphia-1* ATCC, *Salmonella typhimurium* LT2, EHEC H7:O157, and *Shigella flexneri* M90T. The *Bartonella henselae Houston-1* clones were a gift from Rosa de Leo. All effector genes were inserted into TOPO-D pENTR vector (Invitrogen) with manufacturers instructions. pENTR clones were verified by DNA sequencing. Stop codons were introduced into bacterial effector proteins that displayed potential prenylation sites or PDZ-ligand sequences at the COOH-terminus. Effector proteins were cloned into various gateway adaptable vectors using manufacture's protocol for the Gateway system (Invitrogen) unless otherwise mentioned. The Ras rescue plasmid p3S0BL2 was a kind gift of Mark Lemmon (University of Pennsylvania) (Isakoff et al., 1998). To facilitate the rapid transfer of bacterial effector genes into this plasmid, we inserted a Gateway expression cassette (Invitrogen) in between Ras and the HA tag. The resulting plasmid is named pRRD for plasmid Ras Rescue DEST. The entire pENTR effector library was then recombined into the pRRD vector using LR Clonase II (Invitrogen) following manufacturer's instructions. To monitor the subcellular localization of membrane localized effectors in yeast, the p413Gal vector was modified to contain the open reading fame of EGFP with a gateway expression cassette at its 3' end. The sixty effector positive in the Ras Rescue screen were then gateway cloned similarly as with the pRRD vector. For effectors purified with a Strep-tag, effectors were first gateway cloned into pCDNA3.1 GFP–

Strep-tag destination vector. Additionally, IpgB1 and its derivatives were subcloned into pcDNA 3.1 epitope tagged vectors (GFP/mCherry/FLAG) vectors. Site-directed mutagenesis was carried out using the QuickChange Site-Directed Mutagenesis kit (Stratagene). All constructs were verified by DNA sequencing.

Yeast based assays

The following yeast strains were used: INV*Sc*1 **(***MATa his3D1 leu2 trp1-289 ura3-52)* (Invitrogen), the yeast knock-out strains ΔVPS34, ΔFAB1, and ΔLSB6 strains with genetic background BY4741 (MATa his3Δ1 leu2Δ0 met15Δ0 ura3Δ0), and the tetracycline-off strains MSS4, STT4 and PIK1 strains in the genetic background of R1158 (URA::CMV-tTA MATa his3-1 leu2-0 met15-0)(Hughes Tet collection Thermo scientific). The *cdc25ts* yeast strain 352-15A2 (*MATa, ade5, cdc25-2, his7, met10, trp1, ura3-52*) was received from Mark Lemmon, which contains a temperature sensitive allele of *CDC25* (Aronheim *et al*., 1997). BY4742 (MATα ; his3Δ 1 leu2Δ 0 lys2Δ 0 ura3Δ 0) was a gift from Joel Goodman.

A standard lithium acetate protocol (Gietz, Schiestl, Willems, & Woods, 1995) was used for transformation in all the strains except for CDC25ts, which we used a modified LiAc protocol (Isakoff et al., 1998). Briefly, a 5 mL overnight culture of *cdc25ts* yeast, grown at 25°C, was diluted to 50 mL YPDA medium (Clontech) and shaken at 25°C for four hours. Cells were pelleted at 2,000 g for 5 minutes in a room temperature centrifuge and then washed once with 50 mL TE. Cells were repelleted and then resuspended in 100mM LiAc (2 mL). The LiAc: yeast suspension was incubated for 10 minutes at 25°C. Next, 5 µL of carrier DNA (Clontech), 50 µL of LiAc:yeast suspension, and 350 µL of 40% PEG

solution in 100mM LiAc was added to each tube containing the miniprepped DNA. After mixing gently with a pipette, yeast were incubated for 30 minutes at 25°C and then heat shocked at 42°C for 15 minutes. Cells were pelleted, washed with TE (1 mL), plated on glucose plates lacking leucine, and allowed to grow for four days at 25°C. To assay for rescue of the *cdc25ts* allele, transformants were resuspended in media lacking leucine and spotted in duplicate onto a plate grown at 25°C and another grown at the selective temperature, 37°C. Viability was scored between three to ten days after growth as described previously (Isakoff et al., 1998).

Yeast lysis for expression assays were performed as described previously (Salomon & Sessa, 2010). Briefly, 2 mL overnights were pelleted and resuspended in yeast lysis buffer (4% v/v NaOH, 0.5% v/v BME), vortexed for 1 minute, and incubated on ice for 30 minutes. SDS page buffer was added in a 1:1 ratio and samples were boiled at 80°C for 5 minutes. The insoluble fraction was pelleted and the soluble fraction was run on a 10% acrylamide gel and transferred onto nitrocellulose. The membrane was then blocked with 3% skim milk in TBS + 0.1% tween (TBST) for one hour and probed with rabbit anti-Ras (Cell Signaling Technology) or mouse anti-HA (Cell Signaling Technology) at 1:1000 overnight at 4°C. Appropriate HRP conjugated secondary antibodies (Thermo Scientific) were incubated with the membrane for 30 minutes at room temperature. Membranes were developed with Supersignal Fempto Chemiluminescent Substrate (Thermo Scientific)

After two days, transformants were grown overnight in galactose media lacking histidine and visualized on a LSM 510 PASCAL scanning confocal microscope (Zeiss, Thornwood, NY, USA). For the tetracycline-off strains, transformants were grown overnight

in glucose media lacking histidine with the appropriate amount of doxycycline (optimized with the yeast protein Osh2) for repression (50 μg/μL doxycycline for PIK1 and STT4 and 300 μg/μL doxycycline for MSS4). The next day, cultures were pelleted, washed with TE, and grown for another 24 hours in galactose media lacking histidine with the same concentrations of doxycycline. On the third day, yeast were visualized on a LSM 510 PASCAL scanning confocal microscope (Zeiss, Thornwood, NY, USA).

Mammalian cell studies

HeLa and Hek293T cells were maintained in Dulbecco's modified eagle medium containing 10% (v/v) FBS, 2 mM glutamine, and 100 μg/ml penicillin/streptomycin (Thermo Scientific, Waltham, MA, USA) at 37°C in a 5% CO_2 incubator. HeLa cells were seeded onto glass coverslips overnight and transfected at 60-80% confluency with 1.5 μg of DNA using Fugene6 (Roche). After 16 to 18 hours, cells were fixed in 3.7% formaldehyde and visualized on a LSM 510 PASCAL scanning confocal microscope (Zeiss, Thornwood, NY, USA). Colocalization studies were performed with a wide array of transfectable markers including the lipid binding domains of Spo20p (A.A. 51-91), Osh2p (2 tandem copies of the PH domain A.A. 260-421; cDNA kindly provided by Scott Emr), Akt (one PH domain A.A. 1-107; cDNA kindly provided by Michael White), were subcloned into pcDNA 3.1-GFP as has been described previously (Franke, Kaplan, Cantley, & Toker, 1997; Nakanishi, de los Santos, & Neiman, 2004; Stefan et al., 2011). Full length Rac1, Rab5a, and Rab5a^{Q79L} Rab7, and Rab14 was subcloned into pcDNA 3.1-GFP and pcDNA 3.1-mCherry. pEGFP 2xFYVE^{EEA1} and pEGFP 2xPH^{PLC} plasmids have been previously described (Gillooly et al.,

2000; Stauffer, Ahn, & Meyer, 1998). pEGFP Lact-C2 (Addgene plasmid 22852), pmRFP-LC3 (Addgene plasmid 21075), and pEGFP-LAMP1 were kindly provided by Dr. Sergio Grinstein (University of Toronto) and Dr. Paul Luzio (University of Cambridge), respectively. Detection of endocytic membrane microdomains was accomplished using antibodies for Caveolin (BD Biosciences; 1:500 dilution), APPL1 (Cell Signaling; 1:100 dilution), EEA1 (BD Biosciences, 1:500 dilution), and Dynamin (provided by Sandra Schmid; 1:500 dilution).

Recombinant Proteins

For proteins produced with *in vitro* transcription and translation (TNT), 1 μg of effector in pCDNA3.1 GFP destination vector and 40 μCu of S^{35}[Met] was used following manufacturer's protocol (Promega). Expression was verified by autoradiography. For Strep-tag purification of proteins, 10 cm dishes of HEK293T cells were transfected with 10 μg of plasmid DNA using calcium phosphate. After 24 to 48 hours, cells were washed once with cold PBS and lysed in Mammalian Lysis Buffer (0.5% Triton, 4 mM $MgCl_2$ in 10 mM Tris pH 7.5). Strep-tagged effector proteins were purified through affinity chromatography by incubating Strep-Tactin beads (iBA) at 4ºC. Beads were washed three times before the protein was eluted in Strep-tag elution buffer (iBA). Western blots with HRP-conjugated anti-Strep (iBA) confirmed expression.

Lipid interactions

Bacterial effectors proteins expressing a GFP–Strep affinity tag were expressed in mammalian HEK293T cells and purified by Strep-Tactin agarose chromatography. PIP strips (Invitrogen) were blocked in 3% fatty acid free (faf) BSA in TBST for one hour shaking at room temperature. The effector protein of interest was diluted in 750 µL of TBST + 3% fatty acid free BSA and incubated with the PIP strip for 3 hours. The membrane was washed 4 times with TBST + 3% faf-BSA and then incubated with HRP-conjugated anti-Strep (1:5000) for 45 minutes and washed before chemiluminescent detection. Protein lipid interactions were detected by autoradiography or by western blot (HRP-anti-Strep; IBA).

For liposomes pull-down assays, lipids were first purchased in powder form from Avanti Polar Lipids. Liposomes were created by combining PC (75 mol%), NBD-PC (10%), PA (0-20 mol%), and PIPS (20 mol%). Total lipid (1 mM) was solubilized in chloroform, dried under an anhydrous nitrogen stream and immediately suspended in 300mM sucrose. The liposomes (0.1 mM final) were then incubated with Strep-tag purified effector protein (1 µg) in cytosol buffer (25mM HEPES pH 7.2, 25mM KCl, 2.5mM $Mg(C_2H_3O_2)_2$, and 150mM $C_5H_8KNO_4$) for fifteen minutes at 37°C. Samples were subjected to centrifugation at 100,000g in a Beckman TLA55 rotor and a Beckman Ultima MAX TL ultracentrifuge at 12°C for 10 minutes. Supernatant and pellet were isolated, analyzed by SDS-PAGE. Protein was detected by western blot.

Shigella strains and infections

The *ipgB1* and *mxiD* genes were individually disrupted using the λ red recombinase mediated recombination system (Datsenko & Wanner, 2000). Briefly, the PCR primers

IpgB1 5’ (TGAACTAACATATAGGGGGTATCATGCAAATTCTAAACAAAATACTTCCACAGG TGTAGGCTGGAGCTGCTTC) and IpgB1 3’ (AAGATTTAATATAAAAGATTTAATTTG TATTGCTTTGACGGTATACAGCCATATGAATATCCTCCTTAG for *ipgB1* and MxiD 5’ (ATGAAAAAATTTAATATTAAATCTTTGACTCTCTTGATTGTATTGTTACCCAGCC ATATGAATATCCTCCTTAG) and MxiD 3’ (GAAGCAGCTCCAGCCTACACCTACTTTGCT GGAAGACGAAAAATCATTGGTTTCATACTTAAATTACTAA) for *mxiD* were used to amplify the kanamycin resistance marker from the plasmid pKD4. PCR products were electroporated into *Shigella flexneri* strain M90T carrying the red recombinase plasmid pKD46. Transformants were selected by growth on LB agar plates containing kanamycin (50 μg/ml) and simultaneously cured of pKD46 by growth at 42ºC overnight. The kanamycin resistance gene was eliminated through the introduction of the pCP20 helper plasmid, which contains the FLP recombinase. Subsequent curing of pCP20 was carried out by growing strains at 42ºC for 5 hours. Disruption of the *ipgB1* and m*xiD* genes was confirmed through DNA sequencing of the respective genetic loci. Plasmid complementation of ΔIpgB1 strains was achieved by subcloning *ipgB1* into the multiple cloning site of pBadMycHisA (Invitrogen).

For infection of HeLa cells, overnight cultures of *Shigella,* grown in brain heart infusion (BHI) broth at 37°C, were diluted 1:50 in BHI and incubated for 2.5 hours at 37°C.

Next, 500 µl of bacterial culture was collected, washed, and suspended in 1 ml of PBS + 0.003 % Congo red (Sigma). After a 15 minute static incubation at 37°C, *Shigella* (MOI of 10) were added to HeLa cells. Infection was initiated by centrifugation at 1,000 *g* for 10 minutes at room temperature. For imaging the phagocytic cup, cells were fixed and processed for fluorescence microscopy at 35 minutes post-infection. To enumerate bacterial invasion, 90 minutes post infection cells were extensively washed in PBS supplemented with gentamicin (100 µg/ml) and lysed in PBS plus 0.5% Triton X-100. Cellular lysates were diluted to determine colony-forming units (cfu). For *Shigella* persistence assays, cells were initially infected for 90 minutes and washed in a PBS solution containing gentamicin to kill all extracellular bacteria. Fresh media without gentamycin was then added and the infection allowed to proceed for an additional 4 hours to allow bacterial replication. Cells were then lysed to determine bacterial burden (cfu) or fixed and stained for fluorescence microscopy. To quantify the recruitment of lipid binding probes into the *Shigella* phagocytic cup, the mean fluorescence intensity per area of the phagocytic cup, as defined by F-actin ruffles, was calculated using the software ImageJ. Values were normalized by dividing by the total fluorescence intensity per area of the infected cell.

CHAPTER THREE
Development of Screening Techniques to Study Bacterial Effectors that Alter Host Endomembrane Traffic

Introduction

Protein and lipid trafficking are two of the most tightly regulated processes in cell biology. In fact, eukaryotes have established elaborate organelle systems and vesicle transport mechanisms to properly distribute molecules to defined regions in both space and time. The importance of these trafficking systems is reflected in the fact that numerous diseases (such as Danan disease, Tay-Sachs, and Alzheimer's) are caused by mutations that affect protein traffic (Saftig & Klumperman, 2009; Suzuki, Araki, Yamamoto, & Nakaya, 2006). However, studying the molecular basis of disease progression, particularly the transition from a normal to a diseased state, is extremely challenging because diagnosis usually occurs after the disease has already been established. The trafficking of the endolysosomal system can be hijacked by various pathogens through the use of their Type III or Type IV secretion systems. Since disease caused by pathogens can be observed in real time, the characterization of bacterial effectors that alter endomembrane trafficking could be used as a model for studying defects in mammalian cargo transport.

Recently, Rivera et al. established a human growth hormone delivery system utilizing a conditional aggregation domain (CAD) for patients with a human growth deficiency (V. M. Rivera et al., 2000). The CAD is a reversible oligomerization domain that was engineered by ARIAD pharmaceutical based on the rapamycin sensitive FKBP dimerization system (Amara

et al., 1997). When expressed in cells and targeted to the lumen of the endoplasmic reticulum (ER), several CADs interact with each other and form stable protein aggregates that are too large to exit the compartment. Thus, the ER functions as a storage depot for synthetic probes but does not block the trafficking of endogenous proteins (Figure 17A). Addition of AP21998, a cell-permeable chemical ligand dissociates the aggregates in minutes, permitting the proteins to be released from the ER and to enter the secretory pathway. Once hGH enters the Golgi apparatus, the resident enzyme, furin, cleaves off the CADs at an encoded furin cleavage site (FCS). Mature full length hGH then traffics through the exocytic pathway and is released into the extracellular space in a dose-dependent manner (Figure 17A). While this technology was originally developed as a hormone delivery system to treat disease, I thought it could be adapted to study various properties of Type III and Type IV effectors and their interactions with the eukaryotic membrane trafficking systems.

Many pathogens rewire the host endomembrane system through the use of their effector proteins. Unfortunately, the effectors that conduct these changes are largely unknown. Thus, an hGH secretion assay was established to identify bacterial effector proteins that shut down the general secretory pathway (GSP; Figure 17A). Second, a set of probes was developed to study trafficking defects in different arms of the endomembrane system. These probes can be utilized to study trafficking events in real time. As a proof in principle, this technology was applied to identify the point of traffic arrest for the bacterial effectors identified in the hGH screen. Lastly, the CAD was utilized to further understand effector molecules that traffic to multiple points in the endomembrane system. These findings demonstrate a novel strategy through the use of CADs to identify and characterize

bacterial effectors that alter host endomembrane trafficking and to study diseases caused by trafficking defects in humans.

Results

Human Growth Hormone Secretion assay

To establish an experimental assay for global secretory pathway inhibition, cell lines that were amenable to retaining hGH-CAD protein in the ER until the chemical ligand was added were first identified. To this end, HeLa and 293A cells were seeded onto 6 well dishes and transfected with the hGH-CAD construct. The next day, AP21998 (2 mM) was added to the medium the supernatant was collected two hours post drug addition, and extracellular hGH concentrations were monitored via ELISA. As shown in Figure 17B, HeLa cells were capable of retaining hGH-CAD within the ER until released by AP21998, while 293A cells did not show a significant difference in hGH secretion with or without the addition of drug. Therefore, all experiments mentioned hereafter were performed in HeLa cells. Drugs known to inhibit the GSP, such as the potent Arf inhibitor, brefeldin A, and the microtubule destabilizing agent, nocodazole, were used as controls to demonstrate that inhibition of various components necessary for the GSP resulted in low hGH levels secreted into the media (Figure 17C) (Chardin & McCormick, 1999; De Clerck & De Brabander, 1977).

Next, thirty-seven Type III and Type IV effectors were screened for the ability to inhibit global host endomembrane trafficking events. Each of the effectors was cotransfected into HeLa cells with the hGH-CAD construct. The following day, AP21998 (2 mM) was

added to the media for two hours, and the supernatant was subsequently collected to quantify the amount of hGH released with an ELISA. These endeavors identified three effectors, EspG from EHEC and VirA and IpaJ from *Shigella flexneri,* which potently blocked hGH secretion into the extracellular space (Figure 17D).

Construction of a Chemically Regulated Endocytic Trafficking Assay

While this assay was easily utilized to identify effectors with global endomembrane trafficking phenotypes, the precise stage at which the traffic is delayed is unknown. To study this phenomenon, the CAD aggregation system was further adapted to pinpoint the location of inhibition of the global secretory pathway for EspG, VirA, and IpaJ. Representative host proteins for major organelles were selected as probes to study effector mediated endomembrane traffic disruption. This included lysosomal associated membrane protein (LAMP1), a lysosomal acid hydrolase (cathepsin F), the early endosomal mannose-6-phosphate receptor (M6PR), and the Golgi-resident geranylgeranyltransferase, (1,4-GGTase) (Figure 18A). These proteins of interest were fused to GFP and CAD in the proper orientation so that the CAD domain was in the lumen of the ER (Figure 18A). Fluorescent microscopy showed that all four probes were retained in the ER before the addition of the drug (Figure 18B). Upon addition of AP21998, each protein marker was found to arrive at its final destination as shown with colocalization markers (Figure 18B). By monitoring diverse trafficking probes, the role of bacterial pathogen insult on the host membrane trafficking system can be precisely defined. For example, *Salmonella* persists within a vacuole that is positive for LAMP1. As the infection progresses, the effector SifA causes the vacuolar

membrane to produce long tubule structures called *Salmonella*-induced filaments (Sifs; Figure 18C). As a functional readout of these probes, *Salmonella* was incubated with HeLa cells expressing either GFP-LAMP1 or GFP-LAMP1-CAD. After addition of drug, LAMP1-CAD was seen in the *Salmonella* induced filaments, similar to GFP-LAMP1, indicating that this CAD-protein construct traffics normally in the context of *Salmonella* infection (Figure 18C).

These probes were then utilized to determine the point at which EspG, VirA, and IpaJ shutdown the global secretory pathway. To this end, cells were co-transfected with the Golgi-CAD marker and each of the three bacterial effectors. In the case of IpaJ, it was readily apparent that the Golgi-CAD marker was never released from the ER after addition of drug. These findings were similar to cells treated with brefeldin A (Figure 19A and 19B). In the presence of EspG and VirA, the Golgi-CAD marker was released from the ER, but this probe localized to punctae and not to the compact Golgi ribbon as it did in control cells. These findings indicate that EspG and VirA do not block ER exit. (Figure 19C and 19D). Prior to cargo reaching the Golgi apparatus, proteins transgress the ER and the ER to Golgi intermediate compartment (ERGIC). Using an ERGIC specific antibody (p58), it was determined that EspG caused Golgi-resident lumenal enzymes and membrane proteins to be sequestered in the ERGIC (Figure 19C). In contrast, VirA clearly disrupted the ERGIC structure, and Golgi proteins were found in punctae adjacent to the ERGIC (Figure 19D). Importantly, the CAD probes successfully allowed for the determination of subtle differences between these three effectors. This study demonstrates a new system to study endomembrane defects that is applicable to many different pressing questions in the field.

Having determined the different sites of action for these three effectors that disrupt the GSP, bioinformatic analyses were performed to gain potential insight on their enzymatic functions. PSI-BLAST showed that EspG and VirA were sequence homologs of each other but not of any other proteins, resulting in no functional clues. Furthermore, the crystal structure of VirA demonstrated a novel fold unlike any other protein in the database (Davis et al., 2008). Through yeast two hybrid and biochemical studies, Andrey Selyunin in the lab further characterized EspG to bind preferentially to GTP-bound Arf6 (a small GTPase that regulates endomembrane traffic) and locks it in its active state (Selyunin et al., 2011). Mutational analysis demonstrated that residues essential for Arf6 interaction were essential for the down-regulation of hGH secretion (Figure 19E). Furthermore, VirA and EspG were later described by Dong et al. to both have Rab1 GAP activity (Dong et al., 2012). Because the Arf and Rab family of GTPases are master regulators of endomembrane trafficking in eukaryotes, these data fully explain the observation of these effectors' potent inhibition of the general secretory pathway (Hall, 1998; Nobes & Hall, 1995).

Bioinformatic analysis of IpaJ showed homology at the primary sequence level with five other effector proteins – none of which had been characterized. Secondary structure prediction programs, however, classified IpaJ in the C39-like protease family, an enzyme family that shares a conserved catalytic cysteine residue. With over one hundred members and very low sequence homology among the group, only one absolutely conserved cysteine was present. Additionally, a conserved histidine and aspartic acid were also found in IpaJ, completing the catalytic triad necessary for this family's enzymatic activity (Figure 19F). Nikolay Burnaevskiy in the lab further characterized IpaJ as a cysteine protease that cleaves

the N-terminal myristoylated glycine off of Arf1, thereby preventing its localization to the Golgi membrane and its ability to regulate ER to Golgi traffic (Burnaevskiy et al., 2013).

Time-Lapse Studies of Effector Trafficking Using CADs

The dynamics of localization of bacterial effector proteins has not been explored. For example, during the visual screening of GFP-tagged effectors that localize to eukaryotic membranes, I noticed the *Salmonella*-secreted effector SseG was localized to both the ER and the Golgi (see Figure 16A). SseG has been implicated in tethering the *Salmonella* Containing Vacuole (SCV) to the Golgi, since knock out strains have an SCV that moves throughout the cytoplasm (Ramsden, Mota, Munter, Shorte, & Holden, 2007; Salcedo & Holden, 2003). No reports, however, had previously shown SseG localizing to the ER. Since SseG is a transmembrane protein (Abrahams et al., 2006), this raised the question of whether this protein needs the eukaryotic transmembrane insertion machinery (located at the ER and at other organellar surfaces) for proper membrane integration. Alternatively, this protein could be trafficked between the two sites and have an additional function at the ER. To differentiate between these two possibilities, SseG-GFP was fused to the CAD and expressed in HeLa cells. Before addition of the drug, SseG was present in large aggregates of protein (Figure 20A). Two hours after drug exposure, the bacterial effector protein was present at both the ER and Golgi, demonstrating that the fusion of the CAD to SseG did not affect its localization (Figure 20A). Next, the release of SseG-CAD was observed in real time. SseG localized to the ER twelve minutes post drug addition and was not present at the Golgi until 45 minutes after the drug was added (Figure 20B). While further interrogation is required to

understand the purpose of SseG at the endoplasmic reticulum, this tool will allow for the study of virulence factor dynamics in space and time.

Discussion

These studies identified sensitive points in the endomembrane trafficking system that are highly susceptible to pathogenic insult. Interestingly, EspG, VirA, and IpaJ all caused a shutdown of the host exocytic pathway. At first glance, this phenotype seemed as if it would be deleterious to a pathogen, as it would render nutrient delivery to the bacteria at a stand still. However, the pathogens that encode EspG, VirA, and IpaJ do not need normal trafficking pathways to acquire nutrients, since EHEC persists extracellularly and *Shigella* breaks out of its endocytic vacuole minutes after invasion to persist within the cytosol (High, Mounier, Prevost, & Sansonetti, 1992; Marches et al., 2008). These findings do not address the question: What advantage does the exocytic trafficking shutdown give to the microbe? One possibility is that the shutdown of the GSP could serve to prevent antigen presentation on the surface of the cell and, thus, cripple the infected cell's ability to communicate with immunogenic cells. Indeed, several *Salmonella* effectors, when ectopically expressed in tissue culture, prevented MHC presentation of microbial peptides (Halici, Zenk, Jantsch, & Hensel, 2008). More work with infection models will be necessary to fully determine the consequence of these effectors' actions in terms of virulence.

While EspG, VirA, and IpaJ were found to abrogate the GSP, there are likely other effectors from pathogens that persist in a vacuole that block specific arms of the

endomembrane system. For example, intravacuolar pathogens are presented with an antimicrobial challenge of lysosomes routinely fusing with incoming phagosomes. *Salmonella* and *Legionella,* however, orchestrate cell signaling programs aimed at hijacking the endolysosomal trafficking environment of its host. While it is known that co-opting the membrane trafficking network requires fully functional secretion systems for both of these pathogens, the effectors responsible are largely unknown. This small-molecule-regulated probe set can be used to understand the effectors responsible for the spatial and temporal alterations of the endolysosomal system. Additionally, Type III and Type IV secreted effectors, once mechanistically understood, can be used as tools to probe the mechanisms of endomembrane disease onset, development, and progression in a tractable experimental model (Saftig & Klumperman, 2009).

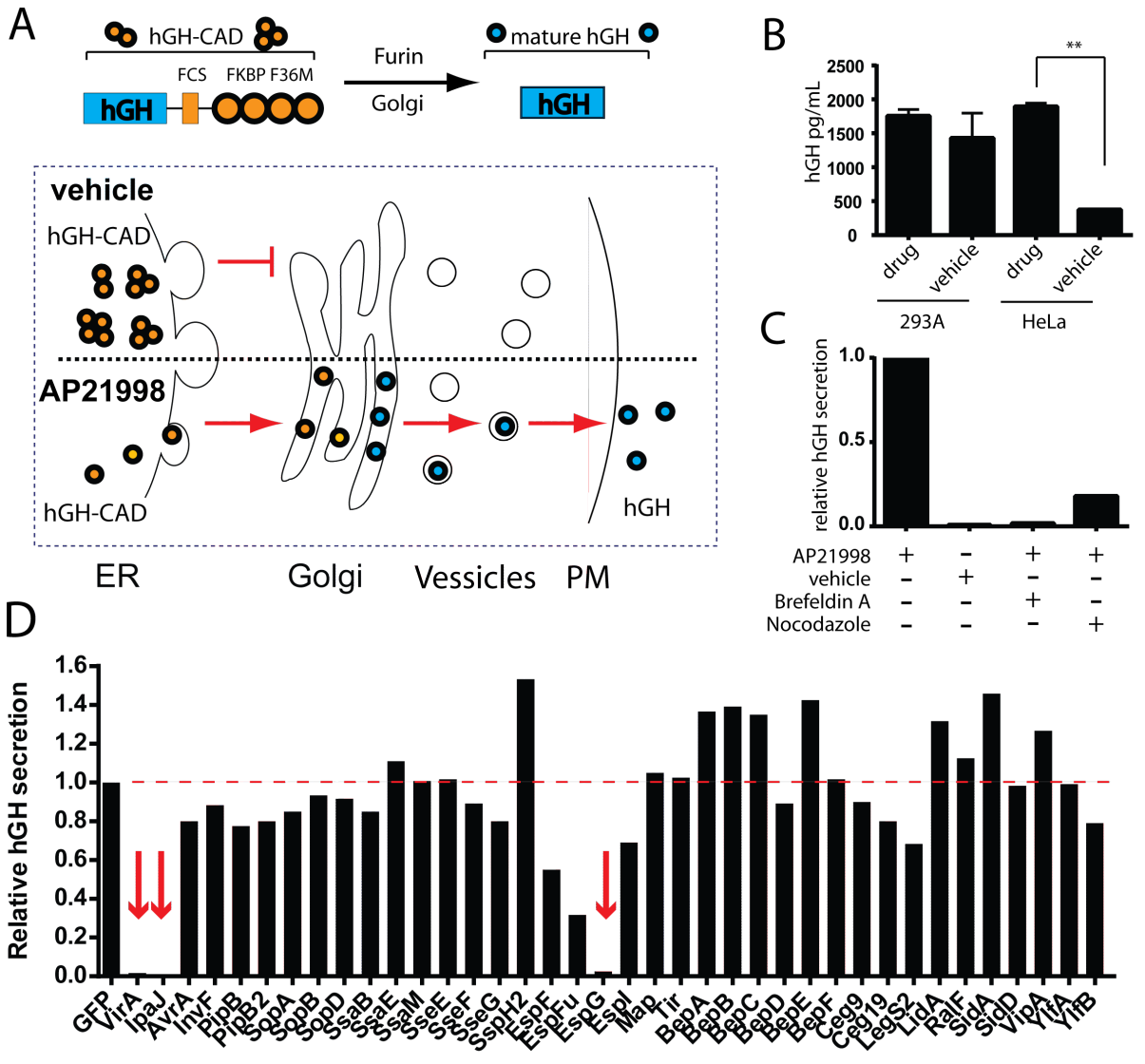

Figure 17: Development and application of a global secretory pathway assay

(A) Schematic diagram of the trafficking and processing of the hGH-CAD fusion protein. hGH-CAD agglomerates in the ER (top) until the drug AP21998 is added to release the aggregation and allow for normal delivery of mature hGH into the supernatant.

(B) Quantification of hGH in the supernatant 2 hours after AP21998 or vehicle is added to HeLa or 293A cells expressing the hGH-CAD construct. Significance determined by ANOVA.

(C) Relative hGH secretion (as compared to GFP construct alone) in the presence of drugs known to inhibit endomembrane trafficking through different mechanisms brefeldin A (Arf inhibitor) or nocodazole (microtubule inhibitor).

(D) Results of the hGH secretion assay comparing the amount of hGH in the supernatant in cells expressing the indicated GFP-effector fusions. Control cells expressing GFP alone are normalized to one, and values are expressed as a relative amount of hGH compared to control cells.

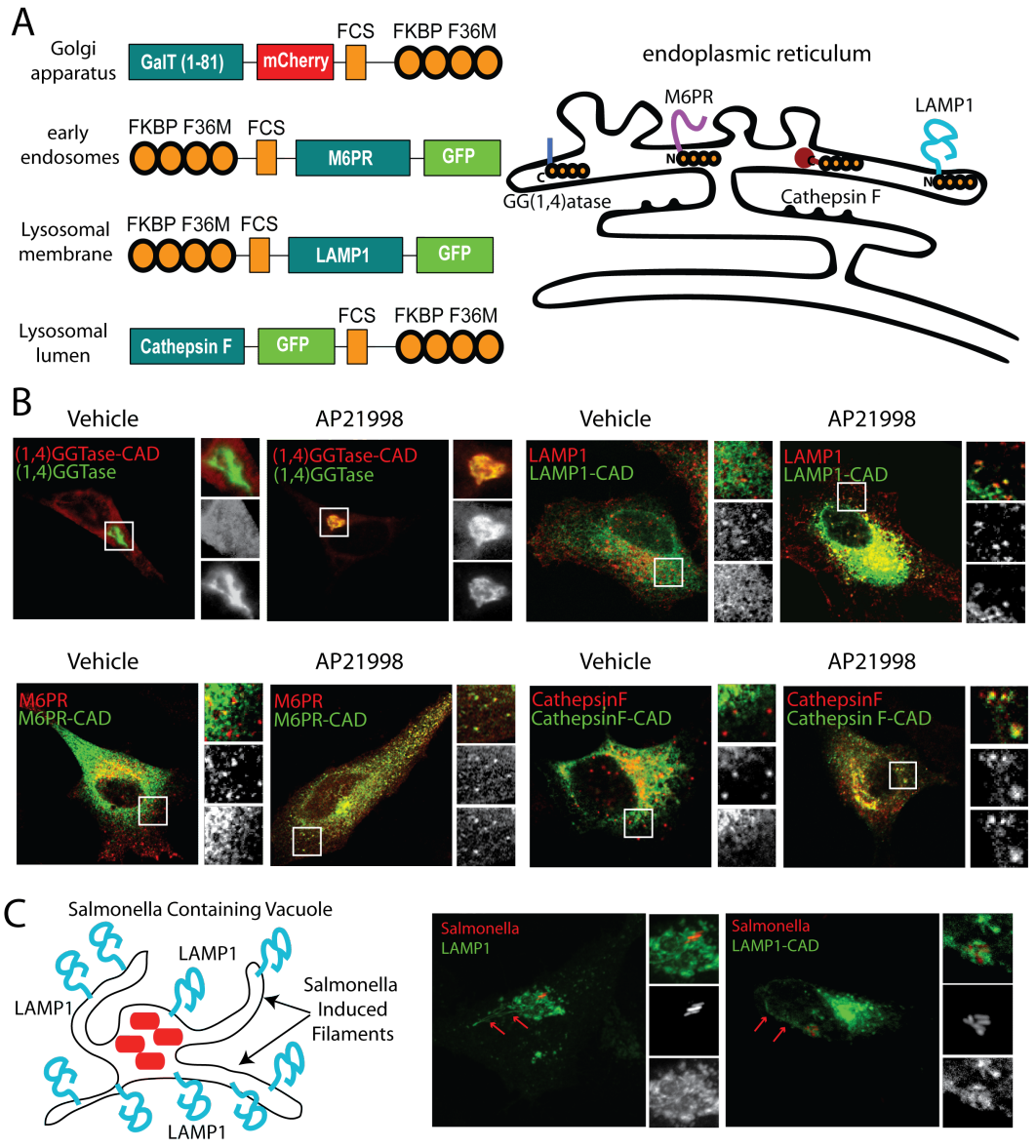

Figure 18: Validation of Endomembrane trafficking probes

(A) Construct architecture of the endomembrane trafficking probes designed in this study. Each probe was oriented so that the CAD would be in the lumen of the ER, allowing for proper detainment until addition of AP21998.

(B) Representative images of each CAD-fusion proteins two hours after vehicle or drug. Final destination of the probe was measure based on colocalization with various endomembrane markers as labeled.

(C) Fluorescent images of internalized *Salmonella* in cells expressing LAMP1-GFP or LAMP1-CAD-GFP 2 hours after addition of AP21998. The *Salmonella*-induced filaments are labeled with the red arrows.

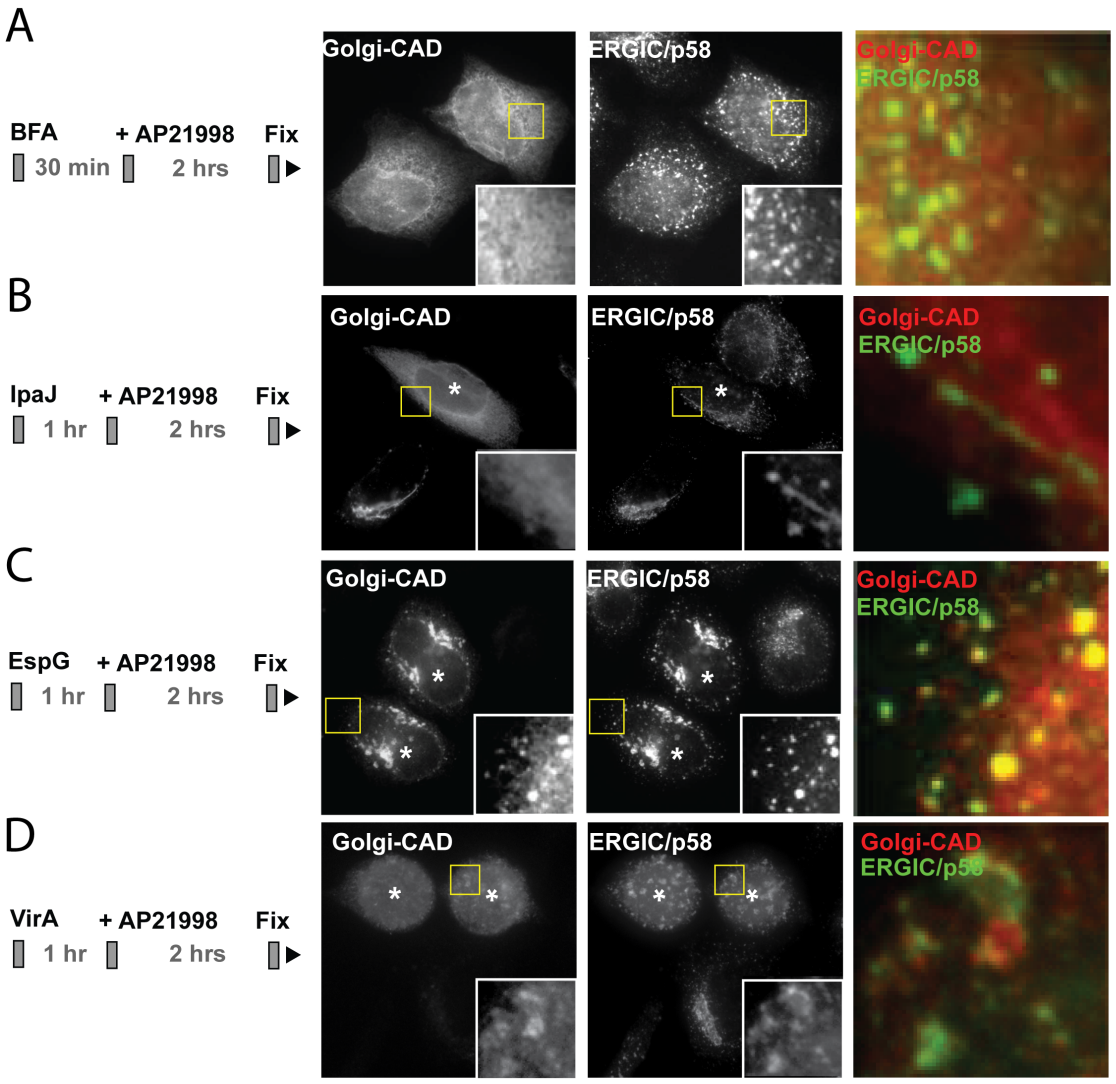

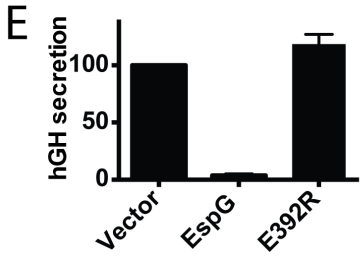

F

```
                                  HHHHHHHHHHHH          EEEEEE    EEEEE
IpaJ  NP_085284        56-RKQMYDNSCGAASLLCAAKELG-79  204-GLHWVLCRPDGS----YMDPAV-221
C39L  Q984Z8_RHILO     23-YVQTTPFTCGAACLMMAMSAVK-44  165-VPHWVLAIGDDGDHILIHDPWV-186
C39L  A6WWZ5_OCHA4     23-YVQTTPFTCGAACLLMAFAHHD-44  165-VPHWVLAHGEDGRHILIHDPWV-186
C39L  A0NWQ4_9RHOB     23-YVQTTPFTCGAACLLMSFACLD-44  165-VPHWVLVHDADDRHLIIHDPWL-186
C39L  Q1Q0J2_9BACT     24-YEQTTDFTCGACCLMMAMGRDI-45  166-FPHWVVVTGFDEKYIYVHDPFV-187
C39L  Q0EX59_9PROT     24-YQQTCEFTCGPCCLMMAMANFD-45  166-SPHWVVVSGFDRRFIYIHEPYV-187
C39F  YP_005047809      8-IKQHDITDCGAACLATISRQYG-33   92-LLHYVVIHKITKKEVIVADPAK-113
C1F   AAB02650        150-KNQGSCGSCWAFSAVVTIEGII-171 290-VDHAVAAVGYGPNYILIKNSWG-311
```

Figure 19: Endomembrane Probes can be used to identify effectors' points of attack

(A-D) Subcellular determination of the Golgi-CAD probe (red) after the addition of AP21998 in EspG, VirA, or IpaJ microinjected cells (asterisk). ERGIC/p58 (green) was used to label intermediary compartments. As a control, Brefeldin A shows Golgi-CAD is retained in the ER.

(E) hGH release assay with wild-type EspG compared to the EspG mutant E392R, a residue critical for EspG:Arf6 interaction. Values are compared to a GFP control (set to 100).

(F) IpaJ alignment to the C39-peptidase like family. Conserved residues important for secondary structure are shown in various colors and catalytic residues are shown in red.

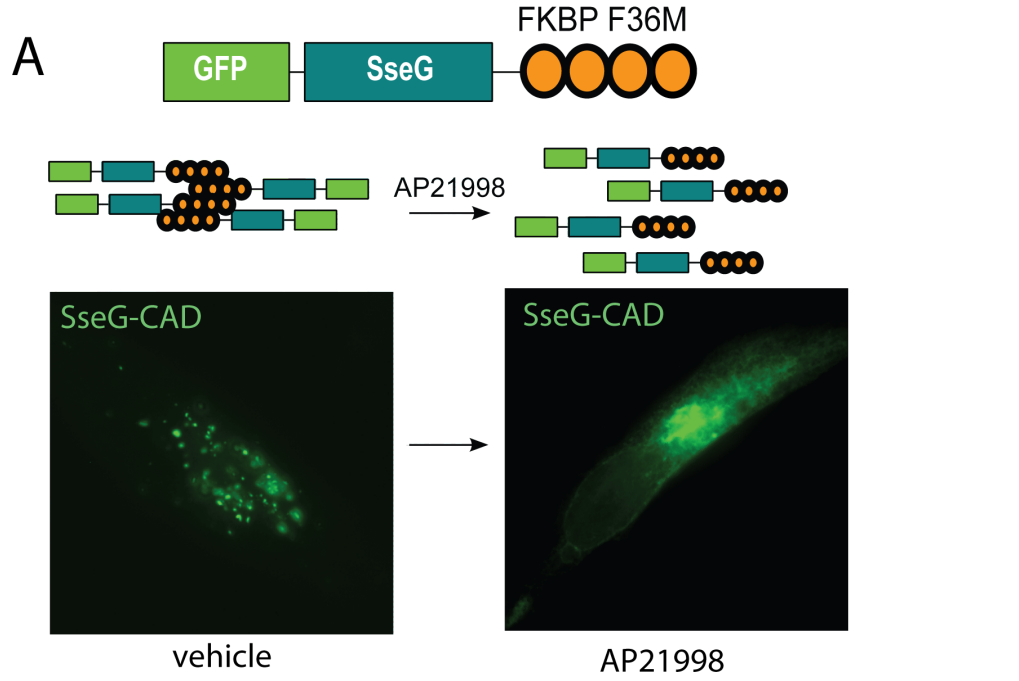
A
FKBP F36M
GFP
SseG
AP21998
SseG-CAD
SseG-CAD
vehicle
AP21998

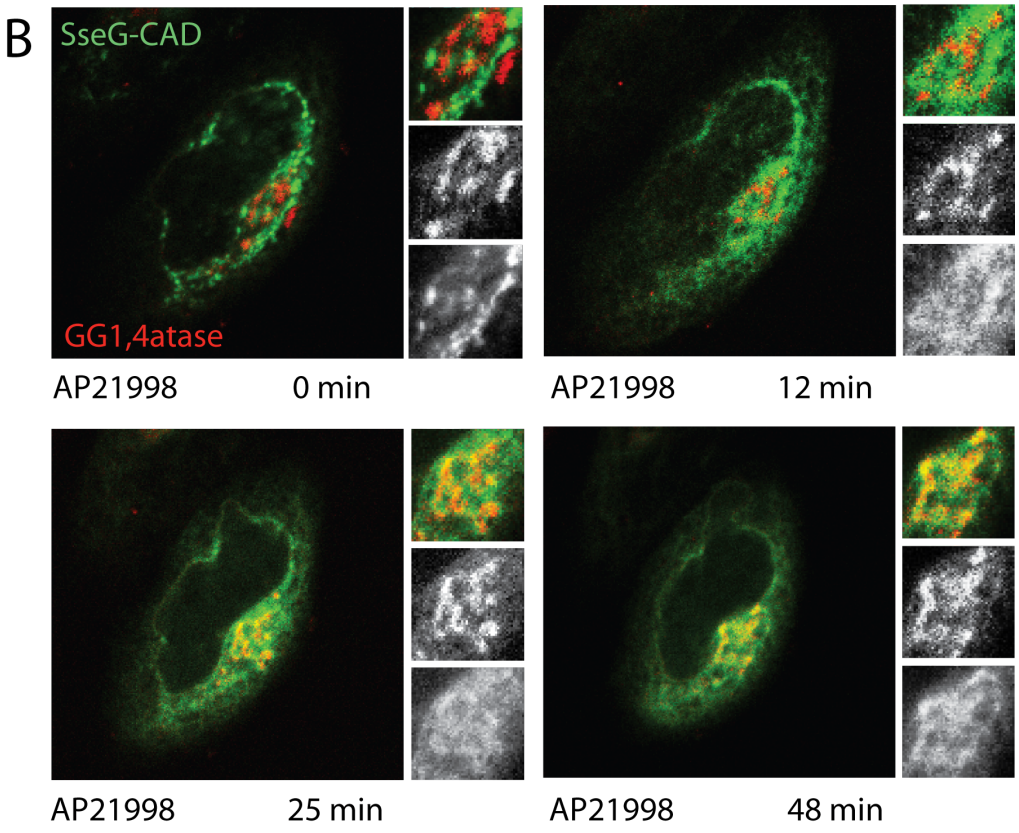
B
SseG-CAD
GG1,4atase
AP21998 0 min
AP21998 12 min
AP21998 25 min
AP21998 48 min

Figure 20: CAD technology can be used to study bacterial effector trafficking

(A) SseG-CAD fusion protein (green) before addition of drug (left) and two hours after drug addition (right).

(B) Still frames at indicated time points taken during live cell microscopy show SseG-CAD (green) coexpressed with the resident Golgi enzyme 1,4GGTase (red).

Materials and Methods

Molecular biology

All effectors used in the hGH secretion assay were cloned as previously mentioned in the material and methods of chapter two into pENTR vectors, and then transferred into a gateway compatible pCDNA3.1 GFP vector. The 4xFKBP-hGH construct was obtained through Ariad Pharmaceutical, Inc.; http://www.ariad.com/regulationkits; source of material, David Bernstein.

The endomembrane probes were subcloned into the CAD vectors as well as pCDNA3.1 vectors containing GFP or mCherry. LAMP1 and 1,4GGTase templates were provided by Dr. Paul Luzio (University of Cambridge) and Clontech, respectively. Cathepsin F and cation dependent (CD) Mannose-6-Phosphate receptor were purchased from ATCC.

hGH trafficking assay

HeLa or 293A cells (50% confluence) were transfected with 0.5 μg of 4xFKBP-hGH and either 1.0 μg eGFP–effector or EGFP control plasmid with Fugene6 (Roche). Sixteen hours later, the medium was replaced with medium containing AP21998 (final concentration, 2 μM) or vehicle control for 2 hours. Where noted brefeldin A (5 μg/mL) or nocodazole (30 μM) were added directly to the media 30 minutes prior to adding AP21998. For all studies, the supernatant was collected and then diluted 100-fold and compared against a hGH standard curve (12.5–400 pg/ml) for the quantification of hGH released using an hGH

enzyme-linked immunosorbent assay (Roche). For no drug controls, 100% ethanol (2 μl) was incubated with the cells for 2 hours.

Bioinformatics

HHpred was used to detect known pfam domains (profile database search used: pfam version 25.0) with distant structural homology relationships to full-length IpaJ (GenInfo Identifier (GI): 12329066) with default parameter settings (Soding, Biegert, & Lupas, 2005). The DUF3335 (C39-like peptidase family) gave a probability score of 90.0. One hundred proteins in the Pfam database contain this domain. PROMALS3D was used to produce a multiple-sequence alignment with the eight IpaJ and 100 DUF3335 family members to identify invariant catalytic residues and confirm conserved secondary and hydrophobicity patterns (Pei, Kim, & Grishin, 2008).

Mammalian cell studies

HeLa cells (50% confluency) were transfected where noted with 1.0 μg GFP, 0.5 μg of Golgi-CAD, 0.5 μg GFP-1,4GGTase, 1.0 μg M6PR-CAD, 1.0 μg M6PR-mcherry, 1.0 μg CathepsinF-CAD, 1.0 μg CathepsinF-mCherry, 1.5 μg of LAMP-CAD, 1.5 μg Lamp-GFP, 1.5 μg SseG-GFP using FuGene6 (Roche) and incubated for 16–18 h. AP21998 (2 μM final) was then added to the media for two hours before cells were fixed and prepared for immunocytochemistry when applicable. Samples were visualized on a LSM 510 PASCAL scanning confocal microscope (Zeiss, Thornwood, NY, USA). The ERGIC was visualized by p58 primary (BD Biosciences) and secondary anti-mouse IgG antibodies (Thermo

Scientific).

Salmonella expressing pDP151 mCherry vector were activated overnight in LB at 37 °C, and then diluted 1:50 and allowed to grow for four more hours. HeLa cells expressing either LAMP-GFP or LAMP-CAD were incubated for ten minutes with activated *Salmonella* (MOI of 5) before washing three times with warm PBS. After the infection persisted for six hours, AP21998 was added to the LAMP-CAD expressing HeLas for two more hours. Cells were then fixed and prepared for microscopy.

For microinjection studies, IpaJ, VirA, and EspG were all subcloned into pGEX4T in order to express recombinant proteins using 0.4 mM IPTG in BL21 DE3 *E. coli* strains. Bacterial pellets were lysed in GST buffer (50mM Tris; 150mM NaCl 2mM DTT pH 7.5) supplemented with protease inhibitors. Proteins were purified using glutathione sepharose (Amersham Biosciences). HeLa cells were microinjected with EspG, IpaJ, or VirA proteins using a semiautomatic InjectMan NI2 (Eppendorf) with a needle concentration of 25 μM.

CHAPTER FOUR
Identification of Secreted Effector Proteins Encoded by *Providencia alcalifaciens*

Introduction

As more and more pathogens are sequenced and found to encode T3SSs, families of effectors across species are being discovered. While bioinformatics may predict proteins with similar enzymatic function, the question remains if these effectors actually serve similar roles or have been functionally repurposed for each pathogen. Therefore, using knowledge of previously described secreted effectors would greatly facilitate the characterization of homologous effector proteins from other microbes.

To gain insight into this critical question, I sought to identify a newly sequenced pathogen, search its genome for genes similar in sequence to other known effectors, and compare the phenotypic properties of the new effectors to those previously characterized. The pathogen *Providencia alcalifaciens* presented a perfect model system to assess the diversification of bacterial effectors. First, genome sequencing revealed a putative T3SS, but no secreted substrates have been characterized to date (Galac & Lazzaro, 2012). Second, it has been observed to cause diarrhea symptoms in a wide array of hosts (Krol, Janeczek, Pliszczak-Krol, Janeczek, & Florek, 2007; Wang et al., 2014; Yoh et al., 2005), allowing for the use of both yeast and mammalian cells to study these effectors as outlined in chapter two.

To begin these studies, a bioinformatic pipeline to find putative bacterial effector candidates was developed. I next identified a secretion system activation protocol that will

allow for future studies with this pathogen. Lastly, a rationale for drawing conclusions on the putative effectors as real substrates of the T3SS in *P. alcalifaciens* was established. This study provides the first identification of Type III secreted effectors in *Providencia alcalifaciens* and a comparative analysis of several homologous virulence factors. These findings suggest that effectors are largely functionally repurposed through the addition of regulatory modules attached to the conserved enzymatic domain that ultimately change the substrate recognition and or localization for each effector.

Results

Bioinformatic identification of effector homologs

Since the T3SS was found collectively within a pathogenicity island, it was intriguing to speculate that the island would also contain the translocated substrates. Unfortunately, bioinformatic searches of the nearby genes did not reveal any proteins homologous to known effectors (data not shown). Therefore, I performed the reverse approach and developed a bioinformatic pipeline using various prediction tools to identify proteins with sequence and structure similarities of known effectors from other species (Figure 21A). First, PSI-BLAST analysis using 214 known Type III and Type IV effectors from seven different pathogens with various lifestyles and host specificities including *Salmonella typhimurium* [*St*], *Shigella flexneri* [*Sf*], enterohemorrhagic *E. coli* O157:H7 [*Ec*], *Yersinia pestis* [Yp], *Pseudomonas syringae* [*Ps*]), *Legionella pneumophila*, and *Bartonella Henselae* was performed to search for effectors encoded in the *Providencia alcalifaciens* genome. Secondary structure

predictions and literature searches were subsequently performed to confirm the conservation of known catalytic residues and structural determinants. In total, fifteen putative effectors were found in the *Providencia alcalifaciens* genome (Figure 21B*)*. Interestingly, the effectors were not found in pathogenicity islands but were rather dispersed throughout the genome, suggesting multiple horizontal transfer events. This dispersion of effectors is also observed in the pathogen *Yersinia enterocolitica*, although the advantage, if any, is unknown (Matsumoto & Young, 2006).

Activation of the T3SS

I next sought to confirm my bioinformatic candidates as bona fide secreted effectors. Traditionally, secreted bacterial effector proteins are confirmed by either translocation assays or proteomics. Unfortunately, *Providencia alcalifaciens* is currently genetically intractable limiting my ability to determine if the Type III apparatus is necessary for virulence. I was unable to transfer DNA through electroporation or conjugation, in spite of many attempts, preventing the genetically manipulation of *P. alcalifaciens.* Since translocation assays require the genetic tractability of species of interest, I next moved to a proteomics approach.

To this end, I first sought to determine how the Type III secretion system of *Providencia alcalifaciens* is activated. Since many protocols for Type III activation have been characterized for other Gram-negative gamma-proteobacteria, *P. alcalifaciens* was cultivated under conditions previously shown to induce the T3SSs of *Salmonella, Shigella, E. coli, Vibrio, or Yersinia* (Figure 22A) (Ando, Abe, Sugimoto, & Tobe, 2007; Bahrani, Sansonetti, & Parsot, 1997; Gode-Potratz, Chodur, & McCarter, 2010; Sherry et al., 2011;

Young & Young, 2002). As a functional readout, activated *P. alcalifaciens* were incubated with HeLa cells for the amount of time necessary for attachment and/or invasion of each of these previously mentioned pathogens and then stained with rhodamine phalloidin and DAPI for fluorescent imaging. *Providencia alcalifaciens* was attached extracellularly to HeLa cells when activated with calcium oxalate to induce low magnesium conditions in DMEM at 37 °C similar to *Vibrio parahaemolyticus* or through a drop in temperature to 26 °C in Luria broth similar to *Yersinia enterocolitica* (Figure 22B*)*. In contrast, little to no bacterial attachment was observed when the *Salmonella, Shigella, or E. coli* activation protocols were used (Figure 22B and data not shown). Though an artificial activation protocol of the T3SS system was developed, the subsequent mass spectroscopy analysis of the proteins released into the supernatant yielded high amounts of periplasmic and surface proteins such as amino acid transporters (data not shown). While the determination of T3SS activation protocols for *Providencia alcalifaciens* can be utilized for future studies, I was left to confirm the candidate effectors as true translocation substrates through a series of alternative methods.

To this end, I rationalized that these proteins are likely effectors if they: (1) localize to a subcellular compartment in eukaryotic cells, (2) interact with a eukaryotic protein, (3) show eukaryotic-like enzymatic function, and/or (4) give a phenotype within eukaryotic cells. From the bioinformatic analysis, I selected three *Providenci*a proteins that were most closely related to effectors with known catalytic residues, enzymatic functions, and/or observable phenotypes, allowing for directed comparison studies to confirm these *Providencia* homologs as effector proteins. From the fifteen putative *Providencia* effectors, the homologs to the SseJ phospholipase family, the SteC kinase family, and the WxxxE GEF family were chosen for

biochemical analysis. Furthermore, this work would also allow for the determination of the conservation of effector protein functions across species.

Analysis of putative SseJ homolog in P. alcalifaciens

SseJ is a glycerophospholipid: cholesterol acyltransferase (GCAT) from *Salmonella typhimurium* that is activated and localized to eukaryotic membranes by the small GTPase RhoA (Christen et al., 2009; Lossi et al., 2008)). Mutation of a single phenylalanine residue in its N-terminus abrogates the interaction and, therefore, membrane localization (Figure 5E) (LaRock et al., 2012). Structural alignments of the homologous *Providencia* protein (referred to as PseJ) to SseJ and other GCAT enzymes showed high conservation in the regions of all three catalytic residues (Figure 23A). Additionally, SseJ homologs were found in two other *Providencia* serovars – *stuarti* and *rustigianii*. While the enzyme core was highly conserved, the N-terminus of PseJ was almost ninety amino acids shorter than the N-terminus of SseJ and was missing the essential phenylalanine for RhoA interaction. To see if PseJ localizes to eukaryotic membranes like SseJ, a temperature sensitive viability screen in *S. cerevisiae* as described in chapter two was performed (Isakoff et al., 1998). Briefly, normal cellular growth and replication of yeast requires the small GTPase Ras to be activated by its GEF, Cdc25p, and to localize to the membrane through a C-terminal farnesylation. A temperature sensitive mutation of Cdc25p prohibits normal function of endogenous Ras at 37°C. Non-farnesylated, constitutively active Ras fused with a protein of interest can rescue this temperature sensitivity only if the fused protein localizes to eukaryotic membranes. Interestingly, PseJ, despite a truncated N-terminus, conferred yeast growth at the non-permissible temperature of

37 °C (Figure 23C). Furthermore, colocalization studies using a constitutively active Rab5 in HeLa cells found both PseJ and SseJ on trafficking vesicles in the endomembrane system (Figure 23B). To test whether PseJ bound to RhoA, the two proteins were coexpressed in HEK cells. Anti-GFP was used to pull-down GFP-PseJ (GFP alone and GFP-SseJ were used as negative and positive controls, respectively). Western bot analysis showed no RhoA-HA associated with PseJ (Figure 23D). While a subcellular localization and interaction with eukaryotic membranes indicates PseJ is a secreted effector, the two homologs differ in their mechanism of membrane association and ability to bind to RhoA.

Analysis of the putative SteC homolog in P. alcalifaciens

SteC is a kinase from *Salmonella* that phosphorylates the Map Kinase MEK (Poh et al., 2008). Bioinformatic predictions show that PteC (*Providencia* homolog) contains the same enzymatic domain and essential residues as the SteC kinase family (Figure 24A). Effectors that alter the MAP kinase pathway cause a growth defect in yeast when grown in the presence of sorbitol (Hao et al., 2008). To test the PteC effector candidate for a growth defect on sorbitol, the *Providencia* protein was transformed into INVSC1 yeast under a galactose inducible promoter. Yeast grew to normal levels when the effector was expressed in the presence of galactose, indicating this effector does not target a pathway generally essential for growth (Figure 24B). In the presence of sorbitol, however, PteC expressing yeast grew several orders of magnitude lower than yeast grown on galactose plates, indicating a conservation of the targeted pathway between SteC and PteC (Figure 24B). Additionally, mutation of the lysine essential for PteC's putative kinase function restored

normal yeast growth (Figure 24B). While the kinase domains seemingly serve similar functions for these two pathogens, SteC also encodes a second domain that binds to the host RhoGEF, Vav1, and causes an actin meshwork to surround the *Salmonella* containing vacuole (Odendall et al., 2012). The *Providencia* homolog, PteC, does not contain this additional domain and gave no actin phenotype when expressed in HeLa cells (similar to GFP alone) (Figure 24C). These studies further demonstrate that effector function can be diversified through the addition of extra domains and implicate PteC as a translocated substrate of the T3SS in *Providencia alcalifaciens*.

Analysis of the putative WxxxE homolog in P. alcalifaciens

Characterized effectors in the WxxxE family are guanine nucleotide exchange factors (Alto et al., 2006). $EspM^{Ec}$, $EspT^{Ec}$, Map^{Ec}, $IpgB1^{Sf}$, and $IpgB2^{Sf}$ each activate specific Rho family GTPases causing cytoskeletal rearrangements that can assist in bacterial attachment or internalization into host cells (Alto et al., 2006; Ohya et al., 2005a; Orchard & Alto, 2012). Other members of the family, such as $SifA^{St}$ and $SifB^{St}$, play roles later in infection, have yet to be demonstrated as GEFs, and do not give altered actin phenotypes (Bulgin et al., 2010). Bioinformatics also identified a WxxxE homolog in *Providencia rustigianii* (Figure 25A). Structural alignments of this family with the candidate *Providencia* homologs demonstrated conserved catalytic and structural residues (Figure 25B). Both *Providencia* homologs localized to the intermediate filament, vimentin (Figure 25B and data not shown). This localization was not governed by the effector's putative GEF domain, as the E81A mutant did not alter localization (Figure 25B). Additionally, the architecture of the intermediate

filaments was similar during ectopic expression of both the wild type and GEF dead mutant *Providencia* WxxxE, suggesting that intermediate filaments is a mode of localization and not a substrate of this enzyme (Figure 25B). Indeed, observations of an intact Golgi apparatus and dispersed endosomes throughout the cytosol further demonstrated that intermediate filaments were not disrupted (Figure 25C). To compare the functional consequence of the *Providencia* WxxxE to characterized WxxxEs from other pathogens, the putative effector was expressed in HeLa cells and the actin cytoskeleton was stained with rhodamine phalloidin to look for an actin phenotype. Similar to GFP expression alone, no stress fibers, lamellipodia, or filopodia were observed in cells expressing the *Providencia* WxxxE (Figure 25D). While the consequence of this subcellular localization in mammalian cells and determination of host substrate remains unclear, it does give indication that this protein is an effector that has greatly diversified its function. Interestingly, phylogenetic analysis of the WxxxE family clustered all the effectors that give actin phenotypes together (Figure 25E). Additionally, the two *Providencia* homologs formed a secondary cluster (Figure 25E). In contrast, SifA and SifB, whose functions are unknown, were present on separate branches on the tree. This functional comparison aids in the categorization of these proteins as effectors and speaks to the power of bioinformatics and phylogenetic analysis to jumpstart effector characterization studies.

Discussion

Here, several lines of evidence indicate that these *Providencia* proteins are secreted

bacterial effectors. First, the bioinformatic strategy was successful in identifying fifteen candidate effectors dispersed throughout the *P. alcalifaciens* genome. Next the *Providencia* homologs to members of the SteC, SseJ, and WxxxE families were all found to have either methods of localization or phenotypes in eukaryotic cells. Moreover, this study discovered that these homologous proteins have been functionally repurposed through accessory domains and likely perform different functions from one another. These diversifications among family members likely play a central role in determining the specific lifestyle of each pathogen.

Protein diversification through the addition of accessory motifs is not a new idea, as it has long been appreciated that eukaryotes implement this strategy. Taken together with the findings on IpgB1 (chapter two), I propose that bacterial effectors employ the same strategy of repurposing effector enzyme activity through the addition of accessory motifs to explore new niches. Indeed, this can be seen with members of the WxxxE family that have been characterized to alter actin dynamics. As shown in chapter two, IpgB1 localizes to eukaryotic membranes through the recognition of phospholipids that are necessary for *Shigella* persistence within the host cytosol. Work done by Robert Orchard showed another member from the WxxxE family, Map, utilizes its PDZ ligand to attach to actin in order to amplify its signaling capabilities in space and time (Orchard et al., 2012). These differences have allowed for the fine-tuning of effector activity critical to the lifestyles of these different pathogens. It is intriguing to speculate how this novel intermediate filament localization regulates the activity of the WxxxE *Providencia* effector. Despite their differences, the application of previous knowledge from studies on homologous effectors could still aid the

field in more rapidly characterizing newly identified effectors in emerging pathogens as shown from the enzymatic and phylogenetic analyses.

Type III secreted effectors are not only of interest because they cause medically relevant diseases, but also because they can be used as tools to understand basic cellular biology. Perturbation of a system with a Type III effector has led to advances in many fields including endomembrane trafficking, signal transduction, membrane fusion, phosphoinositide dynamics, and cell polarity (Orchard et al., 2012; Patel et al., 2009; Selyunin, Reddick, Weigele, & Alto, 2014; Selyunin et al., 2011). Interestingly, several *Providencia* serovars were isolated from the thorax of wild fruit flies and found to be lethal to *Drosophila* (Galac & Lazzaro, 2011). Over a century of studies with *Drosophila* as a model organism has provided a plethora of genetic tools and understanding to the field of biology, since this organism is much simpler, smaller, cheaper, and faster to perform studies on as compared to other typical model organisms. Since *Providencia* serovars are natural *Drosophila* pathogens, these bacterial secreted effectors have the potential to be used to open exciting new avenues in *Drosophila* studies. Taken together, this work with *P. alcalifaciens* demonstrates that a systems biology approach can lead to rapid determination of effector function and development of new tools for basic cellular biology.

A

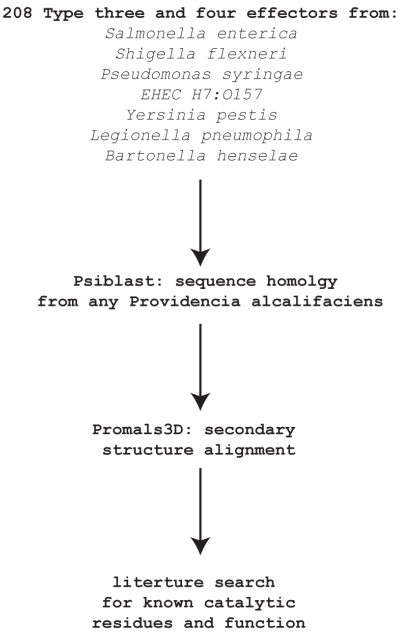

B

Effector	function of at least one family member	P. alcalifaciens homolog
SseJ	phospholipase: activated by RhoA	WP_006661713
SspH2/IpaH/YopM	E3 ubiquitin ligase	WP_006662093
SteB	unknown	WP_006662442
SteC/OspG/NleH/YpkA	kinase	WP_006663275
OspC1/OspC2	unknown	WP_006658374
Map/EspM/EspT/IpgB1/ IpgB2/SifA/SifB	Guanine nucleotide exchange function	WP_006657478
NleF	unknown	WP_006657633
HopA1	suppressor of plant immunity	WP_006661066
HopN1/YopT	protease	WP_006661066
YopH/SptP	tyrosine phosphatase	WP_006660669
VipF	acetyltransferase	WP_006662841
BepA/BepB/BepC	FIC domain	WP_006663466
Ankyrin family	unknown	WP_006658087
LpnE	unknown	WP_006657575
LegS2	sphingosine 1-lyase	WP_0066600500

Figure 21: Identification of *Providencia alcalifaciens* homologs to known Type III and Type IV effectors

(A) A pictorial representation of the bioinformatic pipeline used to identify and confirm sequence and structural homologs to Type III and Type IV effectors in the *P. alcalifaciens* genome.

(B) Table summarizing the proteins found to have homology to effectors from other pathogens.

A

Bacteria	Protocol reference	*Providencia* attachment
S. typhimurium	Sherry et. al 2011	No
S. flexneri	Bahrani et. al 1997	No
EHEC H7:O157	Ando et. al 2007	No
V. parahaemolyticus	Gode-Potratz et. al 2010	Yes
Y. entercolitica	Young and Young 2002	Yes

B

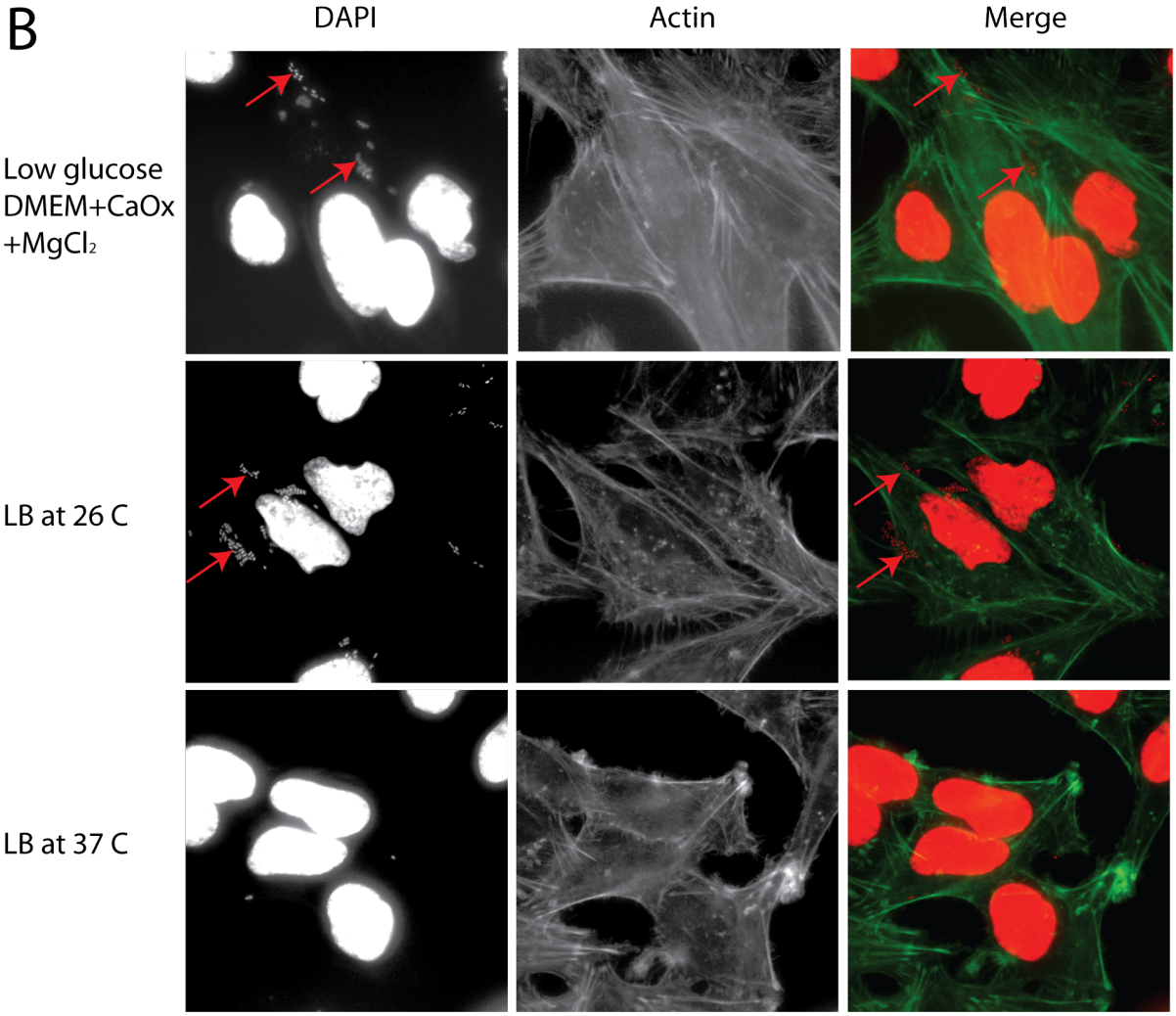

Figure 22: T3SS activation studies with *Providencia alcalifaciens*

(A) Table of T3SS activation protocols tested on *Providencia alcalifaciens*

(B) *P. alcalifaciens*, infections of HeLa cells when activated similarly to *V. parahaemolyticus* (top) or *Y. enterocolitica* (middle), or grown in LB at 37 °C (bottom). DNA in the host cell and bacteria is labeled with DAPI (pseudocolored red) and the actin cytoskeleton is labeled with FITC phalloidin (green) to image the outline of the cells.

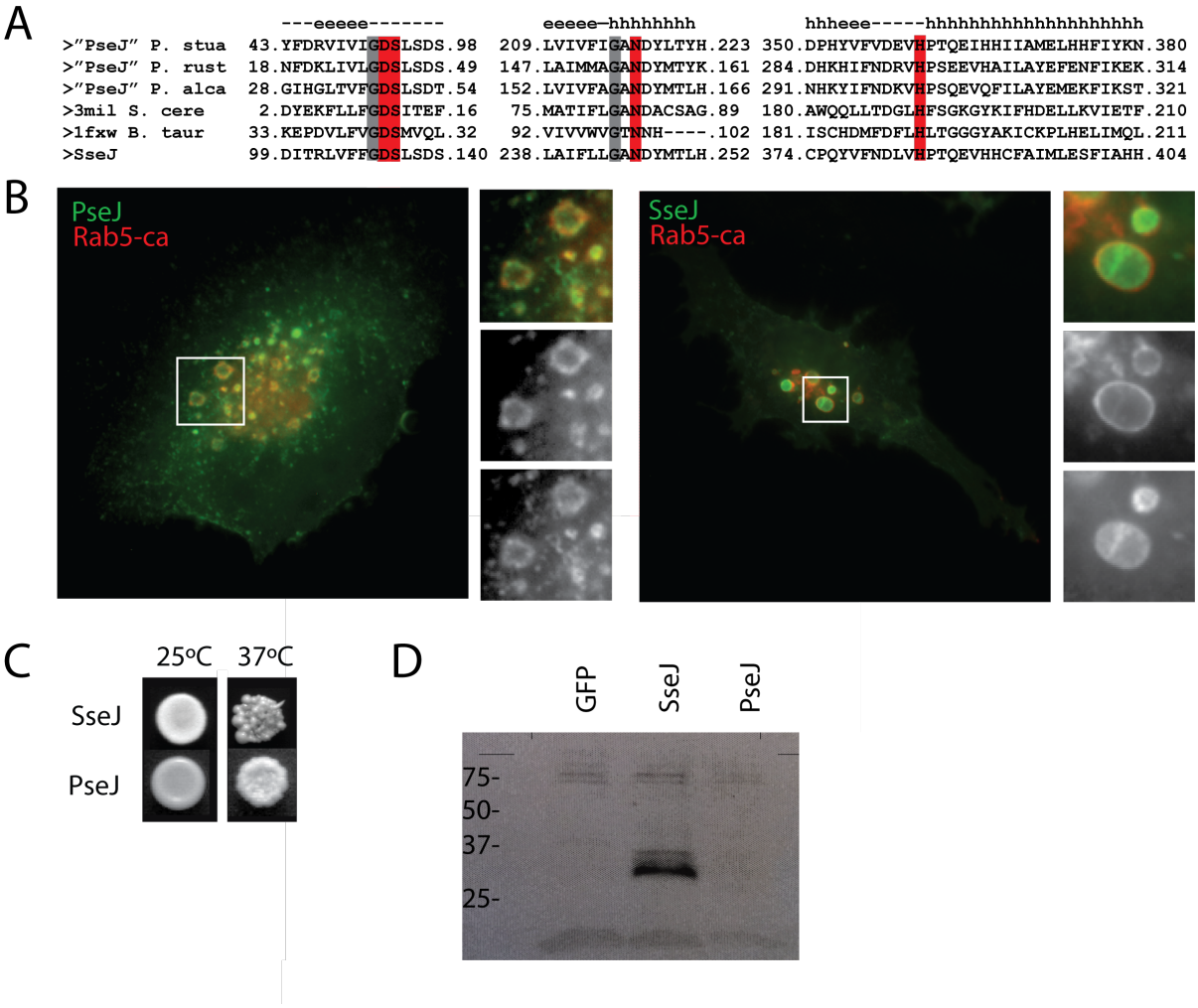

Figure 23: Characterization of the SseJ homolog in *P. alcalifaciens*

(A) Structural alignments of the GCAT family with the putative *Providencia* effector Essential catalytic (red) and structural (grey) residues are highlighted. WP_004924072.1 (*P. stuarti*), WP_006812958.1 (*P. rustigianii*), WP_006661713.1 (*P. alcalifaciens*), 3mil (pdb) *S. cerevisiae*, 1fxw (pdb) *Bos taurus*, SseJ (*Salmonella typhimurium*)

(B) SseJ (green) and its homolog PseJ (green) coexpressed with constitutively active Rab5 (red) in HeLa cells.

(C) Ras rescue temperature sensitive growth assay on PseJ and SseJ. All yeast grow at the permissible temperature of 25 °C, while only yeast that have a protein of interest that localizes to eukaryotic membranes grow at the non-permissible temperature of 37 °C.

(D) GFP co-IP assays of full length GFP_SseJ and GFP_PseJ purified from HEKs. Western blot analysis used anti-HA to probe for HA-RhoA.

A

```
                                --eeeeeeeee---eeeeeeee-----eeeeeeee
>WP_004906754          131.LYLNVTNSLGHGVYGTAYRVG------NFVIKVPF.159
>CDK1 H. sapiens         1.EKYEKIGKIGEGSYGVVFKCRNRDTGQIVAIKKFL.35
>PAK4 H. sapiens        22.SYLDNFIKIGEGSTGIVCIATVRSSGKLVAVKKMD.56
>PLK2 H. sapiens        10.KRYSRGKTLGKGGFAKCYEMTDLTNNKVYAAKIIP.44
>PLK3 H. sapiens         9.RTYLKGRLLGKGGFARCYEATDTETGSAYAVKVIP.43
>SteC                  244.--DIEKNKIGSGSYGTVYRLHD-----DFVVKIPV.271
>YpkA                  134.MRVAETDKFAEGE-SHISIIETKDK-QRLVAKIER.166
>YopO                  131.MRVAETDKFAEGE-SHISIIETKDK-QRLVAKIER.163
>NleH                  131.RLSVPGNVIGKGGNAVVYEDAED---ATKVLKMFT.162
>OspG                   25.TEPILGKLIGQGSTAEIFEDVND---SSALYKKYD.56
```

B

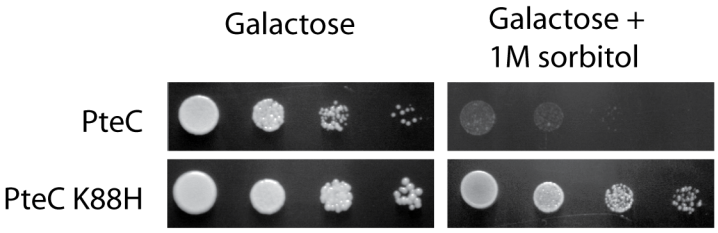

C

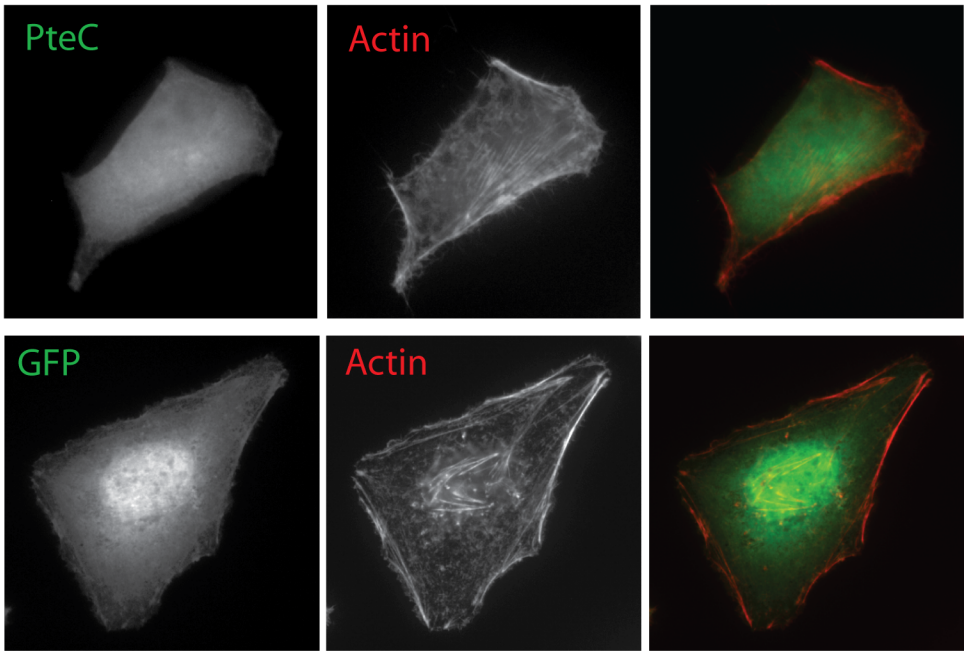

Figure 24: Characterization of the SteC homolog in *P. alcalifaciens*

(A) Structural alignment of the SteC homologs in *Providencia* (WP_004906754.1) with other kinases labeled with either the pdb number or effector name. Essential catalytic and structural residues are highlighted.

(B) Serial dilutions of yeast expressing the SteC homolog (PteC) or kinase dead SteC homolog (PteC K88H) under a galactose inducible promoter on galactose or galactose containing 1M sorbitol plates.

(C) Actin staining (red) on HeLa cells expressing GFP-PteC or GFP alone.

A

```
                        -hhhhhhhhhhhhhhhhhhhhh----          ----hhhhhhhhhhhhh-
>WP_006813499.1   73.AIAHWKEQERVVQLSATFNQAFDAVID. 99   134.QFNKNAAQKSLEHVLRNN.151
>WP_006657478.1   73.AIEHWKKQEKIIQLSSTFNRTFDATRE. 99   134.TFLPNAAQKSIEHILYNN.151
>SifB            191.NLCDWKEQERKAAISSRINLGIAQAGV.217   242.AFEPNYAQSSVTQIVYSC.259
>SifA            193.HLDGWKAQEKATYLAAKIQSGIEKTTR.219   248.EIPPPHTHIPIEKMVKEV.265
>EspT             66.DIDEWIKDERIVYPSRVINQEIDNYCF. 92   117.TLDVKAAQSSINHVIMGS.134
>EspM             66.DIHGWVSDERTVYPSRVINQEIDNCCL. 92   117.TLDVKAAQSSINHIIIGN.134
>IpgB2            58.NITDWKNDEKKVYVSRVVNQCIDKFCA. 84   109.SLDINAAQSSINHLVSGS.126
>Map              70.DTQQWFQQEQTTYISRTVNRTLDDYCR. 96   121.PLDMNGAQSSIGHFLQSN.138
>IpgB1            72.QLFCWMSQERTTYVSSMINRSIDEMAI. 98   124.KLDEKSAQTSISHTALNE.138
```

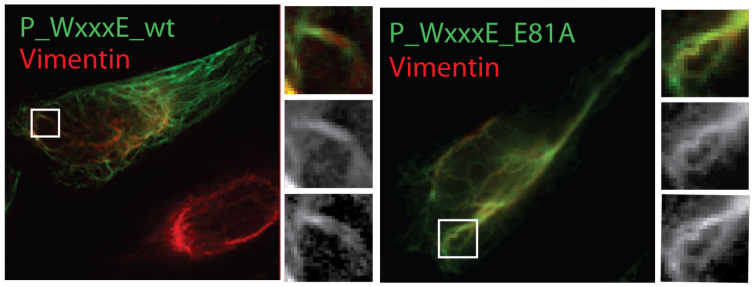

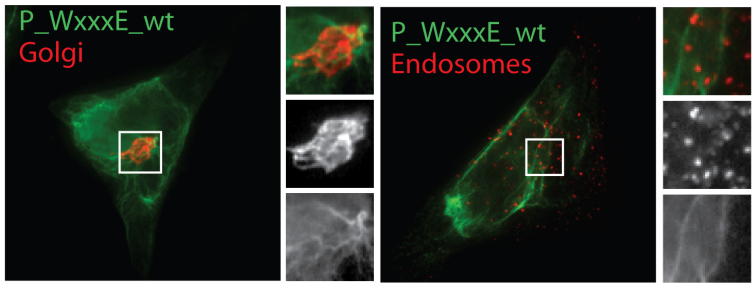

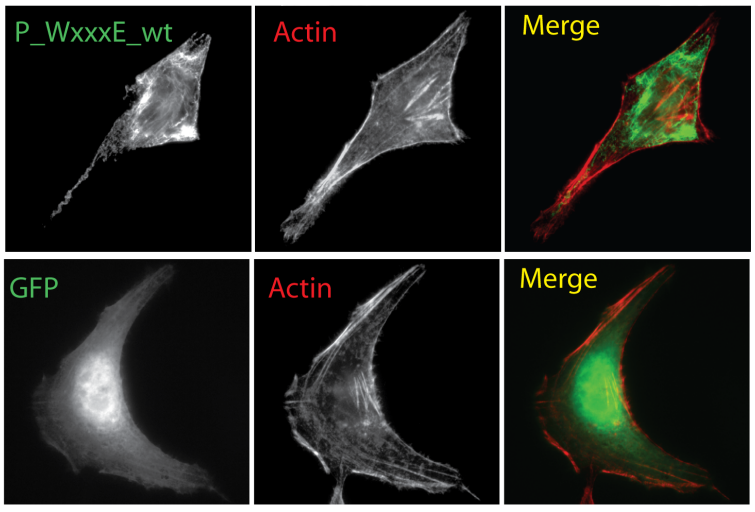

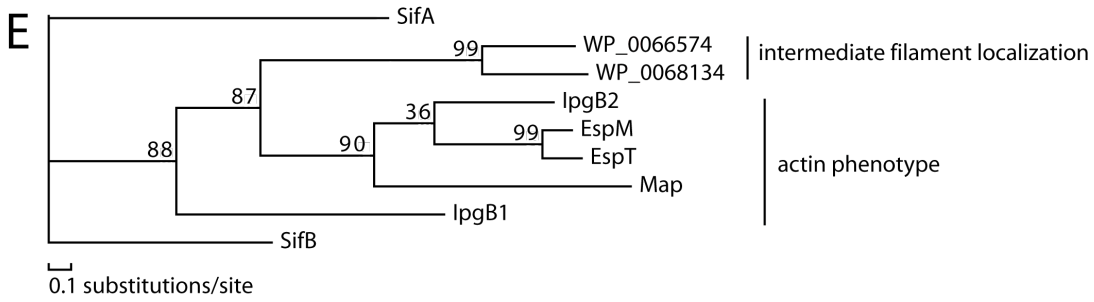

Figure 25: Characterization of the WxxxE homolog in *P. alcalifaciens*

(A) Members of the WxxxE family have the conserved WxxxE motif and the AQSSI catalytic loop as shown. WxxxE from *P. alcalifaciens* labeled (WP_00657478.1). WxxxE from *P. rustigianii* labeled (WP_006813499.1).

(B) Transfection and expression of the GFP-P_WxxxE and GFP-P_WxxxE^{E81A} mutant with the intermediate filament vimentin (red) in HeLa cells.

(C) Representative Golgi architecture (GG1,4atase; red) in HeLa cells expressing GFP-P_WxxxE or GFP alone.

(D) Immunofluorescence of the actin cytoskeleton (red) of cells expressing GFP-P_WxxxE or GFP alone.

(E) Phylogenetic tree of the relationships between the WxxxE family shows three subgroups.

Materials and Methods

Plasmids

PpgB1, PteC, and PseJ were codon optimized and synthesized by IDT. These constructs were then TOPO cloned into pENTR vector and subsequently transferred to various expression vectors using Gateway system (Invitrogen). Vimentin_pLASMID CFP was purchased from ATCC and subcloned into pcDNA3.1-mcherry. RhoA-HA was received from the UMP cDNA resource center. Site-directed mutagenesis was carried out using the QuickChange Site-Directed Mutagenesis kit (Stratagene). All constructs were verified by DNA sequencing.

Bioinformatics

The *Providencia* serovars' genomes were searched using PSI-BLAST with default settings for homologs to each 208 Type III and Type IV effectors in Appendix A. Proteins with expectancy values lower than E^{-10} were then run through PROMALS3D for secondary structure alignments (Pei et al., 2008).

Infection studies

Each activation protocol was carried out as previously mentioned (Ando et al., 2007; Bahrani et al., 1997; Gode-Potratz et al., 2010; Sherry et al., 2011; Young & Young, 2002). After activation, a confluent layer of HeLa cells were then infected with *P. alcalifaciens* with an initial MOI of 100 for four hours. Coverslips were then fixed and stained for immunofluorescent studies.

Yeast based assays

Yeast were transformed as described previously (Gietz et al., 1995). For CDC25ts yeast all incubation were done at 25 °C instead of 30 °C. For the Ras rescue assay, transformants were grown at 25 °C and at 37 °C for three to ten days. For growth assays in INVSC1, 10 fold serial dilutions were spotted on glucose, galactose, or galactose plus 1M sorbitol plates and grown at 30 °C for three days.

Mammalian cell studies

HeLa and HEK293 cells were maintained in DMEM with glutamate and pyruvate supplemented with 10% FBS and 5 mL of pen/strep antibiotics. HeLa cells were transfected with Fugene6 (Roche) at 70% confluency on glass coverslips. For all constructs, 1.5 μg of DNA was used. After sixteen to eighteen hours cells, were fixed in 3.7% formaldehyde, permeabilized with 0.5% Triton, blocked with 1% BSA, and stained with antibodies for immunofluorescence when indicated. DAPI (Life Technologies) was used at a 1:40,000 dilution, rhodamine phalloidin (Invitrogen) was used at a 1:500 dilution, EEA1 was used for endosomes at 1:2500, and GM130 (BD Transduction Laboratories) was used to stain the cis-Golgi apparatus (1:250).

Recombinant protein

GFP-Strep-tagged proteins (7.5 μg per 10 cm plate) and HA-RhoA (7.5 μg per 10 cm plate) were cotransfected into HEK293 cells using as standard calcium phosphate transfection.

Fresh media was added 24 hours after transfection. Two days post transfection, cells were washed once with PBS before they were lysed and scraped in 0.1% Triton and 5 mM EDTA TBS. The cell suspension was vortexed three times every three minutes before separating the soluble and insoluble cellular fractions at 14,000 rpm for 15 minutes at 4 °C. The soluble fraction was then incubated overnight with anti-GFP antibody (ABAffinity) while nutating at 4 °C. The following day, Protein A/G beads were washed in mammalian lysis buffer and added to the soluble cell lysate +antibody mixture for two hours while nutating at room temperature. Beads were washed four times and boiled in 2x laemmli buffer before being run on a 10% acrylamide gel and transferred to nitrocellulose. Western blot analysis using Strep-HRP antibody confirmed expression. To test for pull-down of HA tagged RhoA, a western blot was performed using HA-RhoA (1:1000) overnight at 4 °C and anti-mouse HRP (1:8,000) for 30 minutes at room temperature. HRP was visualized using a chemiluminescent detector.

CHAPTER FIVE
Conclusions and Future Directions

This study, to the best of my knowledge, provides the largest (> 200 proteins) and broadest (6 diverse pathogens) library of bacterial virulence factors to date. By focusing on host membrane-pathogen interactions, an unappreciated mechanism of virulence factor amplification in the host cellular environment has been uncovered. Moreover, the data have far-reaching implications not only for the evolutionary design principles of secreted virulence proteins, but also may uncover unknown regulatory modules and mechanisms in higher order species. Furthermore, this study provides a breadth of tools to push the field forward utilizing a systems biology approach to study virulence factor function.

Origins of Novel lipid binding domains

The search for previously unknown membrane interacting bacterial virulence factors revealed that almost a third of all bacterial effectors tested localized to specific subcellular compartments. Further genetic and biochemical tests identified 16 effectors that directly interact with phospholipids. Prior to this study, only a small number of Type III and Type IV secreted proteins had been shown to interact with different lipid head groups (Brombacher et al., 2009; Haneburger & Hilbi, 2013; Salomon et al., 2013). In total, the effectors known to directly interact with phospholipids has been more than tripled, demonstrating a general necessity of finely tuned localization of secreted factors during infection than previously appreciated.

How did these bacterial membrane-binding domains develop and what do they tell us about virulence factor evolution? Current theory on the origin of eukaryotic protein interactions suggests that two fundamental principles are at play with IpgB1^{Sf} and its host substrate, Rac1. First, IpgB1 likely established an independent plasma membrane localization to bring it into close proximity to where endogenous Rac1 signals. This "colocalization first" strategy would provide an opportunity for a weak interaction to occur more readily, although likely inefficiently. Second, through a series of mutations, IpgB1 gained a site of allosteric regulation, the phospholipid binding module, which looped information flow directly back into the Rac1 signaling cascade. This created a context that would facilitate potent amplification of IpgB1 activity. *Shigella* harboring IpgB1 proteins with a secondary domain that recognizes phospholipids would be naturally selected as it could overcome stochastic fluctuations more efficaciously and allow *Shigella* to have higher rates of infection. While co-localization followed by natural selection has been observed as the process for developing many eukaryotic proteins networks, these findings suggest these principles are also utilized by virulence factors to achieve higher levels of robust signaling through feedback reactions.

Mechanisms to amplify effector protein activity in space and time

How common are feedback loops in amplifying effector protein signaling networks? In spite of the fact that over 50 new membrane-interacting proteins were identified, the catalytic activity for almost 90% are unknown, limiting my ability to determine if membrane localization motifs are commonly utilized in bacterial effector proteins for amplification of

enzymatic activity function, pathogenesis, or both. Still, the global analysis of the mechanisms underlying the subcellular localization of effector proteins predicts that several effectors link their catalytic activity with membrane interactions. For example, the N-WASP activating effector protein $EspFu^{Ec}$ is capable of directly interacting with anionic phospholipids including $PI(4,5)P_2$ (Figure 11). Since it is well known that N-WASP is cooperatively activated by $PI(4,5)P_2$ to induce actin polymerization (G. M. Rivera, Vasilescu, Papayannopoulos, Lim, & Mayer, 2009), it is intriguing to speculate that $EspFu^{Ec}$ may actively cluster $PI(4,5)P_2$ directly underneath the attached bacterium to create a local environment that will robustly induce N-WASP mediated actin polymerization. Similar predictions can be made with the PI phosphatases, $SopB^{St}$ and $SidF^{Lp}$, that both had subcellular localization mechanisms dependent on at least one of the PI kinases in yeast. The assembly of synergistically coupled membrane-binding and catalytic domains provides a mechanism of regulation establishing an effective enzyme concentration that would allow successful signaling cascades necessary for pathogenesis.

Since we speculate the mechanism of feedback directly links localization motifs with enzymatic domains, it will be important to ask if the knowledge of an effector's regulatory domain can be used to predict the target of its enzymatic function. A perfect example is SopA the HECT E3 ligase from *Salmonella* that was identified in this work to bind directly to phospholipids. To date, the host substrate for SopA is unknown, but, as the work with IpgB1 suggests, the nexus between the ligase and phospholipid binding domains may indicate that the host target for SopA is a protein in the phospholipid signaling network.

New tools to study bacterial effectors

While many pathogens have developed methods to rewire the host endomembrane system, the effectors responsible are still unknown. Through the development of the CAD regulated trafficking system, new avenues of research are opened to begin to answer these critical questions. In this study, $EspG^{Ec}$, $VirA^{Sf}$, and $IpaJ^{Sf}$ were all shown to inhibit the global secretory pathway. When probed specifically for the point at which trafficking was arrested, the Golgi-CAD construct easily differentiated the site of obstruction for each of these three effectors. Further applications of this CAD system have the potential to illuminate key insights to questions that have long been unanswered in the field. For example, the various endomembrane trafficking probes can be used in concert with *Salmonella* effector deletion strains to identify which effectors are necessary to properly target LAMP1 and inhibit cathepsin hydrolases from the *Salmonella*-containing vacuole. Furthermore, the notion of effectors directing their own traffic throughout the endomembrane system is a new idea and this technology, as shown with $SseG^{St}$, promises insights into these uncharted territories.

Applying our knowledge

A wide array of both plant and animal pathogens rely on their secretion systems to cause disease, yet the studies on these systems have been limited to only a few species of bacteria (Dean, 2011; Sadarangani, Datta, & Arunachalam, 2013). This limitation is caused by several factors, one of which is the ability to identify and confirm effector substrates.

Bioinformatics using the secretion signal (unique to each bacteria) requires the knowledge of at least a few effectors from the species being studied. Other common practices to identify secreted proteins involve the genetic manipulation of the bacteria followed by translocation assays or the artificial activation of the secretion system followed by mass spectroscopy. If a microbe of interest is not amenable to these techniques, then the secretion systems and the bacterial effectors cannot be studied. Now, in the genome era, a rapid increase in sequenced microbial species coupled with the increase in confirmed bacterial effectors from the few pathogens that have been well characterized has poised the field with new approaches to characterize these essential virulence factors. In this study, a model bioinformatic pipeline and rationale for the classification of putative effectors from the uncharacterized pathogen *P. alcalifaciens* that encodes a Type III secretion system was developed. Previous knowledge of homologous effectors was used to classify Type III effector candidates, PseJ, PteC, and P_WxxxE, as bona fide effectors. From this study, a platform to identify secretion system substrates from uncharacterized species was established.

Conclusions

Through a comprehensive analysis of nearly 200 bacterial Type III and Type IV secreted effector proteins, I present compelling evidence that bacterial virulence factors have evolved membrane targeting motifs that amplify the activity of low abundance secreted enzymes within the host cellular environment. Furthermore, the discovery of 57 bacterial effector proteins that bind intracellular membranes, coupled with the identification of a

membrane-assisted autocatalytic feedback system extends the field's understanding of many bacterial virulence systems. Lastly, the development of new tools to identify and study effector properties provides a resource for future studies.

APPENDIX A
Bacterial effector proteins used in this study

Effector	Organism	Accession number	Expression in CDC25ts	Ras rescue	Literature
AvrPto1	*P. syringae*	NP_793764.1	yes	no	Cunnac et al. 2009
HopA1	*P. syringae*	NP_795084.1	yes	yes	Cunnac et al. 2009
HopAA1-2	*P. syringae*	NP_794461.1	yes	no	Cunnac et al. 2009
HopAB2	*P. syringae*	NP_792881.1	yes	no	Cunnac et al. 2009
HopAG1	*P. syringae*	NP_790740.1	yes	no	Cunnac et al. 2009
HopAH1	*P. syringae*	NP_790744.1	yes	no	Cunnac et al. 2009
HopAH2-1	*P. syringae*	NP_793075.1	yes	no	Cunnac et al. 2009
HopAI1	*P. syringae*	NP_790745.1	yes	no	Cunnac et al. 2009
HopAM1-1	*P. syringae*	NP_790858	no	na	Cunnac et al. 2009
HopAO1	*P. syringae*	NP_794465.1	yes	no	Cunnac et al. 2009
HopAQ1	*P. syringae*	NP_794448.1	yes	no	Cunnac et al. 2009
HopAS1	*P. syringae*	NP_790323.1	yes	yes	Sohn et al. 2012
HopC1	*P. syringae*	NP_790436.1	yes	no	Cunnac et al. 2009
HopD	*P. syringae*	YP_784364.1	yes	no	Cunnac et al. 2009
HopE1	*P. syringae*	NP_794087	yes	no	Cunnac et al. 2009
HopF2	*P. syringae*	NP_790351.1	yes	no	Cunnac et al. 2009
HopG1	*P. syringae*	NP_794468	yes	no	Cunnac et al. 2009
HopH1	*P. syringae*	NP_790435	yes	no	Cunnac et al. 2009
HopI1	*P. syringae*	NP_794511	yes	no	Cunnac et al. 2009
HopK1	*P. syringae*	NP_789904.1	yes	no	Cunnac et al. 2009
HopM1	*P. syringae*	NP_791202.1	yes	no	Cunnac et al. 2009
HopN1	*P. syringae*	NP_791197	yes	no	Cunnac et al. 2009
HopO1-2	*P. syringae*	NP_794345	yes	yes	Cunnac et al. 2009
HopO1-3	*P. syringae*	NP_794343.1	yes	yes	Cunnac et al. 2009
HopP1	*P. syringae*	NP_792485	yes	no	Cunnac et al. 2009
HopQ1-1	*P. syringae*	NP_790716	yes	no	Cunnac et al. 2009
HopQ1-2	*P. syringae*	NP_794471.1	yes	no	Cunnac et al. 2009
HopS1	*P. syringae*	NP_794348.1	yes	yes	Cunnac et al. 2009
HopT1-2	*P. syringae*	NP_794344.1	yes	no	Cunnac et al. 2009
HopU1	*P. syringae*	NP_790350.1	yes	no	Cunnac et al. 2009
HopV1	*P. syringae*	NP_794463.1	yes	yes	Cunnac et al. 2009
HopY1	*P. syringae*	NP_789920.1	yes	no	Cunnac et al. 2009
AvrA	*S. typhimurium*	NP_461786.1	yes	no	Agbor et al. 2011
PipB	*S. typhimurium*	NP_460061.1	yes	yes	Agbor et al. 2011

PipB2	*S. typhimurium*	NP_461706.1	yes	yes	Agbor et al. 2011
SifA-	*S. typhimurium*	NP_460194.1	yes	yes	Agbor et al. 2011
SifB EA	*S. typhimurium*	NP_460561.1	yes	no	Papezova et al. 2007
SipB	*S. typhimurium*	NP_461806.1	yes	no	Agbor et al. 2011
SipC	*S. typhimurium*	NP_461805.1	yes	no	Agbor et al. 2011
SipD	*S. typhimurium*	NP_461804.1	yes	no	Agbor et al. 2011
SopA	*S. typhimurium*	NP_461011.1	yes	yes	Agbor et al. 2011
SopB CS	*S. typhimurium*	NP_460064.1	yes	no	Agbor et al. 2011
SopD	*S. typhimurium*	NP_461866.1	yes	no	Agbor et al. 2011
SopD2	*S. typhimurium*	CBW17005	yes	no	Agbor et al. 2011
SopE2 GV	*S. typhimurium*	NP_460811.1	yes	yes	Agbor et al. 2011
SpiC	*S. typhimurium*	NP_460358.1	yes	no	Agbor et al. 2011
SptP	*S. typhimurium*	NP_461799.1	yes	no	Agbor et al. 2011
SsaB	*S. typhimurium*	NP_460358.1	no	na	Papezova et al. 2007
SsaE	*S. typhimurium*	NP_460361.1	yes	no	Miki et al.. 2009
SsaM	*S. typhimurium*	NP_460378.1	no	na	Yu et al. 2004
SseE	*S. typhimurium*	NP_460367.1	yes	no	Coombes et al. 2004
SseF	*S. typhimurium*	NP_460369.1	no	na	Agbor et al. 2011
SseG	*S. typhimurium*	NP_460370.1	yes	yes	Agbor et al. 2011
SseI	*S. typhimurium*	NP_461184.1	yes	no	Ehrbar and Hardt 2005
SseL	*S. typhimurium*	NP_461229.2	yes	no	Agbor et al. 2011
SseJ	*S. typhimurium*	NP_460590.1	yes	yes	Agbor et al. 2011
SspH2	*S. typhimurium*	NP_461184.1	yes	no	Agbor et al. 2011
SteA	*S. typhimurium*	NP_460542.1	yes	yes	Geddes et al. 2005
SteB	*S. typhimurium*	Q8ZPA6	no	na	Agbor et al. 2011
EspB	*EHEC H7:O157*	NP_290254.1	yes	no	Tobe et al. 2006
EspF	*EHEC H7:O157*	NP_290250.1	yes	yes	Tobe et al. 2006
ESPFu	*EHEC H7:O157*	NP_286906.1	yes	yes	Tobe et al. 2006
EspG	*EHEC H7:O157*	NP_290289.1	yes	no	Tobe et al. 2006
EspH-	*EHEC H7:O157*	NP_290264.1	yes	yes	Tobe et al. 2006
EspJ	*EHEC H7:O157*	NP_288436.1	yes	yes	Tobe et al. 2006
EspK	*EHEC H7:O157*	NP_287316.1	yes	no	Tobe et al. 2006
EspL1	*EHEC H7:O157*	NP_288154.1	yes	no	Tobe et al. 2006
EspL2	*EHEC H7:O157*	NP_289551.1	no	na	Tobe et al. 2006
EspM1	*EHEC H7:O157*	NP_287949.1	yes	no	Tobe et al. 2006
EspM2	*EHEC H7:O157*	NP_289175.1	yes	no	Tobe et al. 2006
EspR1	*EHEC H7:O157*	NP_287686.1	yes	no	Tobe et al. 2006
EspR3	*EHEC H7:O157*	NP_288394.1	yes	no	Tobe et al. 2006
EspT	*EHEC H7:O158*	NP_289175.1	yes	no	Bulgin et al.. 2009
EspW	*EHEC H7:O157*	NP_289177.1	yes	no	Tobe et al. 2006
EspX1	*EHEC H7:O157*	NP_285716.1	no	na	Tobe et al. 2006

EspX2	*EHEC H7:O157*	NP_286562.1	yes	no	Tobe et al. 2006
EspX4	*EHEC H7:O157*	NP_290672.1	no	na	Tobe et al. 2006
EspX5	*EHEC H7:O157*	NP_290699.1	no	na	Tobe et al. 2006
EspY1	*EHEC H7:O157*	NP_285753.1	yes	no	Tobe et al. 2006
EspY2	*EHEC H7:O157*	NP_285765.1	yes	no	Tobe et al. 2006
EspY3	*EHEC H7:O157*	NP_286160.1	yes	no	Tobe et al. 2006
Map	*EHEC H7:O157*	NP_290262.1	yes	no	Tobe et al. 2006
NleA11	*EHEC H7:O157*	NP_287961.1	yes	no	Tobe et al. 2006
NleB1-	*EHEC H7:O157*	NP_286532.1	yes	no	Tobe et al. 2006
NleC	*EHEC H7:O157*	NP_286533.1	yes	no	Tobe et al. 2006
NleD	*EHEC H7:O157*	NP_286535.1	yes	no	Tobe et al. 2006
NleF	*EHEC H7:O157*	NP_287958.1	yes	no	Tobe et al. 2006
NleG7	*EHEC H7:O157*	NP_287535.1	yes	no	Tobe et al. 2006
NleH1	*EHEC H7:O157*	NP_286534.1	yes	yes	Tobe et al. 2006
SepZ	*EHEC H7:O157*	NP_290271.1	no	na	Tobe et al. 2006
Tir	*EHEC H7:O157*	NP_286906.1	yes	yes	Tobe et al. 2006
Ceg7	*L. pneumophila*	YP_094281.1	yes	yes	Heidtman et al. 2009*
Ceg9	*L. pneumophila*	YP_094300.1	yes	yes	Hubber and Roy 2010*
Ceg10	*L. pneumophila*	YP_094338.1	yes	no	Zusman et al. 2008*
Ceg18	*L. pneumophila*	YP_094932.1	yes	yes	Huang et al. 2011*
Ceg19	*L. pneumophila*	YP_095154.1	yes	yes	Hubber and Roy 2010*
Ceg23	*L. pneumophila*	YP_095648.1	yes	no	Zusman et al. 2008*
Ceg29	*L. pneumophila*	YP_096417.1	yes	no	Zusman et al. 2008*
Ceg33	*L. pneumophila*	YP_096596.1	yes	no	Zusman et al. 2008*
CegC1	*L. pneumophila*	YP_094067.1	yes	yes	Lifshitz et al. 2012*
CegC3	*L. pneumophila*	YP_095177.1	yes	no	Zusman et al. 2008*
CegC4	*L. pneumophila*	YP_096212.1	yes	yes	Lifshitz et al. 2012*
LegA2	*L. pneumophila*	YP_096227.1	yes	no	de Felipe et al. 2005*
LegA3	*L. pneumophila*	YP_096309.1	yes	no	de Felipe et al. 2005*
LegA5	*L. pneumophila*	YP_096331.1	yes	yes	de Felipe et al. 2005*
LegA7	*L. pneumophila*	YP_094447.1	yes	no	Huang et al. 2011*
LegA8	*L. pneumophila*	YP_094731.1	yes	no	Hubber and Roy 2010*
LegA9-	*L. pneumophila*	YP_094446.1	yes	no	Huang et al. 2011*
LegA10	*L. pneumophila*	YP_094093.1	yes	no	de Felipe et al. 2005*
LegA11	*L. pneumophila*	YP_094480.1	yes	no	de Felipe et al. 2005*
LegA12	*L. pneumophila*	YP_094527.1	yes	yes	de Felipe et al. 2005*
LegA14	*L. pneumophila*	YP_096459.1	yes	no	de Felipe et al. 2005*
LegA15	*L. pneumophila*	YP_096463.1	yes	no	de Felipe et al. 2005*
LegAS4	*L. pneumophila*	YP_095745.1	yes	no	de Felipe et al. 2008
LegAU13-	*L. pneumophila*	YP_096157.1	yes	no	Hubber and Roy 2010*
LegC3	*L. pneumophila*	YP_095728.1	yes	yes	Hubber and Roy 2010*

LegC4	*L. pneumophila*	YP_095969.1	yes	yes	de Felipe et al. 2005*
LegC5	*L. pneumophila*	YP_095517.1	yes	no	de Felipe et al. 2005*
LegG1-	*L. pneumophila*	YP_095992.1	yes	no	de Felipe et al. 2005*
LegG2	*L. pneumophila*	YP_094330.1	yes	no	de Felipe et al. 2005*
LegK2	*L. pneumophila*	YP_096150.1	yes	no	de Felipe et al. 2005*
LegK3	*L. pneumophila*	YP_096563.1	yes	no	de Felipe et al. 2005*
LegL1	*L. pneumophila*	YP_094979.1	yes	yes	de Felipe et al. 2005*
LegL2	*L. pneumophila*	YP_095629.1	no	no	de Felipe et al. 2005*
LegL3	*L. pneumophila*	YP_095687.1	yes	yes	de Felipe et al. 2005*
LegL5	*L. pneumophila*	YP_095974.1	yes	no	de Felipe et al. 2005*
LegL7-	*L. pneumophila*	YP_096408.1	yes	no	de Felipe et al. 2005*
LegLC4	*L. pneumophila*	YP_095964.1	yes	no	de Felipe et al. 2005*
LegLC8	*L. pneumophila*	YP_095907.1	yes	yes	de Felipe et al. 2005*
LegP	*L. pneumophila*	YP_096991.1	yes	yes	de Felipe et al. 2005*
LegS2	*L. pneumophila*	YP_096188.1	yes	yes	de Felipe et al. 2005*
LegU1-	*L. pneumophila*	YP_094225.1	yes	no	de Felipe et al. 2005*
LegU2	*L. pneumophila*	YP_096825.1	yes	no	Hubber and Roy 2010*
LidA	*L. pneumophila*	YP_094974.1	yes	no	Hubber and Roy 2010*
LirA	*L. pneumophila*	YP_095976.1	yes	yes	Zusman et al. 2008*
LirB	*L. pneumophila*	YP_095978.1	yes	no	Zusman et al. 2008*
LirC	*L. pneumophila*	YP_095979.1	no	na	Zusman et al. 2008*
LirD	*L. pneumophila*	YP_095980.1	no	na	Zusman et al. 2008*
LirF	*L. pneumophila*	YP_095982.1	yes	no	Zusman et al. 2008*
lpg0045	*L. pneumophila*	YP_094100.1	yes	no	*
lpg0081	*L. pneumophila*	YP_094135.1	yes	no	*
lpg0294	*L. pneumophila*	YP_094348.1	yes	no	*
lpg0365	*L. pneumophila*	YP_094409.1	yes	no	Lifshitz et al. 2012*
lpg0518	*L. pneumophila*	YP_094562.1	yes	yes	Lifshitz et al. 2012*
lpg0634	*L. pneumophila*	YP_094670.1	yes	yes	Lifshitz et al. 2012*
lpg0963	*L. pneumophila*	YP_094997.1	yes	no	Lifshitz et al. 2012*
lpg1148	*L. pneumophila*	YP_095181.1	yes	yes	Zusman et al. 2008*
lpg1158	*L. pneumophila*	YP_095191.1	yes	yes	Huang et al. 2011*
lpg1273	*L. pneumophila*	YP_095303.1	yes	yes	*
lpg1689	*L. pneumophila*	YP_095716.1	yes	no	Lifshitz et al. 2012*
lpg1717	*L. pneumophila*	YP_095744.1	yes	yes	Franco et al. 2009*
lpg1751	*L. pneumophila*	YP_095777.1	yes	yes	*
lpg2327	*L. pneumophila*	YP_096336.1	yes	yes	Huang et al. 2011*
lpg2407	*L. pneumophila*	YP_096415.1	yes	yes	Zusman et al. 2008*
lpg2527	*L. pneumophila*	YP_096534.1	yes	no	Lifshitz et al. 2012*
LpnE	*L. pneumophila*	YP_096234.1	no	na	Hubber and Roy 2010*
PieE	*L. pneumophila*	YP_095985.1	yes	yes	Ninio et al. 2009*

PieF	*L. pneumophila*	YP_095988.1	yes	no	Ninio et al. 2009*
PpeB	*L. pneumophila*	YP_095729.1	yes	yes	*
RalF	*L. pneumophila*	YP_095966.1	yes	no	Hubber and Roy 2010*
SdjA-	*L. pneumophila*	YP_096515.1	yes	no	Ninio et al.. 2007*
SetA	*L. pneumophila*	YP_095994.1	yes	no	Hubber and Roy 2010*
SidA	*L. pneumophila*	YP_094657.1	yes	yes	Huang et al. 2011*
SidB	*L. pneumophila*	YP_095669.1	yes	yes	Bruggemann et al. 2006
SidC	*L. pneumophila*	YP_096518.1	yes	no	Hubber and Roy 2010*
SidD	*L. pneumophila*	YP_096472.1	yes	no	Zusman et al. 2008*
SidF	*L. pneumophila*	YP_096589.1	yes	yes	Hubber and Roy 2010*
SidG	*L. pneumophila*	YP_095384.1	yes	no	de Felipe et al. 2005*
SidJ	*L. pneumophila*	YP_096168.1	yes	yes	Hubber and Roy 2010*
SidM	*L. pneumophila*	YP_096471.1	yes	no	Hubber and Roy 2010*
VipA	*L. pneumophila*	YP_094434.1	yes	yes	Hubber and Roy 2010*
VipD	*L. pneumophila*	YP_096826.1	yes	no	Hubber and Roy 2010*
VipF	*L. pneumophila*	YP_094157.1	yes	no	Shohdy et al. 2005*
VpdA	*L. pneumophila*	YP_096418.1	yes	no	Ninio et al.. 2007*
VpdB	*L. pneumophila*	YP_095258.1	yes	no	Ninio et al.. 2007*
WipA	*L. pneumophila*	YP_125080.1	yes	yes	Ninio et al.. 2007*
WipB	*L. pneumophila*	YP_094678.1	yes	yes	Ninio et al.. 2007*
YifA	*L. pneumophila*	YP_096307.1	yes	yes	Hubber and Roy 2010*
YifB	*L. pneumophila*	YP_095901.1	yes	yes	Hubber and Roy 2010*
IpaA	*S. flexneri*	AAK18443.1	yes	no	Parsot 2009
IpaB	*S. flexneri*	AAK18446	yes	no	Parsot 2009
IpaC	*S. flexneri*	AAK18445.1	yes	no	Parsot 2009
IpaD	*S. flexneri*	AAK18444.1	yes	no	Parsot 2009
IpaH1.4	*S. flexneri*	AAK18594.1	yes	no	Parsot 2009
IpaH2.5	*S. flexneri*	AAK18367	yes	no	Parsot 2009
IpaH4.5	*S. flexneri*	AAK18395	yes	no	Parsot 2009
IpaH7.8	*S. flexneri*	AAK18394.1	yes	no	Parsot 2009
IpaH9.8	*S. flexneri*	AAK18544	yes	no	Parsot 2009
IpaJ	*S. flexneri*	AAK18440	no	na	Parsot 2009
IpgB1 EA	*S. flexneri*	CAC05805.1	yes	yes	Parsot 2009
IpgB2 EA	*S. flexneri*	CAC05777.1	yes	no	Parsot 2009
IpgD CS	*S. flexneri*	AAK18452	yes	yes	Parsot 2009
OspB	*S. flexneri*	CAC05770.1	yes	no	Parsot 2009
OspC1	*S. flexneri*	CAC05790.1	yes	no	Parsot 2009
OspC2	*S. flexneri*	AAW64906	yes	no	Parsot 2009
OspD1	*S. flexneri*	AAW64782	yes	no	Parsot 2009
OspD3	*S. flexneri*	AAW64880	yes	no	Parsot 2009
OspE1	*S. flexneri*	AAW64916	yes	no	Parsot 2009

OspE2	*S. flexneri*	AAW64805	yes	no	Parsot 2009
OspF	*S. flexneri*	AAW64770	yes	no	Parsot 2009
OspG	*S. flexneri*	NP_085391	yes	no	Parsot 2009
VirA	*S. flexneri*	AAK18501	yes	no	Parsot 2009
BepA	*B. henselae*	YP_034062.1	yes	no	Schulein et al. 2005
BepB	*B. henselae*	YP_034064.1	yes	no	Schulein et al. 2005
BepC	*B. henselae*	YP_034065.1	yes	no	Schulein et al. 2005
BepD	*B. henselae*	YP_034066.1	yes	yes	Schulein et al. 2005
BepE	*B. henselae*	YP_034067.1	yes	yes	Schulein et al. 2005
BepF	*B. henselae*	YP_034068.1	yes	no	Schulein et al. 2005

*http://microbiology.columbia.edu/shuman/effectors.html

Appendix References:

(Agbor & McCormick, 2011; Bruggemann et al., 2006; Bulgin et al., 2009; Coombes, Brown, Valdez, Brumell, & Finlay, 2004; Cunnac, Lindeberg, & Collmer, 2009; de Felipe et al., 2008; de Felipe et al., 2005; Ehrbar & Hardt, 2005; Franco, Shuman, & Charpentier, 2009; Geddes, Worley, Niemann, & Heffron, 2005; Heidtman et al., 2009; L. Huang et al., 2011; Hubber & Roy, 2010; Lifshitz et al., 2013; T. Miki, Shibagaki, Danbara, & Okada, 2009; Ninio, Celli, & Roy, 2009; Ninio & Roy, 2007; Papezova, Gregorova, Jonuschies, & Rychlik, 2007; Parsot, 2009; Schulein et al., 2005; Shohdy et al., 2005; Sohn et al., 2012; Tobe et al., 2006; J. W. Yu et al., 2004; Zusman, Degtyar, & Segal, 2008)

BIBLIOGRAPHY

Abrahams, G. L., Muller, P., & Hensel, M. (2006). Functional dissection of SseF, a type III effector protein involved in positioning the salmonella-containing vacuole. *Traffic, 7*(8), 950-965. doi: 10.1111/j.1600-0854.2006.00454.x

Agbor, T. A., & McCormick, B. A. (2011). Salmonella effectors: important players modulating host cell function during infection. *Cell Microbiol, 13*(12), 1858-1869. doi: 10.1111/j.1462-5822.2011.01701.x

Allombert, J., Fuche, F., Michard, C., & Doublet, P. (2013). Molecular mimicry and original biochemical strategies for the biogenesis of a Legionella pneumophila replicative niche in phagocytic cells. *Microbes Infect, 15*(14-15), 981-988. doi: 10.1016/j.micinf.2013.09.007

Alto, N. M., Shao, F., Lazar, C. S., Brost, R. L., Chua, G., Mattoo, S., . . . Dixon, J. E. (2006). Identification of a bacterial type III effector family with G protein mimicry functions. *Cell, 124*(1), 133-145.

Alto, N. M., Weflen, A. W., Rardin, M. J., Yarar, D., Lazar, C. S., Tonikian, R., . . . Dixon, J. E. (2007). The type III effector EspF coordinates membrane trafficking by the spatiotemporal activation of two eukaryotic signaling pathways. *J Cell Biol, 178*(7), 1265-1278.

Amara, J. F., Clackson, T., Rivera, V. M., Guo, T., Keenan, T., Natesan, S., . . . Gilman, M. (1997). A versatile synthetic dimerizer for the regulation of protein-protein interactions. *Proc Natl Acad Sci U S A, 94*(20), 10618-10623.

Ando, H., Abe, H., Sugimoto, N., & Tobe, T. (2007). Maturation of functional type III secretion machinery by activation of anaerobic respiration in enterohaemorrhagic Escherichia coli. *Microbiology, 153*(Pt 2), 464-473. doi: 10.1099/mic.0.2006/000893-0

Aurass, P., Schlegel, M., Metwally, O., Harding, C. R., Schroeder, G. N., Frankel, G., & Flieger, A. (2013). The Legionella pneumophila Dot/Icm-secreted Effector PlcC/CegC1 Together with PlcA and PlcB Promotes Virulence and Belongs to a Novel Zinc Metallophospholipase C Family Present in Bacteria and Fungi. *J Biol Chem, 288*(16), 11080-11092. doi: 10.1074/jbc.M112.426049

Bahrani, F. K., Sansonetti, P. J., & Parsot, C. (1997). Secretion of Ipa proteins by Shigella flexneri: inducer molecules and kinetics of activation. *Infect Immun, 65*(10), 4005-4010.

Bakowski, M. A., Braun, V., Lam, G. Y., Yeung, T., Heo, W. D., Meyer, T., . . . Brumell, J. H. (2010). The phosphoinositide phosphatase SopB manipulates membrane surface charge and trafficking of the Salmonella-containing vacuole. *Cell Host Microbe, 7*(6), 453-462. doi: 10.1016/j.chom.2010.05.011

Balla, T. (2005). Inositol-lipid binding motifs: signal integrators through protein-lipid and protein-protein interactions. *J Cell Sci, 118*(Pt 10), 2093-2104. doi: 10.1242/jcs.02387

Banga, S., Gao, P., Shen, X., Fiscus, V., Zong, W. X., Chen, L., & Luo, Z. Q. (2007). Legionella pneumophila inhibits macrophage apoptosis by targeting pro-death

members of the Bcl2 protein family. *Proc Natl Acad Sci U S A, 104*(12), 5121-5126. doi: 10.1073/pnas.0611030104

Baudin, A., Ozier-Kalogeropoulos, O., Denouel, A., Lacroute, F., & Cullin, C. (1993). A simple and efficient method for direct gene deletion in Saccharomyces cerevisiae. *Nucleic Acids Res, 21*(14), 3329-3330.

Bennett, T. L., Kraft, S. M., Reaves, B. J., Mima, J., O'Brien, K. M., & Starai, V. J. (2013). LegC3, an effector protein from Legionella pneumophila, inhibits homotypic yeast vacuole fusion in vivo and in vitro. *PLoS One, 8*(2), e56798. doi: 10.1371/journal.pone.0056798

Bhattacharjee, S., Halane, M. K., Kim, S. H., & Gassmann, W. (2011). Pathogen effectors target Arabidopsis EDS1 and alter its interactions with immune regulators. *Science, 334*(6061), 1405-1408. doi: 10.1126/science.1211592

Boucrot, E., Beuzon, C. R., Holden, D. W., Gorvel, J. P., & Meresse, S. (2003). Salmonella typhimurium SifA effector protein requires its membrane-anchoring C-terminal hexapeptide for its biological function. *J Biol Chem, 278*(16), 14196-14202.

Broberg, C. A., Zhang, L., Gonzalez, H., Laskowski-Arce, M. A., & Orth, K. (2010). A Vibrio effector protein is an inositol phosphatase and disrupts host cell membrane integrity. *Science, 329*(5999), 1660-1662. doi: 10.1126/science.1192850

Brombacher, E., Urwyler, S., Ragaz, C., Weber, S. S., Kami, K., Overduin, M., & Hilbi, H. (2009). Rab1 guanine nucleotide exchange factor SidM is a major phosphatidylinositol 4-phosphate-binding effector protein of Legionella pneumophila. *J Biol Chem, 284*(8), 4846-4856. doi: 10.1074/jbc.M807505200

Browne, S. H., Hasegawa, P., Okamoto, S., Fierer, J., & Guiney, D. G. (2008). Identification of Salmonella SPI-2 secretion system components required for SpvB-mediated cytotoxicity in macrophages and virulence in mice. *FEMS Immunol Med Microbiol, 52*(2), 194-201. doi: 10.1111/j.1574-695X.2007.00364.x

Bruggemann, H., Hagman, A., Jules, M., Sismeiro, O., Dillies, M. A., Gouyette, C., . . . Buchrieser, C. (2006). Virulence strategies for infecting phagocytes deduced from the in vivo transcriptional program of Legionella pneumophila. *Cell Microbiol, 8*(8), 1228-1240. doi: 10.1111/j.1462-5822.2006.00703.x

Brumell, J. H., Goosney, D. L., & Finlay, B. B. (2002). SifA, a type III secreted effector of Salmonella typhimurium, directs Salmonella-induced filament (Sif) formation along microtubules. *Traffic, 3*(6), 407-415.

Bulgin, R., Arbeloa, A., Goulding, D., Dougan, G., Crepin, V. F., Raymond, B., & Frankel, G. (2009). The T3SS effector EspT defines a new category of invasive enteropathogenic E. coli (EPEC) which form intracellular actin pedestals. *PLoS Pathog, 5*(12), e1000683. doi: 10.1371/journal.ppat.1000683

Bulgin, R., Raymond, B., Garnett, J. A., Frankel, G., Crepin, V. F., Berger, C. N., & Arbeloa, A. (2010). Bacterial guanine nucleotide exchange factors SopE-like and WxxxE effectors. *Infect Immun, 78*(4), 1417-1425. doi: 10.1128/IAI.01250-09

Burnaevskiy, N., Fox, T. G., Plymire, D. A., Ertelt, J. M., Weigele, B. A., Selyunin, A. S., . . . Alto, N. M. (2013). Proteolytic elimination of N-myristoyl modifications

by the Shigella virulence factor IpaJ. *Nature, 496*(7443), 106-109. doi: 10.1038/nature12004

Cain, R. J., Hayward, R. D., & Koronakis, V. (2004). The target cell plasma membrane is a critical interface for Salmonella cell entry effector-host interplay. *Mol Microbiol, 54*(4), 887-904. doi: 10.1111/j.1365-2958.2004.04336.x

Campellone, K. G., Cheng, H. C., Robbins, D., Siripala, A. D., McGhie, E. J., Hayward, R. D., . . . Leong, J. M. (2008). Repetitive N-WASP-binding elements of the enterohemorrhagic Escherichia coli effector EspF(U) synergistically activate actin assembly. *PLoS Pathog, 4*(10), e1000191. doi: 10.1371/journal.ppat.1000191

Cascales, E., & Christie, P. J. (2003). The versatile bacterial type IV secretion systems. *Nat Rev Microbiol, 1*(2), 137-149. doi: 10.1038/nrmicro753

Chardin, P., & McCormick, F. (1999). Brefeldin A: the advantage of being uncompetitive. *Cell, 97*(2), 153-155.

Choy, A., Dancourt, J., Mugo, B., O'Connor, T. J., Isberg, R. R., Melia, T. J., & Roy, C. R. (2012). The Legionella effector RavZ inhibits host autophagy through irreversible Atg8 deconjugation. *Science, 338*(6110), 1072-1076. doi: 10.1126/science.1227026

Christen, M., Coye, L. H., Hontz, J. S., LaRock, D. L., Pfuetzner, R. A., Megha, & Miller, S. I. (2009). Activation of a bacterial virulence protein by the GTPase RhoA. *Sci Signal, 2*(95), ra71. doi: 10.1126/scisignal.2000430

Coombes, B. K., Brown, N. F., Valdez, Y., Brumell, J. H., & Finlay, B. B. (2004). Expression and secretion of Salmonella pathogenicity island-2 virulence genes in response to acidification exhibit differential requirements of a functional type III secretion apparatus and SsaL. *J Biol Chem, 279*(48), 49804-49815. doi: 10.1074/jbc.M404299200

Costa, S. C., & Lesser, C. F. (2014). A Multifunctional Region of the Shigella Type 3 Effector IpgB1 Is Important for Secretion from Bacteria and Membrane Targeting in Eukaryotic Cells. *PLoS One, 9*(4), e93461. doi: 10.1371/journal.pone.0093461

Cunnac, S., Lindeberg, M., & Collmer, A. (2009). Pseudomonas syringae type III secretion system effectors: repertoires in search of functions. *Curr Opin Microbiol, 12*(1), 53-60. doi: 10.1016/j.mib.2008.12.003

D'Souza-Schorey, C., & Chavrier, P. (2006). ARF proteins: roles in membrane traffic and beyond. *Nat Rev Mol Cell Biol, 7*(5), 347-358.

Datsenko, K. A., & Wanner, B. L. (2000). One-step inactivation of chromosomal genes in Escherichia coli K-12 using PCR products. *Proc Natl Acad Sci U S A, 97*(12), 6640-6645.

Davis, J., Wang, J., Tropea, J. E., Zhang, D., Dauter, Z., Waugh, D. S., & Wlodawer, A. (2008). Novel fold of VirA, a type III secretion system effector protein from Shigella flexneri. *Protein Sci*.

De Clerck, F., & De Brabander, M. (1977). Nocodazole, a new synthetic antimitotic agent, enhances the production of plasminogen activator by cells in culture. *Thromb Res, 11*(6), 913-914.

de Felipe, K. S., Glover, R. T., Charpentier, X., Anderson, O. R., Reyes, M., Pericone, C. D., & Shuman, H. A. (2008). Legionella eukaryotic-like type IV substrates

interfere with organelle trafficking. *PLoS Pathog, 4*(8), e1000117. doi: 10.1371/journal.ppat.1000117

de Felipe, K. S., Pampou, S., Jovanovic, O. S., Pericone, C. D., Ye, S. F., Kalachikov, S., & Shuman, H. A. (2005). Evidence for acquisition of Legionella type IV secretion substrates via interdomain horizontal gene transfer. *J Bacteriol, 187*(22), 7716-7726. doi: 10.1128/JB.187.22.7716-7726.2005

de Vries, J. S., Andriotis, V. M., Wu, A. J., & Rathjen, J. P. (2006). Tomato Pto encodes a functional N-myristoylation motif that is required for signal transduction in Nicotiana benthamiana. *Plant J, 45*(1), 31-45. doi: 10.1111/j.1365-313X.2005.02590.x

Dean, P. (2011). Functional domains and motifs of bacterial type III effector proteins and their roles in infection. *FEMS Microbiol Rev, 35*(6), 1100-1125. doi: 10.1111/j.1574-6976.2011.00271.x

Degtyar, E., Zusman, T., Ehrlich, M., & Segal, G. (2009). A Legionella effector acquired from protozoa is involved in sphingolipids metabolism and is targeted to the host cell mitochondria. *Cell Microbiol, 11*(8), 1219-1235. doi: 10.1111/j.1462-5822.2009.01328.x

Di Paolo, G., & De Camilli, P. (2006). Phosphoinositides in cell regulation and membrane dynamics. *Nature, 443*(7112), 651-657. doi: 10.1038/nature05185

Dong, N., Liu, L., & Shao, F. (2010). A bacterial effector targets host DH-PH domain RhoGEFs and antagonizes macrophage phagocytosis. *EMBO J, 29*(8), 1363-1376. doi: 10.1038/emboj.2010.33

Dong, N., Zhu, Y., Lu, Q., Hu, L., Zheng, Y., & Shao, F. (2012). Structurally Distinct Bacterial TBC-like GAPs Link Arf GTPase to Rab1 Inactivation to Counteract Host Defenses. *Cell, 150*(5), 1029-1041. doi: 10.1016/j.cell.2012.06.050

Dukes, J. D., Lee, H., Hagen, R., Reaves, B. J., Layton, A. N., Galyov, E. E., & Whitley, P. (2006). The secreted Salmonella dublin phosphoinositide phosphatase, SopB, localizes to PtdIns(3)P-containing endosomes and perturbs normal endosome to lysosome trafficking. *Biochem J, 395*(2), 239-247. doi: 10.1042/BJ20051451

Ehrbar, K., & Hardt, W. D. (2005). Bacteriophage-encoded type III effectors in Salmonella enterica subspecies 1 serovar Typhimurium. *Infect Genet Evol, 5*(1), 1-9. doi: 10.1016/j.meegid.2004.07.004

Fallman, M., Andersson, K., Hakansson, S., Magnusson, K. E., Stendahl, O., & Wolf-Watz, H. (1995). Yersinia pseudotuberculosis inhibits Fc receptor-mediated phagocytosis in J774 cells. *Infect Immun, 63*(8), 3117-3124.

Franco, I. S., Shohdy, N., & Shuman, H. A. (2012). The Legionella pneumophila effector VipA is an actin nucleator that alters host cell organelle trafficking. *PLoS Pathog, 8*(2), e1002546. doi: 10.1371/journal.ppat.1002546

Franco, I. S., Shuman, H. A., & Charpentier, X. (2009). The perplexing functions and surprising origins of Legionella pneumophila type IV secretion effectors. *Cell Microbiol, 11*(10), 1435-1443. doi: 10.1111/j.1462-5822.2009.01351.x

Franke, T. F., Kaplan, D. R., Cantley, L. C., & Toker, A. (1997). Direct regulation of the Akt proto-oncogene product by phosphatidylinositol-3,4-bisphosphate. *Science, 275*(5300), 665-668.

Freeman, J. A., Ohl, M. E., & Miller, S. I. (2003). The Salmonella enterica serovar typhimurium translocated effectors SseJ and SifB are targeted to the Salmonella-containing vacuole. *Infect Immun, 71*(1), 418-427.

Galac, M. R., & Lazzaro, B. P. (2011). Comparative pathology of bacteria in the genus Providencia to a natural host, Drosophila melanogaster. *Microbes Infect, 13*(7), 673-683. doi: 10.1016/j.micinf.2011.02.005

Galac, M. R., & Lazzaro, B. P. (2012). Comparative genomics of bacteria in the genus Providencia isolated from wild Drosophila melanogaster. *BMC Genomics, 13*, 612. doi: 10.1186/1471-2164-13-612

Gao, X., Wan, F., Mateo, K., Callegari, E., Wang, D., Deng, W., . . . Hardwidge, P. R. (2009). Bacterial effector binding to ribosomal protein s3 subverts NF-kappaB function. *PLoS Pathog, 5*(12), e1000708. doi: 10.1371/journal.ppat.1000708

Geddes, K., Worley, M., Niemann, G., & Heffron, F. (2005). Identification of new secreted effectors in Salmonella enterica serovar Typhimurium. *Infect Immun, 73*(10), 6260-6271. doi: 10.1128/IAI.73.10.6260-6271.2005

Gietz, R. D., Schiestl, R. H., Willems, A. R., & Woods, R. A. (1995). Studies on the transformation of intact yeast cells by the LiAc/SS-DNA/PEG procedure. *Yeast, 11*(4), 355-360. doi: 10.1002/yea.320110408

Gillooly, D. J., Morrow, I. C., Lindsay, M., Gould, R., Bryant, N. J., Gaullier, J. M., . . . Stenmark, H. (2000). Localization of phosphatidylinositol 3-phosphate in yeast and mammalian cells. *EMBO J, 19*(17), 4577-4588. doi: 10.1093/emboj/19.17.4577

Gode-Potratz, C. J., Chodur, D. M., & McCarter, L. L. (2010). Calcium and iron regulate swarming and type III secretion in Vibrio parahaemolyticus. *J Bacteriol, 192*(22), 6025-6038. doi: 10.1128/JB.00654-10

Grecco, H. E., Schmick, M., & Bastiaens, P. I. (2011). Signaling from the living plasma membrane. *Cell, 144*(6), 897-909. doi: 10.1016/j.cell.2011.01.029

Halici, S., Zenk, S. F., Jantsch, J., & Hensel, M. (2008). Functional analysis of the Salmonella pathogenicity island 2-mediated inhibition of antigen presentation in dendritic cells. *Infect Immun, 76*(11), 4924-4933. doi: 10.1128/IAI.00531-08

Hall, A. (1998). Rho GTPases and the actin cytoskeleton. *Science, 279*(5350), 509-514.

Haneburger, I., & Hilbi, H. (2013). Phosphoinositide lipids and the legionella pathogen vacuole. *Curr Top Microbiol Immunol, 376*, 155-173. doi: 10.1007/82_2013_341

Hao, Y. H., Wang, Y., Burdette, D., Mukherjee, S., Keitany, G., Goldsmith, E., & Orth, K. (2008). Structural requirements for Yersinia YopJ inhibition of MAP kinase pathways. *PLoS One, 3*(1), e1375. doi: 10.1371/journal.pone.0001375

Heidtman, M., Chen, E. J., Moy, M. Y., & Isberg, R. R. (2009). Large-scale identification of Legionella pneumophila Dot/Icm substrates that modulate host cell vesicle trafficking pathways. *Cell Microbiol, 11*(2), 230-248. doi: 10.1111/j.1462-5822.2008.01249.x

Hemrajani, C., Berger, C. N., Robinson, K. S., Marches, O., Mousnier, A., & Frankel, G. (2010). NleH effectors interact with Bax inhibitor-1 to block apoptosis during enteropathogenic Escherichia coli infection. *Proc Natl Acad Sci U S A, 107*(7), 3129-3134. doi: 10.1073/pnas.0911609106

Hicks, S. W., Charron, G., Hang, H. C., & Galan, J. E. (2011). Subcellular targeting of Salmonella virulence proteins by host-mediated S-palmitoylation. *Cell Host Microbe, 10*(1), 9-20. doi: 10.1016/j.chom.2011.06.003

High, N., Mounier, J., Prevost, M. C., & Sansonetti, P. J. (1992). IpaB of Shigella flexneri causes entry into epithelial cells and escape from the phagocytic vacuole. *EMBO J, 11*(5), 1991-1999.

Hsu, F., Zhu, W., Brennan, L., Tao, L., Luo, Z. Q., & Mao, Y. (2012). Structural basis for substrate recognition by a unique Legionella phosphoinositide phosphatase. *Proc Natl Acad Sci U S A, 109*(34), 13567-13572. doi: 10.1073/pnas.1207903109

Huang, L., Boyd, D., Amyot, W. M., Hempstead, A. D., Luo, Z. Q., O'Connor, T. J., . . . Isberg, R. R. (2011). The E Block motif is associated with Legionella pneumophila translocated substrates. *Cell Microbiol, 13*(2), 227-245. doi: 10.1111/j.1462-5822.2010.01531.x

Huang, Z., Sutton, S. E., Wallenfang, A. J., Orchard, R. C., Wu, X., Feng, Y., . . . Alto, N. M. (2009). Structural insights into host GTPase isoform selection by a family of bacterial GEF mimics. *Nat Struct Mol Biol, 16*(8), 853-860.

Hubber, A., & Roy, C. R. (2010). Modulation of host cell function by Legionella pneumophila type IV effectors. *Annu Rev Cell Dev Biol, 26*, 261-283. doi: 10.1146/annurev-cellbio-100109-104034

Isakoff, S. J., Cardozo, T., Andreev, J., Li, Z., Ferguson, K. M., Abagyan, R., . . . Skolnik, E. Y. (1998). Identification and analysis of PH domain-containing targets of phosphatidylinositol 3-kinase using a novel in vivo assay in yeast. *EMBO J, 17*(18), 5374-5387. doi: 10.1093/emboj/17.18.5374

Ivanov, S. S., Charron, G., Hang, H. C., & Roy, C. R. (2010). Lipidation by the host prenyltransferase machinery facilitates membrane localization of Legionella pneumophila effector proteins. *J Biol Chem, 285*(45), 34686-34698. doi: 10.1074/jbc.M110.170746

Jackson, L. K., Nawabi, P., Hentea, C., Roark, E. A., & Haldar, K. (2008). The Salmonella virulence protein SifA is a G protein antagonist. *Proc Natl Acad Sci U S A, 105*(37), 14141-14146.

Kenny, B., & Finlay, B. B. (1997). Intimin-dependent binding of enteropathogenic Escherichia coli to host cells triggers novel signaling events, including tyrosine phosphorylation of phospholipase C-gamma1. *Infect Immun, 65*(7), 2528-2536.

Knodler, L. A., Vallance, B. A., Hensel, M., Jackel, D., Finlay, B. B., & Steele-Mortimer, O. (2003). Salmonella type III effectors PipB and PipB2 are targeted to detergent-resistant microdomains on internal host cell membranes. *Mol Microbiol, 49*(3), 685-704. doi: 3598 [pii]

Krol, J., Janeczek, M., Pliszczak-Krol, A., Janeczek, W., & Florek, M. (2007). Providencia alcalifaciens as the presumptive cause of diarrhoea in dog. *Pol J Vet Sci, 10*(4), 285-287.

Ku, B., Lee, K. H., Park, W. S., Yang, C. S., Ge, J., Lee, S. G., . . . Oh, B. H. (2012). VipD of Legionella pneumophila targets activated Rab5 and Rab22 to interfere with endosomal trafficking in macrophages. *PLoS Pathog, 8*(12), e1003082. doi: 10.1371/journal.ppat.1003082

Kurushima, J., Nagai, T., Nagamatsu, K., & Abe, A. (2010). EspJ effector in enterohemorrhagic E. coli translocates into host mitochondria via an atypical mitochondrial targeting signal. *Microbiol Immunol, 54*(7), 371-379. doi: 10.1111/j.1348-0421.2010.00218.x

LaRock, D. L., Brzovic, P. S., Levin, I., Blanc, M. P., & Miller, S. I. (2012). A Salmonella typhimurium-translocated glycerophospholipid:cholesterol acyltransferase promotes virulence by binding to the RhoA protein switch regions. *J Biol Chem, 287*(35), 29654-29663. doi: 10.1074/jbc.M112.363598

Layton, A. N., Brown, P. J., & Galyov, E. E. (2005). The Salmonella translocated effector SopA is targeted to the mitochondria of infected cells. *J Bacteriol, 187*(10), 3565-3571. doi: 10.1128/JB.187.10.3565-3571.2005

Lifshitz, Z., Burstein, D., Peeri, M., Zusman, T., Schwartz, K., Shuman, H. A., . . . Segal, G. (2013). Computational modeling and experimental validation of the Legionella and Coxiella virulence-related type-IVB secretion signal. *Proc Natl Acad Sci U S A, 110*(8), E707-715. doi: 10.1073/pnas.1215278110

Lin, D. Y., Diao, J., & Chen, J. (2012). Crystal structures of two bacterial HECT-like E3 ligases in complex with a human E2 reveal atomic details of pathogen-host interactions. *Proc Natl Acad Sci U S A, 109*(6), 1925-1930. doi: 10.1073/pnas.1115025109

Liu, Y., & Luo, Z. Q. (2007). The Legionella pneumophila effector SidJ is required for efficient recruitment of endoplasmic reticulum proteins to the bacterial phagosome. *Infect Immun, 75*(2), 592-603. doi: 10.1128/IAI.01278-06

Lossi, N. S., Rolhion, N., Magee, A. I., Boyle, C., & Holden, D. W. (2008). The Salmonella SPI-2 effector SseJ exhibits eukaryotic activator-dependent phospholipase A and glycerophospholipid : cholesterol acyltransferase activity. *Microbiology, 154*(Pt 9), 2680-2688. doi: 10.1099/mic.0.2008/019075-0

Luo, Y., Frey, E. A., Pfuetzner, R. A., Creagh, A. L., Knoechel, D. G., Haynes, C. A., . . . Strynadka, N. C. (2000). Crystal structure of enteropathogenic Escherichia coli intimin-receptor complex. *Nature, 405*(6790), 1073-1077.

Marches, O., Batchelor, M., Shaw, R. K., Patel, A., Cummings, N., Nagai, T., . . . Frankel, G. (2006). EspF of enteropathogenic Escherichia coli binds sorting nexin 9. *J Bacteriol, 188*(8), 3110-3115.

Marches, O., Covarelli, V., Dahan, S., Cougoule, C., Bhatta, P., Frankel, G., & Caron, E. (2008). EspJ of enteropathogenic and enterohaemorrhagic Escherichia coli inhibits opsono-phagocytosis. *Cell Microbiol, 10*(5), 1104-1115. doi: 10.1111/j.1462-5822.2007.01112.x

Marcus, S. L., Knodler, L. A., & Finlay, B. B. (2002). Salmonella enterica serovar Typhimurium effector SigD/SopB is membrane-associated and ubiquitinated inside host cells. *Cell Microbiol, 4*(7), 435-446.

Matsumoto, H., & Young, G. M. (2006). Proteomic and functional analysis of the suite of Ysp proteins exported by the Ysa type III secretion system of Yersinia enterocolitica Biovar 1B. *Mol Microbiol, 59*(2), 689-706. doi: 10.1111/j.1365-2958.2005.04973.x

Miki, H., Miura, K., & Takenawa, T. (1996). N-WASP, a novel actin-depolymerizing protein, regulates the cortical cytoskeletal rearrangement in a PIP2-dependent manner downstream of tyrosine kinases. *EMBO J, 15*(19), 5326-5335.

Miki, T., Shibagaki, Y., Danbara, H., & Okada, N. (2009). Functional characterization of SsaE, a novel chaperone protein of the type III secretion system encoded by Salmonella pathogenicity island 2. *J Bacteriol, 191*(22), 6843-6854. doi: 10.1128/JB.00863-09

Mizuno-Yamasaki, E., Rivera-Molina, F., & Novick, P. (2012). GTPase networks in membrane traffic. *Annu Rev Biochem, 81*, 637-659. doi: 10.1146/annurev-biochem-052810-093700

Mnaimneh, S., Davierwala, A. P., Haynes, J., Moffat, J., Peng, W. T., Zhang, W., . . . Hughes, T. R. (2004). Exploration of essential gene functions via titratable promoter alleles. *Cell, 118*(1), 31-44. doi: 10.1016/j.cell.2004.06.013

Mukherjee, S., Liu, X., Arasaki, K., McDonough, J., Galan, J. E., & Roy, C. R. (2011). Modulation of Rab GTPase function by a protein phosphocholine transferase. *Nature, 477*(7362), 103-106. doi: 10.1038/nature10335

Muller, M. P., Shkumatov, A. V., Oesterlin, L. K., Schoebel, S., Goody, P. R., Goody, R. S., & Itzen, A. (2012). Characterization of enzymes from Legionella pneumophila involved in reversible adenylylation of Rab1 protein. *J Biol Chem, 287*(42), 35036-35046. doi: 10.1074/jbc.M112.396861

Nakanishi, H., de los Santos, P., & Neiman, A. M. (2004). Positive and negative regulation of a SNARE protein by control of intracellular localization. *Mol Biol Cell, 15*(4), 1802-1815. doi: 10.1091/mbc.E03-11-0798

Neunuebel, M. R., Mohammadi, S., Jarnik, M., & Machner, M. P. (2012). Legionella pneumophila LidA affects nucleotide binding and activity of the host GTPase Rab1. *J Bacteriol, 194*(6), 1389-1400. doi: 10.1128/JB.06306-11

Newton, H. J., Sansom, F. M., Dao, J., McAlister, A. D., Sloan, J., Cianciotto, N. P., & Hartland, E. L. (2007). Sel1 repeat protein LpnE is a Legionella pneumophila virulence determinant that influences vacuolar trafficking. *Infect Immun, 75*(12), 5575-5585. doi: 10.1128/IAI.00443-07

Niebuhr, K., Giuriato, S., Pedron, T., Philpott, D. J., Gaits, F., Sable, J., . . . Payrastre, B. (2002). Conversion of PtdIns(4,5)P(2) into PtdIns(5)P by the S.flexneri effector IpgD reorganizes host cell morphology. *EMBO J, 21*(19), 5069-5078.

Nimchuk, Z., Marois, E., Kjemtrup, S., Leister, R. T., Katagiri, F., & Dangl, J. L. (2000). Eukaryotic fatty acylation drives plasma membrane targeting and enhances function of several type III effector proteins from Pseudomonas syringae. *Cell, 101*(4), 353-363.

Ninio, S., Celli, J., & Roy, C. R. (2009). A Legionella pneumophila effector protein encoded in a region of genomic plasticity binds to Dot/Icm-modified vacuoles. *PLoS Pathog, 5*(1), e1000278. doi: 10.1371/journal.ppat.1000278

Ninio, S., & Roy, C. R. (2007). Effector proteins translocated by Legionella pneumophila: strength in numbers. *Trends Microbiol, 15*(8), 372-380.

Nobes, C. D., & Hall, A. (1995). Rho, rac, and cdc42 GTPases regulate the assembly of multimolecular focal complexes associated with actin stress fibers, lamellipodia, and filopodia. *Cell, 81*(1), 53-62.

Odendall, C., Rolhion, N., Forster, A., Poh, J., Lamont, D. J., Liu, M., . . . Holden, D. W. (2012). The Salmonella kinase SteC targets the MAP kinase MEK to regulate the host actin cytoskeleton. *Cell Host Microbe, 12*(5), 657-668. doi: 10.1016/j.chom.2012.09.011

Ogawa, M., Yoshimori, T., Suzuki, T., Sagara, H., Mizushima, N., & Sasakawa, C. (2005). Escape of intracellular Shigella from autophagy. *Science, 307*(5710), 727-731. doi: 10.1126/science.1106036

Ohlson, M. B., Huang, Z., Alto, N. M., Blanc, M. P., Dixon, J. E., Chai, J., & Miller, S. I. (2008). Structure and function of Salmonella SifA indicate that its interactions with SKIP, SseJ, and RhoA family GTPases induce endosomal tubulation. *Cell Host Microbe, 4*(5), 434-446.

Ohya, K., Handa, Y., Ogawa, M., Suzuki, M., & Sasakawa, C. (2005a). IpgB1 Is a Novel Shigella Effector Protein Involved in Bacterial Invasion of Host Cells: ITS ACTIVITY TO PROMOTE MEMBRANE RUFFLING VIA RAC1 AND CDC42 ACTIVATION. *J Biol Chem, 280*(25), 24022-24034.

Ohya, K., Handa, Y., Ogawa, M., Suzuki, M., & Sasakawa, C. (2005b). IpgB1 is a novel Shigella effector protein involved in bacterial invasion of host cells. Its activity to promote membrane ruffling via Rac1 and Cdc42 activation. *J Biol Chem, 280*(25), 24022-24034. doi: 10.1074/jbc.M502509200

Okada, R., Zhou, X., Hiyoshi, H., Matsuda, S., Chen, X., Akeda, Y., . . . Kodama, T. (2013). The Vibrio parahaemolyticus effector VopC mediates Cdc42-dependent invasion of cultured cells but is not required for pathogenicity in an animal model of infection. *Cell Microbiol*. doi: 10.1111/cmi.12252

Orchard, R. C., & Alto, N. M. (2012). Mimicking GEFs: a common theme for bacterial pathogens. *Cell Microbiol, 14*(1), 10-18. doi: 10.1111/j.1462-5822.2011.01703.x

Orchard, R. C., Kittisopikul, M., Altschuler, S. J., Wu, L. F., Suel, G. M., & Alto, N. M. (2012). Identification of F-actin as the dynamic hub in a microbial-induced GTPase polarity circuit. *Cell, 148*(4), 803-815. doi: 10.1016/j.cell.2011.11.063

Papezova, K., Gregorova, D., Jonuschies, J., & Rychlik, I. (2007). Ordered expression of virulence genes in Salmonella enterica serovar typhimurium. *Folia Microbiol (Praha), 52*(2), 107-114. doi: 10.1007/BF02932148

Parsot, C. (2009). Shigella type III secretion effectors: how, where, when, for what purposes? *Curr Opin Microbiol, 12*(1), 110-116. doi: 10.1016/j.mib.2008.12.002

Patel, J. C., Hueffer, K., Lam, T. T., & Galan, J. E. (2009). Diversification of a Salmonella virulence protein function by ubiquitin-dependent differential localization. *Cell, 137*(2), 283-294.

Pei, J., Kim, B. H., & Grishin, N. V. (2008). PROMALS3D: a tool for multiple protein sequence and structure alignments. *Nucleic Acids Res, 36*(7), 2295-2300. doi: 10.1093/nar/gkn072

Poh, J., Odendall, C., Spanos, A., Boyle, C., Liu, M., Freemont, P., & Holden, D. W. (2008). SteC is a Salmonella kinase required for SPI-2-dependent F-actin

remodelling. *Cell Microbiol, 10*(1), 20-30. doi: 10.1111/j.1462-5822.2007.01010.x

Price, C. T., Jones, S. C., Amundson, K. E., & Kwaik, Y. A. (2010). Host-mediated post-translational prenylation of novel dot/icm-translocated effectors of legionella pneumophila. *Front Microbiol, 1*, 131. doi: 10.3389/fmicb.2010.00131

Ramsden, A. E., Mota, L. J., Munter, S., Shorte, S. L., & Holden, D. W. (2007). The SPI-2 type III secretion system restricts motility of Salmonella-containing vacuoles. *Cell Microbiol, 9*(10), 2517-2529. doi: 10.1111/j.1462-5822.2007.00977.x

Raucher, D., Stauffer, T., Chen, W., Shen, K., Guo, S., York, J. D., . . . Meyer, T. (2000). Phosphatidylinositol 4,5-bisphosphate functions as a second messenger that regulates cytoskeleton-plasma membrane adhesion. *Cell, 100*(2), 221-228.

Reinicke, A. T., Hutchinson, J. L., Magee, A. I., Mastroeni, P., Trowsdale, J., & Kelly, A. P. (2005). A Salmonella typhimurium effector protein SifA is modified by host cell prenylation and S-acylation machinery. *J Biol Chem, 280*(15), 14620-14627.

Rivera, G. M., Vasilescu, D., Papayannopoulos, V., Lim, W. A., & Mayer, B. J. (2009). A reciprocal interdependence between Nck and PI(4,5)P(2) promotes localized N-WASp-mediated actin polymerization in living cells. *Mol Cell, 36*(3), 525-535. doi: 10.1016/j.molcel.2009.10.025

Rivera, V. M., Wang, X., Wardwell, S., Courage, N. L., Volchuk, A., Keenan, T., . . . Clackson, T. (2000). Regulation of protein secretion through controlled aggregation in the endoplasmic reticulum. *Science, 287*(5454), 826-830.

Robert-Seilaniantz, A., Shan, L., Zhou, J. M., & Tang, X. (2006). The Pseudomonas syringae pv. tomato DC3000 type III effector HopF2 has a putative myristoylation site required for its avirulence and virulence functions. *Mol Plant Microbe Interact, 19*(2), 130-138. doi: 10.1094/MPMI-19-0130

Roy, A., & Levine, T. P. (2004). Multiple pools of phosphatidylinositol 4-phosphate detected using the pleckstrin homology domain of Osh2p. *J Biol Chem, 279*(43), 44683-44689. doi: 10.1074/jbc.M401583200

Sadarangani, V., Datta, S., & Arunachalam, M. (2013). New players in the same old game: a system level in silico study to predict type III secretion system and effector proteins in bacterial genomes reveals common themes in T3SS mediated pathogenesis. *BMC Res Notes, 6*, 297. doi: 10.1186/1756-0500-6-297

Saftig, P., & Klumperman, J. (2009). Lysosome biogenesis and lysosomal membrane proteins: trafficking meets function. *Nat Rev Mol Cell Biol, 10*(9), 623-635. doi: 10.1038/nrm2745

Salcedo, S. P., & Holden, D. W. (2003). SseG, a virulence protein that targets Salmonella to the Golgi network. *EMBO J, 22*(19), 5003-5014. doi: 10.1093/emboj/cdg517

Salomon, D., Guo, Y., Kinch, L. N., Grishin, N. V., Gardner, K. H., & Orth, K. (2013). Effectors of animal and plant pathogens use a common domain to bind host phosphoinositides. *Nat Commun, 4*, 2973. doi: 10.1038/ncomms3973

Salomon, D., & Sessa, G. (2010). Identification of growth inhibition phenotypes induced by expression of bacterial type III effectors in yeast. *J Vis Exp*(37). doi: 10.3791/1865

Schoebel, S., Cichy, A. L., Goody, R. S., & Itzen, A. (2011). Protein LidA from Legionella is a Rab GTPase supereffector. *Proc Natl Acad Sci U S A, 108*(44), 17945-17950. doi: 10.1073/pnas.1113133108

Schulein, R., Guye, P., Rhomberg, T. A., Schmid, M. C., Schroder, G., Vergunst, A. C., . . . Dehio, C. (2005). A bipartite signal mediates the transfer of type IV secretion substrates of Bartonella henselae into human cells. *Proc Natl Acad Sci U S A, 102*(3), 856-861. doi: 10.1073/pnas.0406796102

Scidmore, M. A., Fischer, E. R., & Hackstadt, T. (2003). Restricted fusion of Chlamydia trachomatis vesicles with endocytic compartments during the initial stages of infection. *Infect Immun, 71*(2), 973-984.

Scott, J. D., & Pawson, T. (2009). Cell signaling in space and time: where proteins come together and when they're apart. *Science, 326*(5957), 1220-1224.

Selyunin, A. S., Reddick, L. E., Weigele, B. A., & Alto, N. M. (2014). Selective Protection of an ARF1-GTP Signaling Axis by a Bacterial Scaffold Induces Bidirectional Trafficking Arrest. *Cell Rep, 6*(5), 878-891. doi: 10.1016/j.celrep.2014.01.040

Selyunin, A. S., Sutton, S. E., Weigele, B. A., Reddick, L. E., Orchard, R. C., Bresson, S. M., . . . Alto, N. M. (2011). The assembly of a GTPase-kinase signalling complex by a bacterial catalytic scaffold. *Nature, 469*(7328), 107-111. doi: 10.1038/nature09593

Sherry, A. E., Inglis, N. F., Stevenson, A., Fraser-Pitt, D., Everest, P., Smith, D. G., & Roberts, M. (2011). Characterisation of proteins extracted from the surface of Salmonella Typhimurium grown under SPI-2-inducing conditions by LC-ESI/MS/MS sequencing. *Proteomics, 11*(3), 361-370. doi: 10.1002/pmic.200900802

Shohdy, N., Efe, J. A., Emr, S. D., & Shuman, H. A. (2005). Pathogen effector protein screening in yeast identifies Legionella factors that interfere with membrane trafficking. *Proc Natl Acad Sci U S A, 102*(13), 4866-4871. doi: 10.1073/pnas.0501315102

Smith, A. C., Heo, W. D., Braun, V., Jiang, X., Macrae, C., Casanova, J. E., . . . Brumell, J. H. (2007). A network of Rab GTPases controls phagosome maturation and is modulated by Salmonella enterica serovar Typhimurium. *J Cell Biol, 176*(3), 263-268. doi: 10.1083/jcb.200611056

Soding, J., Biegert, A., & Lupas, A. N. (2005). The HHpred interactive server for protein homology detection and structure prediction. *Nucleic Acids Res, 33*(Web Server issue), W244-248. doi: 10.1093/nar/gki408

Sohn, K. H., Saucet, S. B., Clarke, C. R., Vinatzer, B. A., O'Brien, H. E., Guttman, D. S., & Jones, J. D. (2012). HopAS1 recognition significantly contributes to Arabidopsis nonhost resistance to Pseudomonas syringae pathogens. *New Phytol, 193*(1), 58-66. doi: 10.1111/j.1469-8137.2011.03950.x

Sreelatha, A., Bennett, T. L., Zheng, H., Jiang, Q. X., Orth, K., & Starai, V. J. (2013). Vibrio effector protein, VopQ, forms a lysosomal gated channel that disrupts host ion homeostasis and autophagic flux. *Proc Natl Acad Sci U S A, 110*(28), 11559-11564. doi: 10.1073/pnas.1307032110

Stauffer, T. P., Ahn, S., & Meyer, T. (1998). Receptor-induced transient reduction in plasma membrane PtdIns(4,5)P2 concentration monitored in living cells. *Curr Biol, 8*(6), 343-346.

Steele-Mortimer, O. (2008). The Salmonella-containing vacuole: moving with the times. *Curr Opin Microbiol, 11*(1), 38-45. doi: S1369-5274(08)00003-9 [pii]
10.1016/j.mib.2008.01.002

Stefan, C. J., Manford, A. G., Baird, D., Yamada-Hanff, J., Mao, Y., & Emr, S. D. (2011). Osh proteins regulate phosphoinositide metabolism at ER-plasma membrane contact sites. *Cell, 144*(3), 389-401. doi: 10.1016/j.cell.2010.12.034

Stein, M. A., Leung, K. Y., Zwick, M., Garcia-del Portillo, F., & Finlay, B. B. (1996). Identification of a Salmonella virulence gene required for formation of filamentous structures containing lysosomal membrane glycoproteins within epithelial cells. *Mol Microbiol, 20*(1), 151-164.

Strahl, T., & Thorner, J. (2007). Synthesis and function of membrane phosphoinositides in budding yeast, Saccharomyces cerevisiae. *Biochim Biophys Acta, 1771*(3), 353-404. doi: 10.1016/j.bbalip.2007.01.015

Subtil, A., Parsot, C., & Dautry-Varsat, A. (2001). Secretion of predicted Inc proteins of Chlamydia pneumoniae by a heterologous type III machinery. *Mol Microbiol, 39*(3), 792-800.

Suzuki, T., Araki, Y., Yamamoto, T., & Nakaya, T. (2006). Trafficking of Alzheimer's disease-related membrane proteins and its participation in disease pathogenesis. *J Biochem, 139*(6), 949-955. doi: 10.1093/jb/mvj121

Tan, Y., Arnold, R. J., & Luo, Z. Q. (2011). Legionella pneumophila regulates the small GTPase Rab1 activity by reversible phosphorylcholination. *Proc Natl Acad Sci U S A, 108*(52), 21212-21217. doi: 10.1073/pnas.1114023109

Tan, Y., & Luo, Z. Q. (2011). Legionella pneumophila SidD is a deAMPylase that modifies Rab1. *Nature, 475*(7357), 506-509. doi: 10.1038/nature10307

Tanida, I. (2011). Autophagy basics. *Microbiol Immunol, 55*(1), 1-11. doi: 10.1111/j.1348-0421.2010.00271.x

Tobe, T., Beatson, S. A., Taniguchi, H., Abe, H., Bailey, C. M., Fivian, A., . . . Pallen, M. J. (2006). An extensive repertoire of type III secretion effectors in Escherichia coli O157 and the role of lambdoid phages in their dissemination. *Proc Natl Acad Sci U S A, 103*(40), 14941-14946. doi: 10.1073/pnas.0604891103

Tu, X., Nisan, I., Yona, C., Hanski, E., & Rosenshine, I. (2003). EspH, a new cytoskeleton-modulating effector of enterohaemorrhagic and enteropathogenic Escherichia coli. *Mol Microbiol, 47*(3), 595-606.

Van Engelenburg, S. B., & Palmer, A. E. (2010). Imaging type-III secretion reveals dynamics and spatial segregation of Salmonella effectors. *Nat Methods, 7*(4), 325-330. doi: 10.1038/nmeth.1437

Wang, X., Wang, J., Hao, H., Qiu, L., Liu, H., Chen, S., . . . Yang, Z. (2014). Pathogenic Providencia alcalifaciens strain that causes fatal hemorrhagic pneumonia in piglets. *Curr Microbiol, 68*(3), 278-284. doi: 10.1007/s00284-013-0470-y

Weernink, P. A., Meletiadis, K., Hommeltenberg, S., Hinz, M., Ishihara, H., Schmidt, M., & Jakobs, K. H. (2004). Activation of type I phosphatidylinositol 4-phosphate 5-

kinase isoforms by the Rho GTPases, RhoA, Rac1, and Cdc42. *J Biol Chem, 279*(9), 7840-7849. doi: 10.1074/jbc.M312737200

Weflen, A. W., Alto, N. M., Viswanathan, V. K., & Hecht, G. (2010). E. coli secreted protein F promotes EPEC invasion of intestinal epithelial cells via an SNX9-dependent mechanism. *Cell Microbiol, 12*(7), 919-929. doi: 10.1111/j.1462-5822.2010.01440.x

Weiner, O. D., Neilsen, P. O., Prestwich, G. D., Kirschner, M. W., Cantley, L. C., & Bourne, H. R. (2002). A PtdInsP(3)- and Rho GTPase-mediated positive feedback loop regulates neutrophil polarity. *Nat Cell Biol, 4*(7), 509-513. doi: 10.1038/ncb811

Weiss, S. M., Ladwein, M., Schmidt, D., Ehinger, J., Lommel, S., Stading, K., . . . Stradal, T. E. (2009). IRSp53 links the enterohemorrhagic E. coli effectors Tir and EspFU for actin pedestal formation. *Cell Host Microbe, 5*(3), 244-258. doi: 10.1016/j.chom.2009.02.003

Wickner, W. (2010). Membrane fusion: five lipids, four SNAREs, three chaperones, two nucleotides, and a Rab, all dancing in a ring on yeast vacuoles. *Annu Rev Cell Dev Biol, 26*, 115-136. doi: 10.1146/annurev-cellbio-100109-104131

Wong, A. R., Raymond, B., Collins, J. W., Crepin, V. F., & Frankel, G. (2012). The enteropathogenic E. coli effector EspH promotes actin pedestal formation and elongation via WASP-interacting protein (WIP). *Cell Microbiol, 14*(7), 1051-1070. doi: 10.1111/j.1462-5822.2012.01778.x

Yoh, M., Matsuyama, J., Ohnishi, M., Takagi, K., Miyagi, H., Mori, K., . . . Honda, T. (2005). Importance of Providencia species as a major cause of travellers' diarrhoea. *J Med Microbiol, 54*(Pt 11), 1077-1082. doi: 10.1099/jmm.0.45846-0

Young, B. M., & Young, G. M. (2002). Evidence for targeting of Yop effectors by the chromosomally encoded Ysa type III secretion system of Yersinia enterocolitica. *J Bacteriol, 184*(20), 5563-5571.

Yu, J. W., Mendrola, J. M., Audhya, A., Singh, S., Keleti, D., DeWald, D. B., . . . Lemmon, M. A. (2004). Genome-wide analysis of membrane targeting by S. cerevisiae pleckstrin homology domains. *Mol Cell, 13*(5), 677-688.

Yu, Q., Hu, L., Yao, Q., Zhu, Y., Dong, N., Wang, D. C., & Shao, F. (2013). Structural analyses of Legionella LepB reveal a new GAP fold that catalytically mimics eukaryotic RasGAP. *Cell Res, 23*(6), 775-787. doi: 10.1038/cr.2013.54

Zhang, Y., Higashide, W. M., McCormick, B. A., Chen, J., & Zhou, D. (2006). The inflammation-associated Salmonella SopA is a HECT-like E3 ubiquitin ligase. *Mol Microbiol, 62*(3), 786-793. doi: 10.1111/j.1365-2958.2006.05407.x

Zhou, D., Chen, L. M., Hernandez, L., Shears, S. B., & Galan, J. E. (2001). A Salmonella inositol polyphosphatase acts in conjunction with other bacterial effectors to promote host cell actin cytoskeleton rearrangements and bacterial internalization. *Mol Microbiol, 39*(2), 248-259. doi: mmi2230 [pii]

Zusman, T., Degtyar, E., & Segal, G. (2008). Identification of a hypervariable region containing new Legionella pneumophila Icm/Dot translocated substrates by using the conserved icmQ regulatory signature. *Infect Immun, 76*(10), 4581-4591. doi: 10.1128/IAI.00337-08